EGFL7 SIGNALING DURING ORGANOGENESIS OF ENDOCRINE ORGANS: THE PANCREAS AND PLACENTA

A Dissertation

Presented to the Faculty of the Weill Cornell Graduate School

of Medical Sciences

in Partial Fulfillment of the Requirements for the Degree of

Doctor of Philosophy

By

Lauretta Ann Lacko

May 2015

© 2015 Lauretta Ann Lacko

EGFL7 SIGNALING DURING ORGANOGENESIS OF ENDOCRINE ORGANS: THE PANCREAS AND PLACENTA

Lauretta Ann Lacko, Ph.D.

Cornell University 2015

Endocrine organs play a critical role in physiology, growth, and metabolism through secretion of hormones. For example, the hypothalamus controls production of hormones from the pituitary gland to regulate homeostasis, the pancreas produces insulin and glucagon to control blood glucose levels, and the placenta produces hormones necessary for the establishment and maintenance of pregnancy. These organs require a vascular network for hormone secretion in addition to supplying oxygen and nutrients and removing metabolic wastes. *Epidermal growth factor like domain 7* (*Egfl7*) is a secreted angiogenic factor important for vascular development. In this thesis, I have analyzed a role for *Egfl7* in the development of two endocrine organs, the pancreas and placenta.

The first set of studies elucidates a role for *Egfl7* in pancreatic development. Endothelial specific overexpression of *Egfl7* using a transgenic mouse model resulted in increased pancreatic progenitor cell proliferation and decreased differentiation toward insulin-positive endocrine cells. These results were concomitant with collaborative studies demonstrating the stage dependent role of EGFL7 in maintaining pancreatic progenitor self-renewal during directed differentiation of human embryonic stem cells (hESC) along the pancreatic cell lineage, a promising protocol to treat pancreas-associated disorders.

The second set of studies elucidates a role for *Egfl7* in normal and pathological placental development. Analysis of pathological placentation revealed that Egfl7 is downregulated in human preeclamptic term placentas, and in placentas of a mouse model of preeclampsia (PE), prior to the onset of clinical signs of the disease. In addition to placental endothelial cells, Egfl7 expression was uncovered in the trophoblast cell lineage. Analysis of *Egfl7* loss-of-function placentas demonstrated a critical role for *Egfl7* in patterning of the fetoplacental vasculature, resulting in reduced placental perfusion.

Collectively, these studies have elucidated novel roles for *Egfl7* during organogenesis of the pancreas and placenta. The stage dependent role of EGFL7 in hESC differentiation may enhance strategies used for treatment of diabetes mellitus, the seventh leading cause of death in the United States. The functional role of *Egfl7* in placental development and its early downregulation in PE suggest that it could be a potential novel diagnostic tool and/or therapeutic target for treating PE.

BIOGRAPHICAL SKETCH

Lauretta Ann Lacko was born and raised in suburban Chicago, and graduated from Amos Alonzo Stagg High School in June 2004. Lauretta attended the University of Illinois at Urbana-Champaign, where was awarded the Jonathon Baldwin Turner Scholarship and honored as a James Scholar and an American Society of Animal Science Scholar. She earned her Bachelor of Science in Animal Sciences with a minor in Chemistry with honors in May 2008. She was honored with the Bronze Tablet Award for graduating in the top 3% of her class.

Lauretta has an extensive and diverse research background in reproductive physiology. Her undergraduate thesis work involved optimizing artificial insemination and estrus resynchronization protocols in beef cattle. Lauretta was an ANSC-USDA Research intern at the Research Centre Foulum in Viborg, Denmark in 2006, where she examined lying behavior and its relation to early detection of lameness in dairy cattle under Dr. Lene Munksgaard, as well as studying thermoregulation mechanisms in mink kits. In addition to her studies, Lauretta was actively involved in working with faculty on maximizing study abroad experiences as a Learning Abroad and Global Awareness Program Leader. She aided in the establishment an exchange program between the University of Illinois and the National Taiwan University.

Following her undergraduate studies, Lauretta was awarded a prestigious Fulbright Postgraduate Fellowship to study the role of progesterone receptors in breast cancer using a novel 3D *in vitro* model system in the laboratory of a leading breast cancer biologist, Dr. Christine Clarke, at the

Westmead Institute for Cancer Research at the University of Sydney in Australia, from July 2008 through August 2009.

In September of 2009, Lauretta entered the Physiology, Biophysics, and Systems Biology graduate program at Weill Cornell Graduate School of Medical Sciences. The following July, Lauretta became a member of the laboratory of Dr. Heidi Stuhlmann, and began her thesis research investigating the role of *Epidermal Growth Factor Like Domain 7* (*Egfl7*) in pancreatic and placental development. She has presented her work annually at the Vincent DuVigneaud Graduate School Symposium at Weill Cornell, as well as at national and international conferences, including the North American Vascular Biology Organization (NAVBO) and the International Federation of Placenta Associations (IFPA). Lauretta has been awarded three best poster presentation awards as well as a best oral presentation award at local and national conferences. She was awarded the NIH T32 Developmental Biology training fellowship from 2011-2013. Lauretta has mentored two undergraduate summer students and two first-year rotation students, and has worked as a teaching assistant in the Summer Academy in Molecular Biology program for high school students.

Lauretta's Ph.D. work has resulted in three publications and a fourth in preparation. Following completion of her Ph.D., Lauretta plans to continue her training in scientific research in the field of reproductive physiology.

This work is dedicated to my parents, Shirley and Tony Lacko,
for their endless love and support, and their tireless encouragement of their
little girl to dream big and keep asking 'why'.

ACKNOWLEDGMENTS

I want to take this opportunity to express my gratitude, as I am truly lucky to have received a tremendous amount of support as I endeavored to complete my Ph.D.

Firstly, I wish to thank my thesis advisor, Dr. Heidi Stuhlmann, for her guidance, support, and continuous encouragement. I am grateful for your mentorship and the opportunity to pursue a project outside of the current focus of the lab. Your constant reassuring words and mentoring and your enthusiasm for science provided a foundation for me to grow and mature as a scientist. Thank you. And thank you for always encouraging me to pursue ideas for new experiments. I also wish to thank my thesis committee members and faculty members at WCMC. I would like to thank Dr. Doris Herzlinger for the honorary membership in her lab, for constantly stimulating scientific discussion, and for her guidance and support throughout my graduate school career. I am grateful to Drs. Carl Blobel and Robin Davisson for their careful attention to my work and their guidance. I would like to acknowledge my committee chairperson and collaborator, Dr. Shuibing Chen, for allowing me to work on an exciting project with her lab and for her complimentary words. I would like to thank the PBSB chairperson, Dr. Harel Weinstein, for providing me the confidence to pursue my Ph.D. and for demonstrating a true passion for science and education.

I am grateful for professors of my undergraduate education, Dr. Walter Hurley, Dr. White, and Dr. Katzenellenbogen, for taking the time to guide me as I ventured into a scientific career. I want to thank Drs. Dinny Graham and Christine Clarke, for their gracious mentoring and support throughout my

Fulbright fellowship and showing me my true potential as a scientist. My time in your lab was life-changing.

Also deserving recognition are the past and present members of the Stuhlmann Laboratory, including Dr. Kathryn Bambino, Samantha Hinds, Abhijeet Sharma, Dr. Donna Nichol, and Dr. Pauline Ocaya. I owe many thanks to Dr. Kathryn Bambino for her constant moral support, scientific discussions, and for being a great friend and colleague. I want to thank Samantha Hinds for keeping a positive and organized atmosphere in the lab, and for her encouragement and ability to put our accomplishments into the big picture.

Much of the work in my thesis could not have been done without the support of the core facilities at WCMC and MSKCC. I want to thank the MSKCC Transgenic Core Facility, Dr. Jason McCormack at the WCMC Cell Sorting Core, Drs. Jenny Xiang and Tuo Zhang at the WCMC Genomics Core Facility, and Lee Cohen-Gould and her team at the WCMC Electron Microscopy Core Facility. Furthermore, I would like to thank Nick Gale from Regeneron for the Egfl7 knockout ESCs. I would like to thank the funding sources for this work, including the NIH T32 Training Grant in developmental biology, March of Dimes (MOD #6-FY14-411), and the National Institutes of Health (R01 HL082098). I am also grateful for the friendships and support of my fellow PBSB students, including Peipei Guo and William Chang.

I would like to thank my parents for their unwavering support and for instilling in me the discipline and values needed to pursue higher education. I am forever grateful for their endless love and encouragement, and for all they sacrificed to give a better life to my brother and me. They are truly an inspiration. I owe endless gratitude to my brother, A.J., who has been a pillar in my education and in my life. I would like to thank my friends, Stephanie

Richard, Megan Smyrniotis, Katie Rooney, and Sarah Blount, for their constant love and support.

Finally, words cannot express the gratitude I have to my fiancé, Dr. Romulo Hurtado, without whom I could not have accomplished this work. I am eternally grateful for his support both scientifically and emotionally. I want to thank you for your mentorship, our scientific discussions, your technical advice, and our collaborative studies. I want to thank you for challenging me to my highest potential as a scientist and as a person. The confidence I've gained from your support has allowed me to achieve more than I've ever thought possible. Your patience is astounding. Dr. Romulo Hurtado: Thank you. I am truly lucky to have found you and cannot wait for the many scientific and life successes that are in our future.

TABLE OF CONTENTS

LIST OF FIGURES

LIST OF TABLES

LIST OF ABBREVIATIONS

Akt	Protein Kinase B
Akt-HUVEC-CM	Conditioned Medium from Akt-HUVECs
Akt-HUVECs	AKT-activated Human Umbilical Vein Endothelial Cells
ANG1	Angiopoietin-1
ANGPT2	Angiopoietin-2
BJ	human skin fibroblast cells
bp	base pairs
BPH/5	Blood pressure high strain 5
CASZ1	Castor zinc finger 1
CCL13	Chemokine (C-C motif) Ligand 13
CD31/PECAM1	Cluster of Differentiation 31/Platelet Endothelial Cell Adhesion Molecule 1
CDX2	Caudal-type homeobox 2
CK	Cytokeratin
CM	Conditioned medium
CNS	Central nervous system
COUP-TFII	Chicken ovalbumin upstream promoter-transcription factor II
Csf1	Colony stimulating factor 1
DAPT	N-[N-(3,5-Difluorophenacetyl)-L-alanyl]-S-phenylglycine t-butyl ester (γ-secretase inhibitor)
DE	Definitive endoderm
Dll4	Delta like protein 4
DSL	Delta, Serrate, Lag-2
E	Embryonic Day
EC	Endothelial Cell(s)
ECM	Extracellular matrix
EdU	5-ethynyl-2'-deoxyuridine
EGF	Epidermal growth factor
Egfl7	Epidermal growth factor like domain 7
EGFP	enhanced green fluorescent protein
EGFR	EGF receptor

ERG	ETS related gene
ERK	Extracellular signal related kinase
ESC	Embryonic stem cells
ETS	E-twenty-six
FACS	Fluorescence activated cell sorting
FAK	Focal Adhesion Kinase
FE	Foregut endoderm
FGF10	Fibroblast Growth Factor 10
Fgf2	basic Fibroblast Growth Factor
FOXA2	Forkhead box A2
Fzd5	Frizzled class receptor 5
GATA2	GATA binding protein 2
Gcm1	Glial cells missing 1
GFP	Green fluorescent protein
GO	Gene Ontology
GSIS	Glucose Stimulated Insulin Secretion
GTT	Glucose Tolerance Test
hESC	Human embryonic stem cells
Hey1/2	Hairy/enhancer of split related with YRPW motif protein 1/2
HNF4α	Hepatocyte Nuclear Factor 4 alpha
HNF6	Hepatocyte Nuclear Factor 6
HUVECs	Human Umbilical Vein Endothelial Cells
ICAM1	Intercellular adhesion molecule 1
IL24	Interleukin-24
iPSCs	Induced pluripotent stem cells
ISH	In situ hybridization
IUGR	Intrauterine growth restriction
kb	Kilobase
kDa	KiloDalton
Klf2a	Kruppel like factor 2a
KO	Knockout
MAPK	Mitogen activated protein kinase
MEF	Mouse embryonic fibroblasts

mg	milligram
miR	microRNA
mL	milliliter
mm	millimeter
mm Hg	Millimeters Mercury
MPEC-CM	Conditioned medium from MPECs
MPECs	Mouse pancreas islet endothelial cells
mRNA	messenger RNA
NFκB	Nuclear Factor Kappa-Light-Chain-Enhancer of activated B-Cells
ng	Nanogram
NGN3	Neurogenin 3
NKX6.1	NK6 homeobox 1
p85β/PIK3R2	Phosphoinositide-3-Kinase Regulatory Subunit 2
PDGF-BB	Platelet derived growth factor homodimeric protein BB
PDGFB	Platelet derived growth factor B
PDGFRβ	Platelet derived growth factor receptor beta
Pdx1	Pancreatic and duodenal homeobox 1
PE	Preeclampsia
PI3K	Phosphoinositide 3-kinase
PLAU	Plasminogen activator, Urokinase
PlGF	Placental growth factor
PODXL	Podocalyxin
PP	Pancreatic progenitor
Prap1	Proline rich acidic protein 1
Ptf1a	Pancreas specific transcription factor 1a
qRT-PCR	Quantitative reverse transcription polymerase chain reaction
Rasip1	Ras interacting protein 1
RNA	Ribonucleic acid
RNA-Seq	RNA sequencing
ROCK	Rho-associated protein kinase
Rpbj	Recombination Signal Binding Protein For Immunoglobulin Kappa J Region
RT-PCR	reverse transcription polymerase chain reaction

sEng	Soluble Endoglin
sFlt1	Soluble fms-like tyrosine kinase 1
Shh	Sonic Hedgehog
shRNA	Short hairpin RNA
SOX17	Sex determining region Y (SRY)-box 17
SOX9	Sex determining region Y (SRY)-box 9
Spred1	Sprouty-related EVH1 domain containing 1
TG	Transgenic
TGC	Trophoblast giant cell
TGFβ	Transforming Growth Factor beta
TIE2	Angiopoietin-1 Receptor/Tunica Interna Endothelial Cell Kinase
Tmprss4	Transmembrane protease serine 4
TSC	Trophoblast stem cells
VCAM1	Vascular cell adhesion molecule 1
VEGF	Vascular endothelial growth factor
VEGF-A	Vascular endothelial growth factor-A
VEGFR2/KDR/Flk-1	VEGF Receptor 2/Kinase insert domain receptor/Fetal liver kinase-1
WT	Wild type

LIST OF SYMBOLS

α	alpha or anti
β	beta
γ	gamma
μ	micro

Chapter 1 – Introduction

1.1 – Vasculogenesis and Angiogenesis

Organogenesis requires a functional, arborized vascular network for proper development and homeostasis. The vasculature conducts blood in order to supply oxygen and nutrients to tissues while removing metabolic wastes, and is necessary for distant tissues to communicate. Abnormal vessel growth contributes to the pathology and progression of many diseases, such as cancer and myocardial infarction. Blood vessels form by two distinct processes, vasculogenesis and angiogenesis. Vasculogenesis, or the de novo formation of blood vessels during development, involves the differentiation of mesoderm-derived angioblasts into endothelial cells that form a primitive vascular plexus (**Figure 1.1**) (*1-3*). Angiogenesis is the formation of blood vessels from pre-existing vessels. Blood vessels are stabilized through recruitment of pericytes and smooth muscle cells to form a mature vascular network (**Figure 1.1**) (*1-3*).

Blood vessel formation begins after gastrulation when mesodermal clusters of cells differentiate into angioblasts, or endothelial precursor cells, in the embryo. These cells proliferate, migrate to specified locations, and coalesce to form vascular cords (*1-3*). Vascular Endothelial Growth Factor-A (VEGF-A) is the predominant signaling molecule required for vascular development, and plays an important role in the migration of endothelial progenitor cells and the formation of the primitive vascular plexus (*4*). Indeed, loss of a single *Vegfa* allele results in embryonic lethality at midgestation (Embryonic Day 11.5-12.5) due to defective endothelial cell differentiation and irregular blood vessel development (*5, 6*). The importance of the VEGF signaling pathway during vascular development is further demonstrated by deficiency in VEGF-A's two

predominant receptors, Flt-1/VEGFR1 and Flk-1/VEGFR2/KDR, resulting in the overgrowth or absence of a structured blood vessel network, respectively (*7, 8*).

The primitive vascular plexus expands and matures through branching and sprouting angiogenesis. Several elegant studies have elucidated the mechanism controlling angiogenesis (Reviewed in (*2, 3, 9, 10*)). In response to proangiogenic and chemotactic signaling molecules, certain endothelial cells acquire a tip cell phenotype, developing filopodia to sense environmental cues and becoming the leading migratory edge of a nascent vascular sprout (*2, 9-12*). Tip cell expression of matrix metalloproteinases facilitates the degradation of the surrounding basement membrane proteins, allowing for the migration and invasion of endothelial cells (*12*). Adjacent to tip cells are endothelial stalk cells, which proliferate in order to elongate the vessel and also form lumens. Tip cells anastomose, often with the aid of macrophages, with neighboring vessel sprouts to build the branched, vascular network (*1-3, 10, 11*). Tip and stalk cell phenotypes are transient, and endothelial cells go through iterative cycles of sprouting and branching morphogenesis during vascular development (*10, 13*). Lateral inhibition and a negative feedback loop between VEGF signaling and NOTCH signaling are integrated to designate tip and stalk cell phenotypes (*10*). Notch signaling is an evolutionarily conserved pathway important for cell fate specification and branching morphogenesis, among other processes. Members of the Notch signaling pathway include five Delta-Serrate-Lag2 (DSL) ligands (Jagged1, Jagged2, Delta-like1/3/4), as well as four transmembrane receptors (Notch1/2/3/4) (*10*). VEGF-A signaling through VEGFR2 induces Dll4 signaling in tip cells. Dll4/NOTCH signaling regulates tip/stalk cell fate specification as evidenced by increased number of tip cells and branching defects in Dll4-mutant mice (*14*).

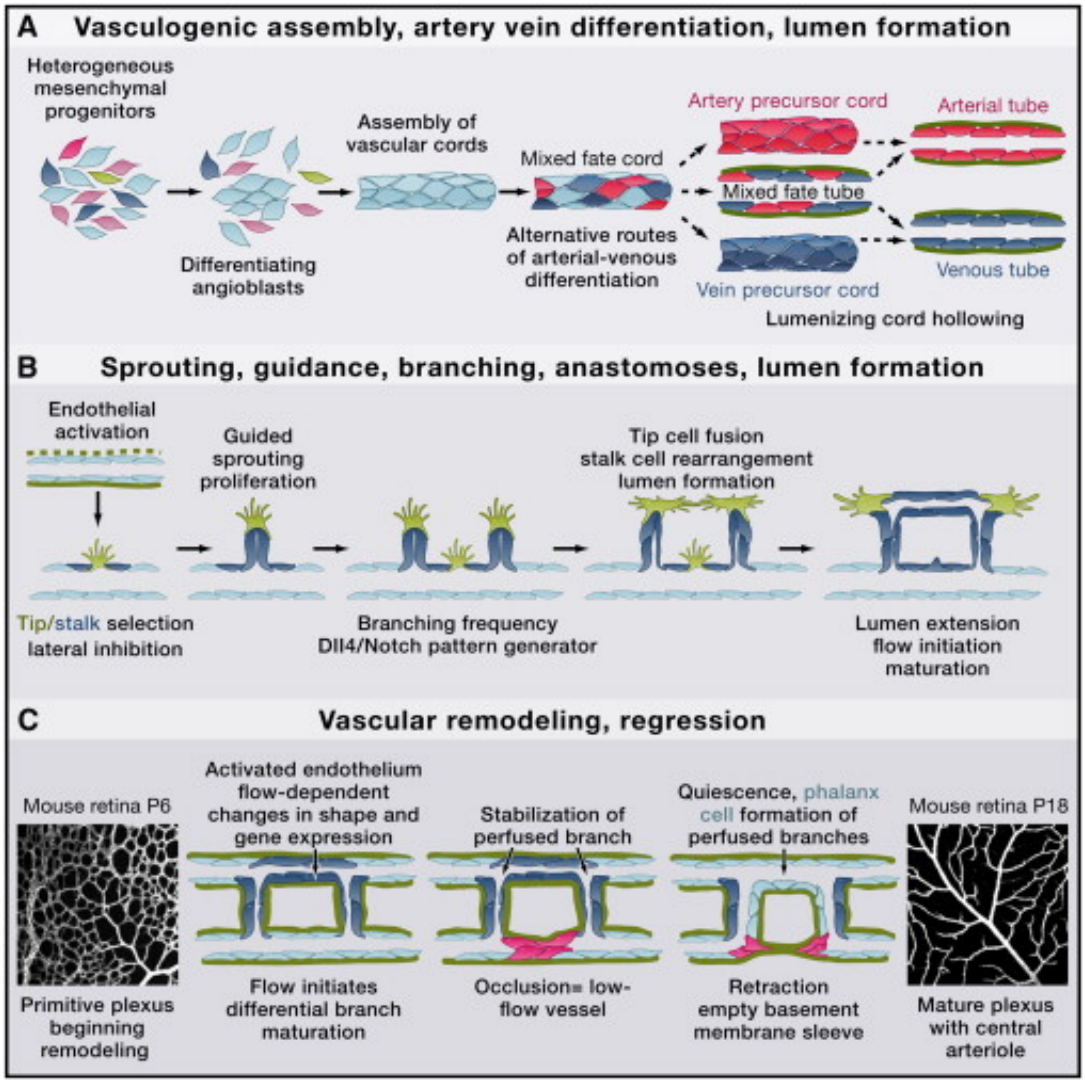

FIGURE 1.1 Hallmarks of development of a functional vasculature.

Borrowed from Potente *et al,* (2011) Cell 146(6): 873-887

1.2 – Vascular Lumen Formation

Lumen formation is another important step required for normal vascular development, irrespective of the vessels arising from vasculogenesis or angiogenesis. Vascular lumen formation can occur by different mechanisms, which likely depend on the vascular bed, but require a few common, critical steps (*3, 15, 16*). The first step in vascular lumen formation is to establish apical-basal polarity in order to determine the luminal surface of the cells and then to rearrange their cell-cell junctions. In addition to several polarity and cell adhesion molecules, β1-integrin signaling plays an important role in this process, as β1-deficient mouse embryos have occluded lumens and mislocalized expression of the polarity molecule Par3, as well as the junctional molecule, VE-cadherin (*17*). Next, endothelial cell shape changes begin to establish a lumen. VEGF-A/VEGFR2 signaling activates Rho-associated protein kinase (ROCK) signaling, resulting in rearranging of non-muscle myosin II and F-actin fibers (*16*). Additionally, glycoproteins such as CD34 and Podocalyxin (PODXL) accumulate on the luminal side of the endothelial cells, and studies suggest they also recruit other proteins (Moesin and F-actin) to the apical surface and their repulsive charges facilitate tube formation (*18*). An endothelial specific regulator of GTPase signaling, Ras interacting protein 1 (Rasip1), has been implicated tubulogenesis. Rasip1-deficient mice fail to form patent vascular lumens through dysregulation of cell polarity and cellular adhesion molecules (*19*).

1.3 Arterio-venous Specification and Vessel Stabilization

The primitive vascular network must be specified into arteries and veins, which carry different hemodynamic loads. Arterial and venous endothelial cells are molecularly distinct, and the initial expression of arterial and venous markers occurs early during development (*3, 20, 21*). Eph-Ephrin signaling establishes arterio-venous boundaries. Analyses of Lacz knock-in mice demonstrated that Ephrin-B2 marks arterial endothelial cells while Eph-B4 is preferentially expressed by venous endothelial cells, prior to the onset of circulation (*22*). Ephrin-B2 and Eph-B4 may mark arterial and venous endothelial cells early. However, Eph-Ephrin signaling is not required for initial cell fate specification but arterio-venous maintenance and remodeling, as deficient mice exhibit defects in remodeling and not spatial localization of arteries and veins (*21*).

Arterial endothelial cell specification is driven by a Sonic hedgehog (Shh)-VEGF-Notch signaling pathway (*21*). Mutant mice of members of the Notch signaling pathway, including Dll4, Rpbj, and Hey1/Hey2 result in failed arterial differentiation and altered Ephrin-B2 and Eph-B4 expression (Reviewed in (*21*)). Venous specification requires nuclear receptor COUP-TFII (Chicken ovalbumin upstream promoter-transcription factor II) to repress Notch signaling. Furthermore, hemodynamic forces drive arterio-venous specification and maintenance (*20*). Arteries are covered by layers of vascular smooth muscle cells and carry a high-pressure gradient, while veins are low-pressure vessels encased by few smooth muscle cells.

Blood vessels are stabilized via recruitment of vascular mural cells. Pericytes and smooth muscle cells interact with endothelial cells and engage in intercellular communication (*23*). Endothelial expressed Platelet-derived Growth Factor B (PDGFB) signals to its receptor, PDGFR-β, on vascular mural

cells, to stimulate their proliferation and recruitment to blood vessels (*24*). Indeed, PDGFB or PDGFR-β deficient mice exhibit hemorrhaging or embryonic lethality (*24*). Additionally, Angiopoeitin-1 (ANG1) activates its endothelial receptor, TIE2, to promote pericyte adhesion, stabilize vessels, and stimulate endothelial cell quiescence (*25*). Ang1 and Tie2 deficient mice exhibit reduced pericyte coverage, defective angiogenesis, and embryonic lethality (*26, 27*).

Blood vessels mature through pruning and remodeling, in which the hierarchal, blood-conducting vascular system is formed and contains arteries, arterioles, capillaries, venules and veins. Tissue-specific phenotypes are further acquired to adapt to the specific requirements of that tissue, and endothelial cells become quiescent.

1.4 – Physiological and Pathological Angiogenesis

Although most endothelial cells in the adult are quiescent, they can become activated during physiological and pathological angiogenesis. Angiogenesis is required for normal physiologic processes such as the cyclic changes in the female reproductive tract, during wound healing, and in response to exercise (*28-30*). It is required for formation of the corpus luteum in the ovary, in the endometrium during the menstrual cycle, as well as in the uterus and placenta during pregnancy (*28*). New blood vessel formation is a critical requirement for wound repair and tissue regeneration (*29*). Increased vascularity in skeletal muscle is induced by exercise (*30*).

Pathologic processes and diseases such as diabetic retinopathy, rheumatoid arthritis, and tumorigenesis also require angiogenesis. Abnormal retinal angiogenesis is implicated in diabetic patients, as diabetic retinopathy is one of the leading causes of blindness in the United States (*31*). Angiogenesis plays a

role in the invasiveness of the synovium and the development of rheumatoid arthritis (*32*). Furthermore, pathological angiogenesis in tumors has been shown to play a key role in tumor progression and metastasis, and has been a preferential target for therapeutic treatment (*33*).

In addition to the signaling pathways mentioned above, many other factors play a role in regulating blood vessel development. Thus, it is important to elucidate the molecular mechanisms that control blood vessel formation during development, in order to understand pathological vascular development as well as to effectively treat patients in need of anti-angiogenic therapy.

1.5 – Epidermal Growth Factor Like Domain 7

Another angiogenic factor that has been implicated during vasculogenesis and angiogenesis is Epidermal Growth Factor Like Domain 7 (Egfl7), also known as VE-Statin, Zneu1, or Notch4-like protein. The Stuhlmann Lab identified *Egfl7* using a retroviral gene entrapment screen for genes with restricted expression during mouse embryogenesis and embryonic stem cell differentiation (*34*). *Egfl7* was independently discovered by two other laboratories as a gene involved in early cardiovascular development (*35, 36*). EGFL7 is a unique angiogenic factor in that it is a secreted factor predominantly expressed by endothelial cells, while other secreted angiogenic factors, such as VEGF, are predominately expressed by non-endothelial cell types. The *Egfl7* gene spans 11.5kb on mouse chromosome 2 and human chromosome 9, and contains 11 exons with the protein coding region extending from exon 3 to exon 10 (*34, 35*). A microRNA, miR-126, is embedded between exon 7 and exon 8 of *Egfl7*. The 1.4kb Egfl7 transcript encodes a putative 278 amino acid, 29-kDa protein. The native EGFL7 protein runs at ~41kDa, suggesting posttranslational modifications of several potential N- and O-linked glycosylation sites (*34, 35*).

EGFL7 contains an N-terminal signal peptide, an EMI-like domain, and two centrally located EGF-like domains, one of which contains a region conserved in Notch ligands required for receptor binding, termed the DSL domain, and the second containing a calcium binding domain. Mouse EGFL7 is 73% identical to human, 88% identical to rat, and 45% identical to *Xenopus laevis* orthologs, including conservation of the signal peptide and EGF domains (*34*).

The signal peptide domain within Egfl7 is common to many secreted proteins. When overexpressed *in vitro*, EGFL7 localizes to organelles of the secretory pathway, including the endoplasmic reticulum and the Golgi apparatus, and can be detected in conditioned medium from these cells (*34, 35*). Moreover, EGFL7 is found tightly associated with the extracellular matrix (ECM) (*37*). Fibronectin and type I collagen facilitate EGFL7 deposition into the ECM, supporting the notion that EGFL7 is associated with the 'provisional matrix', or the environment encountered by nascent blood vessels (*38*).

1.6 – Egfl7 Expression and Function

Egfl7 expression in largely restricted to actively proliferating endothelial cells, including endothelial cells undergoing vasculogenesis, physiological angiogenesis, and pathological angiogenesis. Egfl7 is also expressed in embryonic stem cells and neural stem cells, as well as in primordial germ cells, and pre- and peri-implantation embryos beginning at the 8-cell stage of development (*34-36, 39, 40*).

Egfl7 is a marker of the endothelial cell lineage and their precursors, with an expression profile similar to, but preceding, Flk-1 (*34, 41, 42*). Egfl7 is expressed by endothelial progenitors of the developing embryo such as mesodermal cell clusters migrating from the posterior primitive streak, and of

extraembryonic tissues such as blood islands in the yolk sac (*34-36, 41*). Its expression becomes restricted to endothelial cells, peaking at E9.5 and becoming downregulated in the adult, quiescent endothelium (*34, 36*). Egfl7 is, however, expressed in the adult lung and kidney, albeit at low levels, as well as in both tip and stalk cells of the postnatal retina (*38, 40, 41*).

Egfl7 is upregulated during physiological angiogenesis, such as in reproductive structures like the uterus, whose cyclic changes in angiogenesis supply the nutrients and hormones necessary for the establishment and maintenance of pregnancy (*28, 36, 43*). Egfl7 is also upregulated during pathological angiogenesis, such as in oxygen-induced retinopathy (*41*), vascular injury (*43, 44*), and in several tumors (*45-47*).

A role for EGFL7 has been demonstrated in key cellular processes involved in development and maturation of a stable, vascular network, such as proliferation, migration, adhesion, sprouting, and patterning (*35, 36, 38, 40, 43, 48*). *In vitro*, knockdown of Egfl7 results in decreased proliferation of both embryonic stem cells (*48*) and Human Umbilical Vein Endothelial Cells (HUVECs) (*40*), and increased proliferation of neural stem cells (*49*). EGFL7 affects migration by acting as a chemoattractant for endothelial cells (*43*) and inhibiting PDGF-BB induced aortic smooth muscle cell migration (*35*). Using *in vitro* angiogenesis assays, Egfl7 knockdown resulted in decreased migration of HUVECs, while overexpression and knockdown of Egfl7 resulted in aberrant or no capillary sprouting, respectively (*40*).

Egfl7 functions to promote weak endothelial cell adhesion and a permissive environment for the migration and sprouting of endothelial cells (*36, 37, 50, 51*). EGFL7 has been shown to bind to $\alpha V\beta 3$ integrin on the ECM, but does not play a structural role in the matrix, resembling members of the ‘matricellular

proteins' family (*37, 52*). EGFL7 promotes cell shape changes and mild adhesion of endothelial cells to the ECM via binding of $\alpha V\beta 3$ integrin, activation of focal adhesion kinase (FAK), and upregulation of RhoA GTPase (*36, 37, 50*). In contrast to fibronectin and other traditional cell adhesion molecules that promote stress fiber formation and a non-migratory phenotype, EGFL7 stimulates the development of filopodia, allowing endothelial cells to attach and migrate more efficiently.

Additionally, EGFL7 has been shown to modulate ECM rigidity by blocking lysyl oxidase mediated conversion of tropoelastin to elastin through interaction with the enzyme's catalytic site (*51*). Inhibition of elastin fiber deposition results in control of vascular elastogenesis, and provides a possible mechanism by which Egfl7 controls cell migration and invasion. In support, mature quiescent endothelial cells do not express Egfl7 but do accumulate elastin fibers, a mechanism in line with blood vessel development and maturation.

In vivo studies in mice and zebrafish demonstrate that EGFL7 affects vascular patterning (*36, 38, 40, 50*). Endothelial specific overexpression of Egfl7 in mice results in abnormal vascular patterning and remodeling, including accumulation of endothelial cell aggregates, collapsed arterial vessels, hyperbranched and tortuous vessels in the head vasculature and postnatal retina, as well as aberrant positioning of endothelial and smooth muscle cells at branch points of the dorsal aorta (*40*). Egfl7 loss-of-function mice exhibited defects in the collective migration and spatial organization of endothelial cells, as well as hemorrhaging, vascular patterning, and partial embryonic lethality (*36, 38*). It is important to note, that studies involving Egfl7 knockout mice have been complicated by the presence of miR-126, which will be discussed in detail below. However, studies involving knockdown and overexpression of Egfl7

while maintaining miR-126 levels demonstrate that Egfl7 plays an important role during formation of a functioning vasculature (*40, 48*).

Furthermore, Egfl7 has been shown to play a role in tubulogenesis and lumen formation (*36, 50, 53*). Egfl7 knockdown in zebrafish and *Xenopus laevis* results in defective reorganization of junctional proteins and failed lumen formation (*36, 50, 53*).

1.7 – Egfl7 function in disease and vascular injury

In addition to a role for Egfl7 during vascular development, Egfl7 has been implicated to function in response to vascular injury and disease. EGFL7 expression is transiently upregulated in the endothelium of two models of arterial injury, and high levels are detected in human atherosclerotic plaques (*43*).

Egfl7 plays a protective role in pathologic hypoxic or hyperoxic tissues. Upregulation of Egfl7 in response to hypoxia is seen in cultured endothelial cells, the immature rat brain, and in the mouse retina (*41, 44, 54*). In human coronary artery endothelial cells, Egfl7 exhibits anti-inflammatory characteristics by repressing ICAM1 expression and NFκB activation in response to hypoxia-reoxygenation injury or calcineurin-inhibition induced injury (*44, 55*). Egfl7 protects endothelial cells *in vitro* from hyperoxia-induced cell death via prevention of cytochrome c release, therefore inhibiting activation of the caspase cascade (*56*).

In cancer, EGFL7 has been shown to promote cell motility and metastasis, as well as tumor growth. In hepatocellular carcinoma, EGFL7 stimulates focal adhesion kinase phosphorylation and subsequent tumor cell migration (*57*).

Furthermore, EGFL7 promotes tumor progression by reducing the expression of endothelial molecules that mediate leukocyte adhesion and infiltration of immune cells, including ICAM1 and VCAM1 (*58, 59*).

The role of Egfl7 in cancer has been further corroborated. Expression of Egfl7 is elevated in many tumors and cancer cell lines. A recent study found that EGFL7 is overexpressed in ten human epithelial tumors, including lung, breast, prostate, ovarian, renal, colorectal, gastric, and esophageal cancers, as well as hepatocellular carcinoma, and malignant glioma (*45*). Additionally, Egfl7 is widely expressed in pancreatic cancer cell lines (*60*), as well as in the serum of many cancer patients (*45*). High levels of EGFL7 correlate with higher tumor grade, poor prognosis, and higher metastatic score (*57, 60-62*). Therefore, Egfl7 may be a useful, novel predictive factor for progression of certain cancers, including ovarian cancer, gastric carcinoma, malignant glioma, laryngeal squamous cell carcinoma, and pancreatic cancer (*60-64*).

Based on the knowledge of the functional role of Egfl7 during vascular development, vascular injury, and cancer, efforts are underway to explore the use of anti-EGFL7 therapy. Preclinical trials using anti-EGFL7 monoclonal antibodies in combination with anti-VEGF therapy showed promising results regarding inhibition of tumor growth in human cancer xenograft mouse models and genetically engineered mouse models, when compared to anti-VEGF therapy alone (*65*). Phase II clinical trials for anti-EGFL7 therapy (Parsatuzumab) are currently in progress to determine the effect of this therapy in treatment on progression-free survival and tumor growth in patients with certain cancers, including non-small cell lung cancer (Genentech; MEGF0444A, RG7414; Roche; http://sigma.larvol.com/merge/sigma/product.php?e1=69&tab=newstrac).

1.8 – miR-126

As mentioned previously, determining the role of Egfl7 during mammalian vascular development has been complicated by the presence of a microRNA, miR-126, located between exon 7 and exon 8 of the Egfl7 transcript (*66, 67*). However, several studies have demonstrated an integral role for Egfl7 in vascular development without altering miR-126 expression (*37, 40, 48, 50*). Several groups have demonstrated Egfl7-specific functions during pathological development, such as oxygen-induced-retinopathy (*41*) and in cancer cells.

Several possible explanations are considered to reconcile these seemingly conflicting results. The lack of phenotype seen by Kuhnert *et al* in the Egfl7-specific knockout mice could be due to compensatory factors or to the mixed genetic background in which the studies were performed (*66*). It is important to note that while EGFL7 is secreted and found associated with the extracellular matrix, miR-126 exerts its function within the cell (*34, 36, 37, 67, 68*).

MicroRNAs are a family of small non-coding RNAs (~20-25nt) that regulate expression of target mRNAs through destabilization and degradation or translation inhibition (*69*). The first studies using two different Egfl7 loss-of-function mice demonstrated vascular defects and partial embryonic lethality, however, the levels of miR-126 were never measured (*38*). A later study demonstrated that Egfl7 loss-of-function mice that maintained miR-126 expression did not exhibit any overt vascular defects (*66*). In contrast, a miR-126-specific knockout mouse that maintained Egfl7 expression resulted in a vascular phenotype similar to the one described for the original Egfl7 knockout in Schmidt *et al* (*38, 66*), suggesting that the mutant phenotype was due to the loss of miR-126 rather than the loss of Egfl7.

Egfl7 and miR-126 share a 5.4kb regulatory promoter region that controls their vascular specific expression profile during development (*67*). Additionally, Klf2a, a transcription factor upregulated in response to hemodynamic forces, has been shown to upregulate miR-126 in zebrafish (*70*). miR-126 knockout in mice results in partial embryonic lethality, leaky vessels, and hemorrhaging, as well as aberrant endothelial cell proliferation and migration (*67*). miR-126 loss-of-function mice and zebrafish exhibit impaired angiogenesis and defective vascular integrity via de-repression of angiogenic signaling pathways. Specifically, miR-126 directly targets Spred1 and p85β/PIK3R2, both inhibitors of the VEGF signaling pathway (*67, 68*). Two reports also indicate that miR-126 can regulate Egfl7 expression directly or indirectly, in non-small cell lung cancer cells (*71*) or in HUVECs, respectively (*68*).

Collectively, several groups have demonstrated an important role for both Egfl7 and miR-126 during formation of a functional vasculature, and it is plausible that both cooperate to achieve this result.

1.9 – Egfl7 signaling pathways

Egfl7 has been shown to be directly regulated by GATA2 and ERG in endothelial cells through GATA and ETS- binding sites located in the proximal promoter region (*72*). Both binding sites are common to many genes of early blood and endothelial development (*73*). Two evolutionarily conserved ETS binding sites are located in the 5.4kb promoter region upstream of the Egfl7 transcriptional start site, the minimal region demonstrated as sufficient to drive expression of Egfl7 during embryogenesis (*67*). The Egfl7 promoter also contains a GATA2 consensus binding site (*72*). A recent study has elucidated that the zinc transcription factor, CASZ1, directly regulates and activates Egfl7 *in vitro* and in Xenopus embryos to control tubulogenesis (*50*).

Downstream, Egfl7 executes its role in blood vessel development through modulation of the Notch signaling pathway (*40, 49*). Notch signaling is important for vascular development, specifically playing a role in sprouting, branching, and proliferation (*10*). EGFL7 interacts with NOTCH1 and NOTCH4, as well as their ligand, DLL4, suggesting that EGFL7 can block NOTCH ligand-receptor binding. EGFL7 modulates Notch signaling differentially, depending on the vascular bed. Egfl7 acts as a Notch agonist in developing embryos (*40*). On the other hand, overexpression of Egfl7 in endothelial cells *in vitro* represses Notch reporter activity and inhibits Jagged1/Jagged2-mediated Notch activation (*40, 49*). Furthermore, endothelial overexpression of Egfl7 in the postnatal retina results in reduction of Notch target gene expression, or actions as a Notch antagonist (*40*). The phenotype observed in the postnatal retina of Egfl7 gain-of-function mice mildly, yet incompletely, recapitulates Notch loss-of-function (*40*). These results suggest that Egfl7 refines Notch signaling and may act, at least in part, through additional signaling pathways to exert an important function during blood vessel development.

Several studies have demonstrated that Egfl7 promotes cell migration and invasion through activation of the Epidermal Growth Factor Receptor (EGFR) signaling pathway in cancer cells (*57, 74*). In hepatocellular carcinoma, EGFL7 promotes EGFR-mediated FAK activation, while EGFL7 in gastric cancer cells stimulates EGFR-AKT signaling and thus epithelial-mesenchymal transition (*57, 74*).

EGFL7 may function through autocrine or paracrine pathways, or both. EGFL7 is tightly associated with the ECM and known to affect the spatial organization of endothelial cells. This could result from EGFL7 secretion affecting signaling on the same cell, neighboring endothelial cells, or both. Additionally, EGFL7's

modulation of NOTCH signaling involves interaction with the transmembrane bound ligands and receptors. However, EGFL7's association with the ECM would not provide enough force to activate Notch signaling itself, therefore it has been suggested that EGFL7 may block the interaction of Notch ligands and receptors that either activate or repress Notch receptor signaling (*40, 49*), and this can be performed on cells that secreted EGFL7 or on neighboring cells.

1.10 – Summary and Significance

EGFL7 plays a critical role in the development of a functional, hierarchal vascular system, particularly during embryogenesis and during physiological and pathological angiogenesis. Dysregulated and abnormal vascularization contributes to the development and progression of many diseases, including tumorigenesis. Irregularly patterned vessels impair perfusion and thus oxygen and nutrient delivery to tissues. Despite numerous efforts to elucidate the mechanisms controlling developmental and pathological blood vessel formation, the detailed molecular mechanisms and regulatory factors remain incomplete.

The function of the endocrine system is to produce and secrete hormones, and thus requires a well-defined vascular network. Two endocrine organs that require tightly regulated vascular patterning and development are the pancreas and the placenta. Disruptions in the signaling pathways involved in their organogenesis may result in pathologies such as diabetes mellitus or preeclampsia. It is important to elucidate the molecular mechanisms controlling normal development in order to better understand the pathophysiology and potential treatments of disease states.

Due to the functional role of *Egfl7* during developmental and physiological angiogenesis, and the important role of the vasculature in the pancreas and the placenta, we hypothesized that *Egfl7* plays an important role in their development. To test this, I utilized *Egfl7* gain- and loss-of-function mice, as well as a mouse model of PE. In this dissertation, I describe the effect of modulation of Egfl7 on the development of both the pancreas and the placenta, and investigate the significance and implications of alterations of Egfl7 during development of these vascular organs. Importantly, to address the complication of the embedded microRNA within the Egfl7 transcript, miR-126 levels are unchanged in all models used for these studies.

Secreted factors from the endothelium have been shown to support and induce pancreatic organogenesis (*75, 76*). In chapter two, I will demonstrate the effect of endothelial-specific overexpression of Egfl7 on pancreatic development in the mouse. Using confocal microscopy imaging techniques, I will reveal a functional role for endothelial EGFL7 in pancreatic progenitor cells in the mouse embryo.

Furthermore, placental development requires formation of a dense fetal capillary network bathed in maternal blood delivered by remodeled maternal spiral arteries. Tightly regulated angiogenic signaling is required for these processes. Indeed, dysregulated angiogenic signaling and aberrantly vascularized placentas have been implicated in placental pathologies, such as preeclampsia (PE). In chapters 3 and 4, I will demonstrate a role for EGFL7 in normal and pathological placental development. Using a mouse model of PE and a global Egfl7-knockout mouse, I will reveal the spatiotemporal expression profile of Egfl7 in normal and PE placentas, and define the function of EGFL7 in formation of the densely patterned fetal vasculature.

REFERENCES

1. W. Risau, Mechanisms of angiogenesis. *Nature* **386**, 671-674 (1997).
2. P. Carmeliet, Mechanisms of angiogenesis and arteriogenesis. *Nat Med* **6**, 389-395 (2000).
3. M. Potente, H. Gerhardt, P. Carmeliet, Basic and therapeutic aspects of angiogenesis. *Cell* **146**, 873-887 (2011).
4. V. L. Bautch, VEGF-directed blood vessel patterning: from cells to organism. *Cold Spring Harb Perspect Med* **2**, a006452 (2012).
5. P. Carmeliet, V. Ferreira, G. Breier, S. Pollefeyt, L. Kieckens, M. Gertsenstein, M. Fahrig, A. Vandenhoeck, K. Harpal, C. Eberhardt, C. Declercq, J. Pawling, L. Moons, D. Collen, W. Risau, A. Nagy, Abnormal blood vessel development and lethality in embryos lacking a single VEGF allele. *Nature* **380**, 435-439 (1996).
6. N. Ferrara, K. Carver-Moore, H. Chen, M. Dowd, L. Lu, K. S. O'Shea, L. Powell-Braxton, K. J. Hillan, M. W. Moore, Heterozygous embryonic lethality induced by targeted inactivation of the VEGF gene. *Nature* **380**, 439-442 (1996).
7. F. Shalaby, J. Ho, W. L. Stanford, K. D. Fischer, A. C. Schuh, L. Schwartz, A. Bernstein, J. Rossant, A requirement for Flk1 in primitive and definitive hematopoiesis and vasculogenesis. *Cell* **89**, 981-990 (1997).
8. G. H. Fong, J. Rossant, M. Gertsenstein, M. L. Breitman, Role of the Flt-1 receptor tyrosine kinase in regulating the assembly of vascular endothelium. *Nature* **376**, 66-70 (1995).
9. H. M. Eilken, R. H. Adams, Dynamics of endothelial cell behavior in sprouting angiogenesis. *Curr Opin Cell Biol* **22**, 617-625 (2010).
10. L. K. Phng, H. Gerhardt, Angiogenesis: a team effort coordinated by notch. *Dev Cell* **16**, 196-208 (2009).
11. P. Carmeliet, Angiogenesis in health and disease. *Nat Med* **9**, 653-660 (2003).
12. F. De Smet, I. Segura, K. De Bock, P. J. Hohensinner, P. Carmeliet, Mechanisms of vessel branching: filopodia on endothelial tip cells lead the way. *Arterioscler Thromb Vasc Biol* **29**, 639-649 (2009).
13. L. Jakobsson, C. A. Franco, K. Bentley, R. T. Collins, B. Ponsioen, I. M. Aspalter, I. Rosewell, M. Busse, G. Thurston, A. Medvinsky, S. Schulte-Merker, H. Gerhardt, Endothelial cells dynamically compete for the tip cell position during angiogenic sprouting. *Nat Cell Biol* **12**, 943-953 (2010).
14. M. Hellström, L. K. Phng, J. J. Hofmann, E. Wallgard, L. Coultas, P. Lindblom, J. Alva, A. K. Nilsson, L. Karlsson, N. Gaiano, K. Yoon, J. Rossant, M. L. Iruela-Arispe, M. Kalén, H. Gerhardt, C. Betsholtz, Dll4

signalling through Notch1 regulates formation of tip cells during angiogenesis. *Nature* **445**, 776-780 (2007).
15. M. L. Iruela-Arispe, G. E. Davis, Cellular and molecular mechanisms of vascular lumen formation. *Dev Cell* **16**, 222-231 (2009).
16. M. Zeeb, B. Strilic, E. Lammert, Resolving cell-cell junctions: lumen formation in blood vessels. *Curr Opin Cell Biol* **22**, 626-632 (2010).
17. A. C. Zovein, A. Luque, K. A. Turlo, J. J. Hofmann, K. M. Yee, M. S. Becker, R. Fassler, I. Mellman, T. F. Lane, M. L. Iruela-Arispe, Beta1 integrin establishes endothelial cell polarity and arteriolar lumen formation via a Par3-dependent mechanism. *Dev Cell* **18**, 39-51 (2010).
18. S. P. Herbert, D. Y. Stainier, Molecular control of endothelial cell behaviour during blood vessel morphogenesis. *Nat Rev Mol Cell Biol* **12**, 551-564 (2011).
19. K. Xu, A. Sacharidou, S. Fu, D. C. Chong, B. Skaug, Z. J. Chen, G. E. Davis, O. Cleaver, Blood vessel tubulogenesis requires Rasip1 regulation of GTPase signaling. *Dev Cell* **20**, 526-539 (2011).
20. E. A. Jones, F. le Noble, A. Eichmann, What determines blood vessel structure? Genetic prespecification vs. hemodynamics. *Physiology (Bethesda)* **21**, 388-395 (2006).
21. M. R. Swift, B. M. Weinstein, Arterial-venous specification during development. *Circ Res* **104**, 576-588 (2009).
22. H. U. Wang, Z. F. Chen, D. J. Anderson, Molecular distinction and angiogenic interaction between embryonic arteries and veins revealed by ephrin-B2 and its receptor Eph-B4. *Cell* **93**, 741-753 (1998).
23. A. Armulik, A. Abramsson, C. Betsholtz, Endothelial/pericyte interactions. *Circ Res* **97**, 512-523 (2005).
24. P. Lindahl, B. R. Johansson, P. Levéen, C. Betsholtz, Pericyte loss and microaneurysm formation in PDGF-B-deficient mice. *Science* **277**, 242-245 (1997).
25. H. G. Augustin, G. Y. Koh, G. Thurston, K. Alitalo, Control of vascular morphogenesis and homeostasis through the angiopoietin-Tie system. *Nat Rev Mol Cell Biol* **10**, 165-177 (2009).
26. T. N. Sato, Y. Tozawa, U. Deutsch, K. Wolburg-Buchholz, Y. Fujiwara, M. Gendron-Maguire, T. Gridley, H. Wolburg, W. Risau, Y. Qin, Distinct roles of the receptor tyrosine kinases Tie-1 and Tie-2 in blood vessel formation. *Nature* **376**, 70-74 (1995).
27. C. Suri, P. F. Jones, S. Patan, S. Bartunkova, P. C. Maisonpierre, S. Davis, T. N. Sato, G. D. Yancopoulos, Requisite role of angiopoietin-1, a ligand for the TIE2 receptor, during embryonic angiogenesis. *Cell* **87**, 1171-1180 (1996).
28. H. M. Fraser, S. F. Lunn, Angiogenesis and its control in the female reproductive system. *Br Med Bull* **56**, 787-797 (2000).
29. M. G. Tonnesen, X. Feng, R. A. Clark, Angiogenesis in wound healing. *J*

Investig Dermatol Symp Proc **5**, 40-46 (2000).
30. T. Gustafsson, W. E. Kraus, Exercise-induced angiogenesis-related growth and transcription factors in skeletal muscle, and their modification in muscle pathology. *Front Biosci* **6**, D75-89 (2001).
31. T. N. Crawford, D. V. Alfaro, J. B. Kerrison, E. P. Jablon, Diabetic retinopathy and angiogenesis. *Curr Diabetes Rev* **5**, 8-13 (2009).
32. E. M. Paleolog, J. M. Miotla, Angiogenesis in arthritis: role in disease pathogenesis and as a potential therapeutic target. *Angiogenesis* **2**, 295-307 (1998).
33. S. M. Weis, D. A. Cheresh, Tumor angiogenesis: molecular pathways and therapeutic targets. *Nat Med* **17**, 1359-1370 (2011).
34. M. J. Fitch, L. Campagnolo, F. Kuhnert, H. Stuhlmann, Egfl7, a novel epidermal growth factor-domain gene expressed in endothelial cells. *Dev Dyn* **230**, 316-324 (2004).
35. F. Soncin, V. Mattot, F. Lionneton, N. Spruyt, F. Lepretre, A. Begue, D. Stehelin, VE-statin, an endothelial repressor of smooth muscle cell migration. *EMBO J* **22**, 5700-5711 (2003).
36. L. H. Parker, M. Schmidt, S. W. Jin, A. M. Gray, D. Beis, T. Pham, G. Frantz, S. Palmieri, K. Hillan, D. Y. Stainier, F. J. De Sauvage, W. Ye, The endothelial-cell-derived secreted factor Egfl7 regulates vascular tube formation. *Nature* **428**, 754-758 (2004).
37. I. Nikolic, N. D. Stankovic, F. Bicker, J. Meister, H. Braun, K. Awwad, J. Baumgart, K. Simon, S. C. Thal, C. Patra, P. N. Harter, K. H. Plate, F. B. Engel, S. Dimmeler, J. A. Eble, M. Mittelbronn, M. K. Schäfer, B. Jungblut, E. Chavakis, I. Fleming, M. H. Schmidt, EGFL7 ligates αvβ3 integrin to enhance vessel formation. *Blood* **121**, 3041-3050 (2013).
38. M. Schmidt, K. Paes, A. De Mazière, T. Smyczek, S. Yang, A. Gray, D. French, I. Kasman, J. Klumperman, D. S. Rice, W. Ye, EGFL7 regulates the collective migration of endothelial cells by restricting their spatial distribution. *Development* **134**, 2913-2923 (2007).
39. L. Campagnolo, I. Moscatelli, M. Pellegrini, G. Siracusa, H. Stuhlmann, Expression of EGFL7 in primordial germ cells and in adult ovaries and testes. *Gene Expr Patterns* **8**, 389-396 (2008).
40. D. Nichol, C. Shawber, M. J. Fitch, K. Bambino, A. Sharma, J. Kitajewski, H. Stuhlmann, Impaired angiogenesis and altered Notch signaling in mice overexpressing endothelial Egfl7. *Blood* **116**, 6133-6143 (2010).
41. K. Bambino, L. A. Lacko, K. A. Hajjar, H. Stuhlmann, Epidermal growth factor-like domain 7 is a marker of the endothelial lineage and active angiogenesis. *Genesis* **52**, 657-670 (2014).
42. N. Kabrun, H. J. Bühring, K. Choi, A. Ullrich, W. Risau, G. Keller, Flk-1 expression defines a population of early embryonic hematopoietic precursors. *Development* **124**, 2039-2048 (1997).

43. L. Campagnolo, A. Leahy, S. Chitnis, S. Koschnick, M. J. Fitch, J. T. Fallon, D. Loskutoff, M. B. Taubman, H. Stuhlmann, EGFL7 is a chemoattractant for endothelial cells and is up-regulated in angiogenesis and arterial injury. *Am J Pathol* **167**, 275-284 (2005).
44. M. V. Badiwala, L. C. Tumiati, J. M. Joseph, R. Sheshgiri, H. J. Ross, D. H. Delgado, V. Rao, Epidermal growth factor-like domain 7 suppresses intercellular adhesion molecule 1 expression in response to hypoxia/reoxygenation injury in human coronary artery endothelial cells. *Circulation* **122**, S156-161 (2010).
45. C. Fan, L. Y. Yang, F. Wu, Y. M. Tao, L. S. Liu, J. F. Zhang, Y. N. He, L. L. Tang, G. D. Chen, L. Guo, The expression of Egfl7 in human normal tissues and epithelial tumors. *Int J Biol Markers* **28**, 71-83 (2013).
46. S. Gao, X. Yang, S. Li, Q. Tang, [The study on clinical significance of the expression of EGFL7 in laryngeal squamous cell carcinoma]. *Lin Chung Er Bi Yan Hou Tou Jing Wai Ke Za Zhi* **27**, 147-150 (2013).
47. G. Philippin-Lauridant, M. C. Baranzelli, C. Samson, C. Fournier, S. Pinte, V. Mattot, J. Bonneterre, F. Soncin, Expression of Egfl7 correlates with low-grade invasive lesions in human breast cancer. *Int J Oncol* **42**, 1367-1375 (2013).
48. A. Durrans, H. Stuhlmann, A role for Egfl7 during endothelial organization in the embryoid body model system. *J Angiogenes Res* **2**, 4 (2010).
49. M. H. Schmidt, F. Bicker, I. Nikolic, J. Meister, T. Babuke, S. Picuric, W. Müller-Esterl, K. H. Plate, I. Dikic, Epidermal growth factor-like domain 7 (EGFL7) modulates Notch signalling and affects neural stem cell renewal. *Nat Cell Biol* **11**, 873-880 (2009).
50. M. S. Charpentier, K. S. Christine, N. M. Amin, K. M. Dorr, E. J. Kushner, V. L. Bautch, J. M. Taylor, F. L. Conlon, CASZ1 promotes vascular assembly and morphogenesis through the direct regulation of an EGFL7/RhoA-mediated pathway. *Dev Cell* **25**, 132-143 (2013).
51. E. Lelièvre, A. Hinek, F. Lupu, C. Buquet, F. Soncin, V. Mattot, VE-statin/egfl7 regulates vascular elastogenesis by interacting with lysyl oxidases. *EMBO J* **27**, 1658-1670 (2008).
52. P. Bornstein, Matricellular proteins: an overview. *J Cell Commun Signal* **3**, 163-165 (2009).
53. A. De Mazière, L. Parker, S. Van Dijk, W. Ye, J. Klumperman, Egfl7 knockdown causes defects in the extension and junctional arrangements of endothelial cells during zebrafish vasculogenesis. *Dev Dyn* **237**, 580-591 (2008).
54. M. Gustavsson, C. Mallard, S. J. Vannucci, M. A. Wilson, M. V. Johnston, H. Hagberg, Vascular response to hypoxic preconditioning in the immature brain. *J Cereb Blood Flow Metab* **27**, 928-938 (2007).
55. M. V. Badiwala, D. Guha, L. Tumiati, J. Joseph, A. Ghashghai, H. J.

Ross, D. H. Delgado, V. Rao, Epidermal growth factor-like domain 7 is a novel inhibitor of neutrophil adhesion to coronary artery endothelial cells injured by calcineurin inhibition. *Circulation* **124**, S197-203 (2011).
56. D. Xu, R. E. Perez, I. I. Ekekezie, A. Navarro, W. E. Truog, Epidermal growth factor-like domain 7 protects endothelial cells from hyperoxia-induced cell death. *Am J Physiol Lung Cell Mol Physiol* **294**, L17-23 (2008).
57. F. Wu, L. Y. Yang, Y. F. Li, D. P. Ou, D. P. Chen, C. Fan, Novel role for epidermal growth factor-like domain 7 in metastasis of human hepatocellular carcinoma. *Hepatology* **50**, 1839-1850 (2009).
58. S. B. Pinte, F. Soncin, Egfl7 promotes tumor escape from immunity. *Oncoimmunology* **1**, 375-376 (2012).
59. S. Delfortrie, S. Pinte, V. Mattot, C. Samson, G. Villain, B. Caetano, G. Lauridant-Philippin, M. C. Baranzelli, J. Bonneterre, F. Trottein, C. Faveeuw, F. Soncin, Egfl7 promotes tumor escape from immunity by repressing endothelial cell activation. *Cancer Res* **71**, 7176-7186 (2011).
60. L. Zhou, J. Li, Y. P. Zhao, J. C. Guo, Q. C. Cui, W. X. Zhou, T. P. Zhang, W. M. Wu, L. You, H. Shu, Prognostic significance of epidermal growth factor-like domain 7 in pancreatic cancer. *Hepatobiliary Pancreat Dis Int* **13**, 523-528 (2014).
61. C. H. Huang, X. J. Li, Y. Z. Zhou, Y. Luo, C. Li, X. R. Yuan, Expression and clinical significance of EGFL7 in malignant glioma. *J Cancer Res Clin Oncol* **136**, 1737-1743 (2010).
62. J. Oh, S. H. Park, T. S. Lee, H. K. Oh, J. H. Choi, Y. S. Choi, High expression of epidermal growth factor-like domain 7 is correlated with poor differentiation and poor prognosis in patients with epithelial ovarian cancer. *J Gynecol Oncol* **25**, 334-341 (2014).
63. J. J. Li, X. M. Yang, S. H. Wang, Q. L. Tang, Prognostic role of epidermal growth factor-like domain 7 protein expression in laryngeal squamous cell carcinoma. *J Laryngol Otol* **125**, 1152-1157 (2011).
64. X. Wang, X. Yao, X. Ji, J. Chen, L. Li, H. Zhu, [Construction of lentivirus vector of interference of EGFL7 gene and its inhibitive role on the invasion of laryngeal cancer cell]. *Lin Chung Er Bi Yan Hou Tou Jing Wai Ke Za Zhi* **25**, 1135-1138, 1141 (2011).
65. L. Johnson, M. Huseni, T. Smyczek, A. Lima, S. Yeung, J. H. Cheng, R. Molina, D. Kan, A. De Mazière, J. Klumperman, I. Kasman, Y. Zhang, M. S. Dennis, J. Eastham-Anderson, A. M. Jubb, O. Hwang, R. Desai, M. Schmidt, M. A. Nannini, K. H. Barck, R. A. Carano, W. F. Forrest, Q. Song, D. S. Chen, L. Naumovski, M. Singh, W. Ye, P. S. Hegde, Anti-EGFL7 antibodies enhance stress-induced endothelial cell death and anti-VEGF efficacy. *J Clin Invest* **123**, 3997-4009 (2013).
66. F. Kuhnert, M. R. Mancuso, J. Hampton, K. Stankunas, T. Asano, C. Z. Chen, C. J. Kuo, Attribution of vascular phenotypes of the murine Egfl7

locus to the microRNA miR-126. *Development* **135**, 3989-3993 (2008).
67. S. Wang, A. B. Aurora, B. A. Johnson, X. Qi, J. McAnally, J. A. Hill, J. A. Richardson, R. Bassel-Duby, E. N. Olson, The endothelial-specific microRNA miR-126 governs vascular integrity and angiogenesis. *Dev Cell* **15**, 261-271 (2008).
68. J. E. Fish, M. M. Santoro, S. U. Morton, S. Yu, R. F. Yeh, J. D. Wythe, K. N. Ivey, B. G. Bruneau, D. Y. Stainier, D. Srivastava, miR-126 regulates angiogenic signaling and vascular integrity. *Dev Cell* **15**, 272-284 (2008).
69. Y. Zhao, D. Srivastava, A developmental view of microRNA function. *Trends Biochem Sci* **32**, 189-197 (2007).
70. S. Nicoli, C. Standley, P. Walker, A. Hurlstone, K. E. Fogarty, N. D. Lawson, MicroRNA-mediated integration of haemodynamics and Vegf signalling during angiogenesis. *Nature* **464**, 1196-1200 (2010).
71. Y. Sun, Y. Bai, F. Zhang, Y. Wang, Y. Guo, L. Guo, miR-126 inhibits non-small cell lung cancer cells proliferation by targeting EGFL7. *Biochem Biophys Res Commun* **391**, 1483-1489 (2010).
72. A. Le Bras, C. Samson, M. Trentini, B. Caetano, E. Lelievre, V. Mattot, F. Beermann, F. Soncin, VE-statin/egfl7 expression in endothelial cells is regulated by a distal enhancer and a proximal promoter under the direct control of Erg and GATA-2. *PLoS One* **5**, e12156 (2010).
73. I. J. Donaldson, M. Chapman, S. Kinston, J. R. Landry, K. Knezevic, S. Piltz, N. Buckley, A. R. Green, B. Göttgens, Genome-wide identification of cis-regulatory sequences controlling blood and endothelial development. *Hum Mol Genet* **14**, 595-601 (2005).
74. B. H. Luo, F. Xiong, J. P. Wang, J. H. Li, M. Zhong, Q. L. Liu, G. Q. Luo, X. J. Yang, N. Xiao, B. Xie, H. Xiao, R. J. Liu, C. S. Dong, K. S. Wang, J. F. Wen, Epidermal growth factor-like domain-containing protein 7 (EGFL7) enhances EGF receptor-AKT signaling, epithelial-mesenchymal transition, and metastasis of gastric cancer cells. *PLoS One* **9**, e99922 (2014).
75. D. Eberhard, M. Kragl, E. Lammert, 'Giving and taking': endothelial and beta-cells in the islets of Langerhans. *Trends Endocrinol Metab* **21**, 457-463 (2010).
76. E. Lammert, O. Cleaver, D. Melton, Induction of pancreatic differentiation by signals from blood vessels. *Science* **294**, 564-567 (2001).

Chapter 2 – Endothelial Cells Control Pancreatic Cell Fate at Defined Stages through EGFL7 Signaling[*†]

2.1 – Rationale

The mammalian pancreas regulates blood glucose homeostasis and arises from the fusion of ventral and dorsal buds. Signaling from blood vessels directs growth, morphogenesis, and differentiation throughout pancreatic organogenesis (*1*). Step-wise inductive events occur to pattern and differentiate the pancreas. The pancreas develops from *Pdx1*-positive foregut endoderm, initiated at the contact site between the notochord and the dorsal endoderm at embryonic day (E)9.0 (*2, 3*). *Pdx1*, or Pancreatic and Duodenal Homeobox gene-1, is essential for pancreatic morphogenesis, as evidenced by apancreatic Pbx1-null mice (*3, 4*). Following fusion of the dorsal aortae and contact with the *Pdx1*-positive foregut endoderm, pancreatic buds begin to evaginate, and endocrine cell differentiation initiates (*1*). The splanchnic mesoderm containing small vessels then separates the dorsal aorta from the foregut endoderm. Insulin expression is upregulated at contact sites with the portal vein at E10.5 (*1*). At E11.5, the gut tube begins to rotate, bringing the dorsal and ventral pancreatic buds in close proximity for fusion (*5*). Subsequent branching morphogenesis and remodeling processes in addition to differentiation along the three pancreatic lineages occurs to form an arborized,

---

[*] Kao D, **Lacko LA**, Ding B, Huang C, Phung K, Gu G, Rafii S, Stuhlmann H, and Chen S. Endothelial Cells Control Pancreatic Cell Fate at Defined Stages through EGFL7 Signaling. *Stem Cell Reports,* 4(2):181-9 (2015).

[†] *NOTE:* Human studies, *in vitro* studies, and explant studies were performed by Kao D, Ding B, Huang C, Phung K, Gu G, Rafii S, and Chen S.

mature pancreas (*5*). The mature pancreatic endocrine cells make up the Islets of Langerhans, which are established after birth and are tightly associated with blood vessels (*1, 6*).

Early seminal studies demonstrate the critical role of blood vessel signaling during pancreatic organogenesis. First, insulin expression and epithelial buds were induced by recombined aortic endothelium but not by the notochord in pre-patterned dorsal endoderm (*1*). Next, removal of the aorta from *Xenopus* embryos fails to induce endocrine gene expression. Moreover, ectopic insulin expressing cells and epithelial buds were found in the posterior stomach epithelium, adjacent to ectopic endothelial cells of mice expressing VEGF-A under control of the *Pdx1* promoter (*1*). Several animal studies have since begun to elucidate the precise mechanism by which endothelial cells control pancreatic development. For example, interaction of aortic endothelial cells with the dorsal pancreatic bud stimulates Ptf1a expression and early pancreatic growth (*7*). Endothelial cell ablation and forced hypervascularization experiments demonstrate a role for blood vessels in controlling pancreas size via branching morphogenesis and differentiation of early endocrine progenitor cells, in part through modulation of the Notch signaling pathway (*8*).

Understanding the diverse, instructive steps required for pancreatic organogenesis in the mouse will have implications for translation to humans in order to study the mechanism of disease progression and to develop functional pancreatic endocrine cells for transplantation treatment of pancreatic diseases such as diabetes. Diabetes is characterized by chronic hyperglycemia resulting

from defects in production or action of insulin, which over time can seriously damage other tissues in the body (*9*). Its prevalence is predicted to double by the year 2030, resulting in the classification as a potential epidemic (*10*). Thus, the need for models of disease progression and the development of successful therapeutic treatments is essential. Dissecting the cellular biological and molecular mechanisms of pancreatic development in the mouse has contributed to the development of cell replacement therapies. Specifically, researchers have established controlled conditions *in vitro* to differentiate human embryonic stem cells (hESC) and induced pluripotent stem cells (iPSCs) into functional, insulin-producing beta cells (*11*), but strategies remain inefficient.

The laboratory of Dr. Shuibing Chen established that secreted factors from endothelial cells affect pancreatic progenitor cell self-renewal during directed differentiation of hESCs into beta cells (*12*). Indeed, they discovered that EGFL7 was the only factor that could alone promote pancreatic progenitor cell proliferation (*12*). In this chapter, I will demonstrate a stage-dependent role for *Epidermal growth factor like domain 7* (*Egfl7)* in pancreatic growth and development *in vivo*, using a transgenic mouse overexpressing Egfl7 under the control of the Tie2 promoter. Results of these studies and those of Kao *et al* demonstrate that Egfl7 controls pancreatic cell fate at the progenitor cell stage both *in vivo* and *in vitro*, and can be used to increase the efficiency of producing large numbers of pancreatic endocrine cells, which can potentially be applied to future transplantation studies (*12*).

2.2 – Abstract

Although endothelial cells have been shown to affect mouse pancreatic development, their precise function in human development remains unclear. Using a co-culture system containing human embryonic stem cell (hESC)-derived progenitors and endothelial cells, we found that endothelial cells play a stage-dependent role in pancreatic development, in which they maintain pancreatic progenitor (PP) self-renewal and impair further differentiation into hormone-expressing cells. The mechanistic studies suggest that the endothelial cells act through the secretion of EGFL7. Consistently, endothelial overexpression of EGFL7 *in vivo* using a transgenic mouse model resulted in an increase of PP proliferation rate and a decrease of differentiation toward endocrine cells. These studies not only identified the novel role of EGFL7 as the molecular handle involved in the crosstalk between endothelium and pancreatic epithelium, but also provide a paradigm for using hESC stepwise differentiation to dissect the stage-dependent roles of signals controlling organogenesis.

2.3 – Introduction

During embryonic development, cell fate is determined by both intrinsic programs and the external cell niche. The animal studies suggested that the endothelial cell niche provides both supportive and inductive roles throughout pancreas development (*6*). Early studies showed that signals from endothelial cells are essential for the induction of pancreatic organogenesis (*1*).

Endothelial cells specifically promote early dorsal pancreas development by inducing Ptf1a^{+} pancreatic progenitors (PPs) by activating FGF10 signaling (*7*) (*13*). Interestingly, some groups recently reported that the endothelial cell niche could restrain epithelium branching and endocrine development. One group showed that blood vessel ablation results in increased pancreatic organ size (*14*). Another group showed that elimination of endothelial cells increases the size of pancreatic buds (*8*). Similarly, another group showed that over-expressing VEGF-A increases embryonic endothelial cell populations and perturbs pancreatic endocrine differentiation (*15*). However, a complete understanding of the role of endothelial cells in human pancreatic development is still missing.

Human embryonic stem cells (hESCs) provide an *in vitro* platform to study human development. To better understand the signaling from the endothelial cell niche in pancreatic differentiation, we have developed a co-culture system of endothelial cells with hESC-derived progenitors under serum-free, chemically-defined conditions. By using the co-culture system, we found that endothelial cells maintain PP self-renewal and impair further differentiation into hormone-expressing cells by secreting EGFL7.

2.4 – Results and Discussion

2.4.1 – Endothelial cells promote the proliferation of PDX1^{+} cells in the chemically defined environment.

To systematically probe the role of an endothelial cell niche in human pancreatic development, we set up a co-culture system using endothelial cells and hESC-derived progenitors. The co-culture system is established in a chemically defined culture condition to mimic the serum-free environment during embryonic development. The endothelial cells used in this study were AKT-HUVECs (AKT-activated human umbilical vein endothelial cells) (*16*) or MPECs (mouse pancreas islet endothelial cells). BJ cells, which are human skin fibroblasts, were used as a control for cell type specificity. To explore the stage-dependent effect of endothelial cells, HUES8 cells were differentiated into three different stages: definitive endoderm (DE), foregut endoderm (FE), or PP populations, using a previously established strategy (*17*). The hESC-derived populations were cultured together with MPECs or AKT-HUVECs at different ratios and examined for their capacities to self-renew or differentiate (**Figure 2.1A**). The self-renewal ability was determined by immunostaining with antibodies against a proliferation marker (Ki67) and stage dependent self-renewal markers, including SOX17 for DE, HNF4α for FE, and PDX1 for PPs. The differentiation ability was determined by immunostaining with antibodies against differentiation markers, including HNF4α for DE, PDX1 for FE, and insulin/glucagon/somatostatin for PPs.

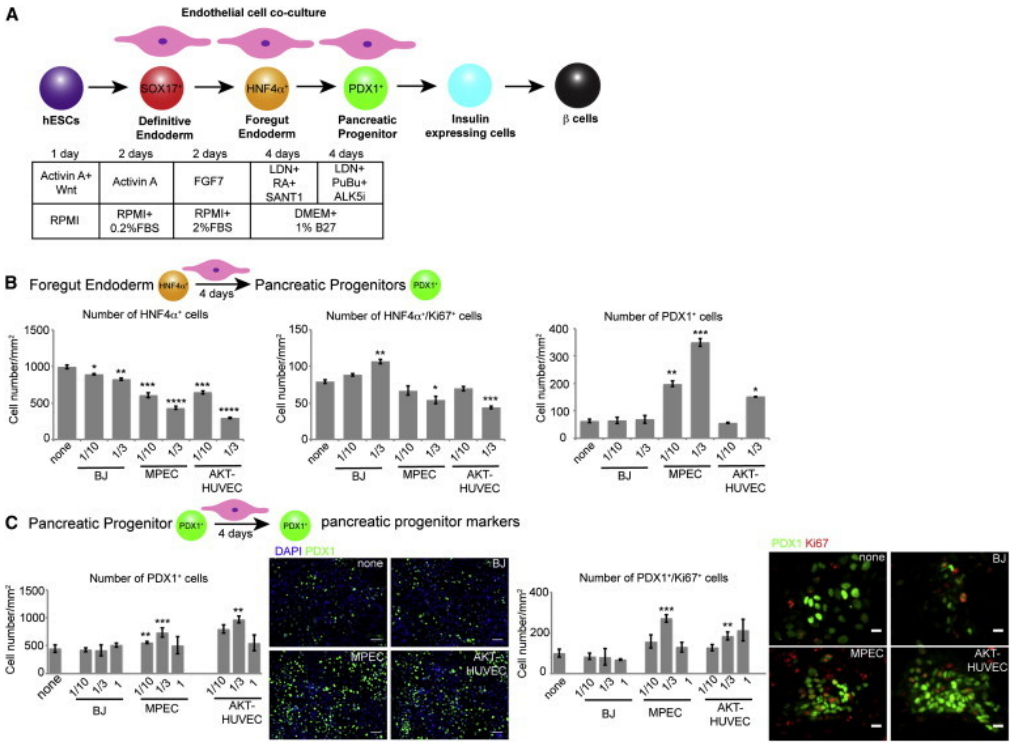

Figure 2.1 The Role of Endothelial Cells in Human Pancreatic Differentiation. (A) Scheme of co-culture between endothelial cells and hESC-derived progenitors. (B) Cell number per mm^2 after HUES8-derived FE population were co-cultured with BJ cells, MPECs, or AKT-HUVECs at indicated ratios (n = 3). (C) Cell number per mm^2 (n = 3) and representative images after HUES8-derived PP population were co-cultured with BJ cells, MPECs or AKT-HUVECs. The left scale bar represents 50 µm. The right scale bar represents 10 µm. Data presented mean ± standard deviation in each independent experiment, and $*P < 0.05$, $**P < 0.01$, $***P < 0.001$, $****P < 0.0001$.

In the co-culture condition of MPECs or AKT-HUVECs with the hESC-derived DE population, neither the number of $SOX17^+/Ki67^+$ cells nor the number of $HNF4\alpha^+$ cells changed significantly (**Supplemental Figure 2.1A**), suggesting that endothelial cells do not affect either self-renewal or differentiation of DE. In the co-culture condition with the hESC-derived FE population, the number of $PDX1^+$ cells was significantly increased in the presence of MPECs and AKT-HUVECs, but not BJ cells (**Figure 2.1B**). In addition, when the hESC-derived PP population was cultured with MPECs and AKT-HUVECs, the number of $PDX1^+$ cells was significantly elevated as compared to BJ cells (**Figure 2.1C**). The results suggest that endothelial cells, not fibroblasts, promote the generation of $PDX1^+$ cells at the FE and PP stages.

Next, we asked if the generation of $PDX1^+$ cells is due to cell proliferation, by examining the proliferation marker Ki67. In co-cultures using the HUES8-derived PP population, the number of $PDX1^+/Ki67^+$ cells is significantly higher in the presence of MEPCs and AKT-HUVECs than control conditions (**Figure 2.1C**). To further validate that endothelial cells promote PP proliferation, we generated a transgenic *Pdx1*-EGFP HUES8 cell line, which contains the mouse *Pdx1* promoter driving expression of EGFP. The *Pdx1*-EGFP HUES8 cell line was validated by Flow Cytometry. After 14 days of differentiation, about 45% of cells were $EGFP^+$, most of which were positively stained by PDX1 antibody (**Supplemental Figure 2.1B**). *Pdx1*-$EGFP^+$ cells were sorted and co-cultured with MPECs, AKT-HUVECs, or BJ cells (**Supplemental Figure 2.1C**). The result confirmed that endothelial cells can support the isolated $PDX1^+$ cell proliferation. Interestingly, when we co-cultured the PP population with

endothelial cells, we observed that the differentiation of PPs to hormone-expressing cells was impaired (**Supplemental Figures 2.1D, E**). In addition, endothelial cells show similar capacities to increase the number of $PDX1^+$ cells and $PDX1^+/Ki67^+$ cells when co-cultured with H1-derived PP population (**Supplemental Figure 2.1F**), suggesting that the effect of endothelial cells is not hESC line dependent. These data together suggest that endothelial cells provide a niche to maintain proliferation and impair differentiation of $PDX1^+$ cells toward hormone-expressing cells.

2.4.2 – $PDX1^+$ cells after co-culture with endothelial cells retain PP signature gene expression.

To determine the cellular identity of $PDX1^+$ cells after co-culture with endothelial cells, cells were stained with other antibodies against progenitor markers. Immunocytochemistry suggested that most $PDX1^+$ cells grew in the presence of endothelial cells expressed PP markers, HNF6, SOX9 and FOXA2 and endocrine marker, NKX6.1 (**Figure 2.2A**). The quantified results suggest that the number of $PDX1^+/NKX6.1^+$ cells, $PDX1^+/FOXA2^+$ cells, $PDX1^+/HNF6^+$ cells and $PDX1^+/SOX9^+$ cells were higher in the endothelial cell co-culture conditions than in control cells (**Figure 2.2B**).We further tested the mRNA expression of PP markers (*FOXA2, HNF6*, and *SOX9*) and endocrine progenitor markers (*NKX6.1*, *NKX2.2* and *NGN3*) in the purified *Pdx1*-GFP^+ cells. qRT-PCR suggested that the expression of PP markers (*FOXA2*, *HNF6*, and *SOX9*, **Supplemental Figure 2.2B, D, E**) and endocrine progenitor markers (*NKX6.1*, **Supplemental Figure 2.2C**) in sorted *Pdx1*-$EGFP^+$ cells

Figure 2.2 The Cellular Identity of PDX1$^+$ PPs Expanded in Endothelial Cell Niche. (A) Representative figures of PDX1$^+$ cells co-stained with another PP marker, FOXA2, HNF6, or SOX9 and endocrine progenitor marker, NKX6.1 under co-culture conditions. Scale bar represents 50 μm. (B) Relative cell number of PDX1$^+$ cells co-stained with another progenitor marker (n = 3). The relative cell number normalized to control (none) as one. (C) Quantified results of the relative cell numbers of PDX1$^+$/Ki67$^+$ cells co-stained with another progenitor marker (n = 3). (D) Transcriptome analysis by RNA-seq of *Pdx1*-EGFP$^+$ cells before and after co-cultured with endothelial cells. The scatter plot showed mRNA expression level in sorted *Pdx1*-EGFP$^+$ cells before co-culture versus after co-culture with AKT-HUVECs (left) or after co-culture with BJ cells versus after co-culture with AKT-HUVECs (right). Data were presented as mean ± SD.

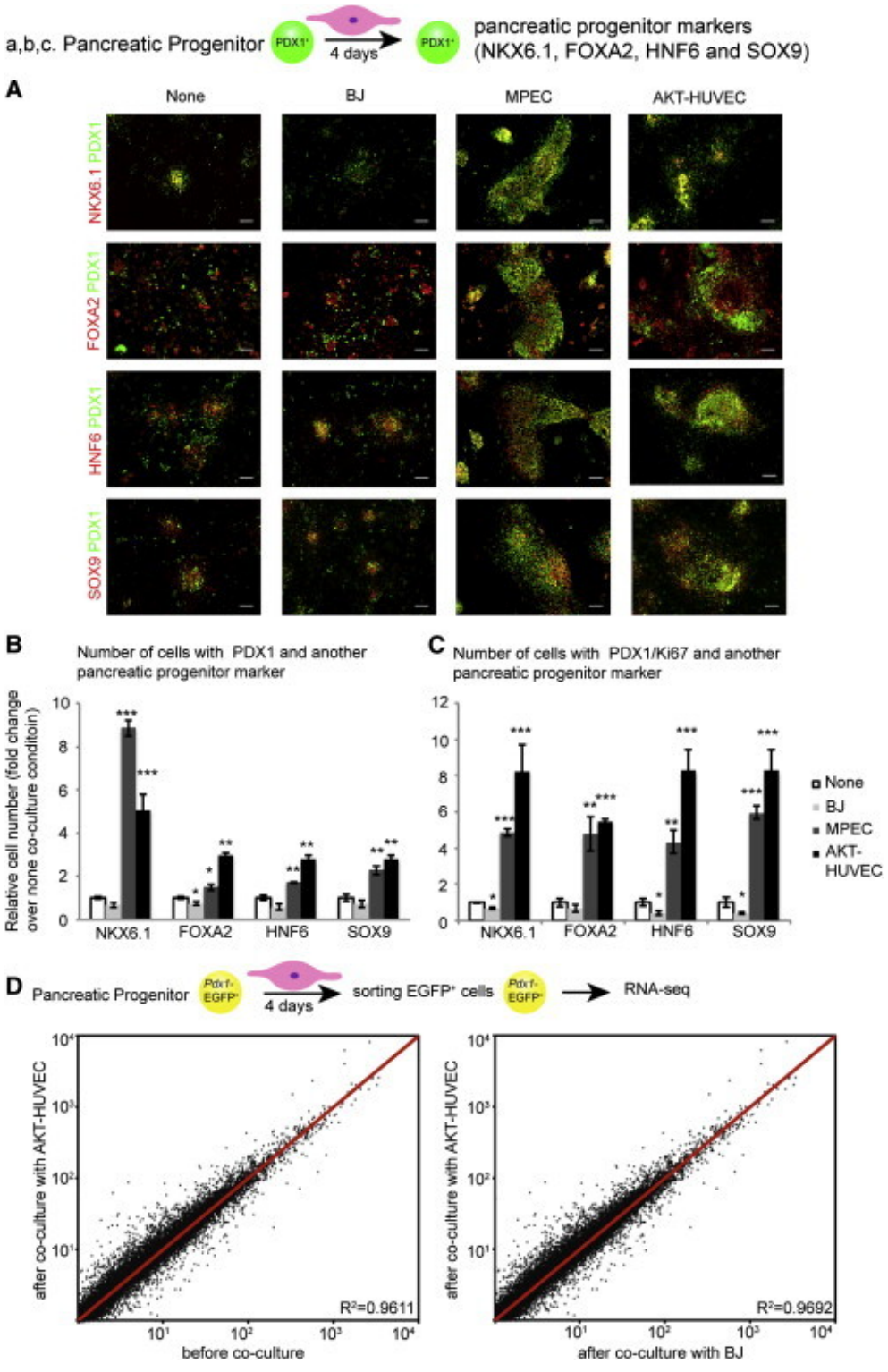
a,b,c. Pancreatic Progenitor
PDX1+
4 days
PDX1+
pancreatic progenitor markers
(NKX6.1, FOXA2, HNF6 and SOX9)
A
None
BJ
MPEC
AKT-HUVEC
NKX6.1 PDX1
FOXA2 PDX1
HNF6 PDX1
SOX9 PDX1
B
Number of cells with PDX1 and another pancreatic progenitor marker
Relative cell number (fold change over none co-culture conditoin)
NKX6.1
FOXA2
HNF6
SOX9
C
Number of cells with PDX1/Ki67 and another pancreatic progenitor marker
None
BJ
MPEC
AKT-HUVEC
D
Pancreatic Progenitor
Pdx1-EGFP+
4 days
sorting EGFP+ cells
Pdx1-EGFP+
RNA-seq
after co-culture with AKT-HUVEC
before co-culture
R²=0.9611
after co-culture with BJ
R²=0.9692

was elevated in MPEC co-culture condition; but the expression of endocrine progenitor markers (*NGN3* and *NKX2.2*, **Supplemental Figure 2.2F-G**) did not significantly differ between BJ and MPEC co-culture conditions (**Supplemental Figure 2.2F**, at day 4, P=0.1274 for none versus MPEC; P=0.8968 for BJ versus MPEC). It suggested that PDX1$^+$ cells after co-culture with endothelial cells bias to endocrine fate, but have not expressed the endocrine progenitor markers yet. Next, we investigated whether the increased PP population under co-culture conditions was due to cell proliferation by measuring the number of PDX1$^+$/Ki67 cells that are also positive for other PP markers (**Figure 2.2C**). When co-cultured with MPECs and AKT-HUVECs, the number of proliferating PPs increased about 5-fold and 6-8 fold, respectively, compared to none co-culture conditions. Sometimes, the number of the proliferating PPs in the presence of BJ cells was lower than none co-culture condition. This might be due to the high cell density in the co-culture condition, which might affect PP proliferation.

Transcriptome profiling provides a way to systematically compare gene expression in different cell populations. PPs before or after co-culture with endothelial cells were profiled by RNA-seq. To purify the PDX1$^+$ PPs, EGFP$^+$ cells were sorted from the *Pdx1*-EGFP HUES8 cell-derived cells before or after co-culture with MPECs or AKT-HUVECs. The global gene expression of PPs before and after co-culture with endothelial cells showed very high similarity (R^2=0.9611 in the presence of AKT-HUVECs, **Figure 2.2D** left; and R^2=0.9378 in the presence of MPECs, **Supplemental Figure 2.2A**). In addition, the global gene expression pattern of PPs expanded in the presence of either AKT-

HUVECs or BJ cells showed high similarity (R^2=0.9692, **Figure 2.2D** right). These data confirm that PPs maintain cellular identity after expansion by endothelial cells.

2.4.3 – Endothelial cells maintain human PP self-renewal by secreting EGFL7.

In the co-culture system, endothelial cells might function through a secreted factor(s) or by direct cell-cell contact. To test these possibilities, HUES8 cell-derived PP populations were treated with conditioned medium (*18*) collected from MPECs (MPEC-CM) or from AKT-HUVECs (AKT-HUVEC-CM). CM retained similar, but slightly lower activity compared to intact cells for promoting PP self-renewal (**Figure 2.3A**). This data suggests that endothelial cells function, at least in part, through a secreted factor(s). We further analyzed the gene expression profiles of AKT-HUVECs, MPECs and BJ cells to identify candidate secreted factors (**Figure 2.3B and Supplemental Figure 2.3A**). Genes encoding secreted proteins, whose expression in endothelial cells is at least 30-fold higher than in the BJ cells, were selected for further analysis. Among the genes encoding secreted molecules (**Supplemental Table 2.1**), we tested the abilities of recombinant proteins ANGPT2, EGFL7, CCL13, IL24, PLAU, DHH, and PDGFB to expand human PPs (**Figure 2.3C**). Only EGFL7 was able to promote PP proliferation (**Figure 2.3C, D, E**). To determine whether EGFL7 was required for the endothelial cell effect, we used shRNA to knockdown EGFL7 expression in AKT-HUVECs. EGFL7 mRNA expression level was decreased by about 63.5% in AKT-HUVECs infected with EGFL7

Figure 2.3 Endothelial Cells Promote PP Proliferation by Secretion of EGFL7. (A) Cell number per mm^2 4 days after HUES8-derived PPs were co-cultured with endothelial cells or treated with CM (n = 3). (B) Transcriptome analysis of gene expression in BJ cells and AKT-HUVECs by RNA-seq. The blue line indicates the cutoff line of a 30-fold increase in gene expression in AKT-HUVECs as compared with BJ cells. The red dot indicates EGFL7. (C) Number of $PDX1^+$ cells per mm^2 4 days after hESC-derived PPs were treated with different recombinant proteins (300 ng/ml) (n = 3). (D) $PDX1^+$ (left) or $PDX1^+/Ki67^+$ cell number per mm^2 (right) 4 days after HUES8-derived PPs were treated with CM or 300 ng/ml EGFL7 (n = 3). (E) Representative images of (D). (F) $PDX1^+/Ki67^+$ cell number per mm^2 4 days after HUES8-derived PPs were co-cultured with AKT-HUVECs carrying shRNA targeting EGFL7 (shRNA-EGFL7) or AKT-HUVECs carrying scrambled control shRNA (scrambled) (n = 3). (G) Representative images of (F). Data were presented as mean ± SD.

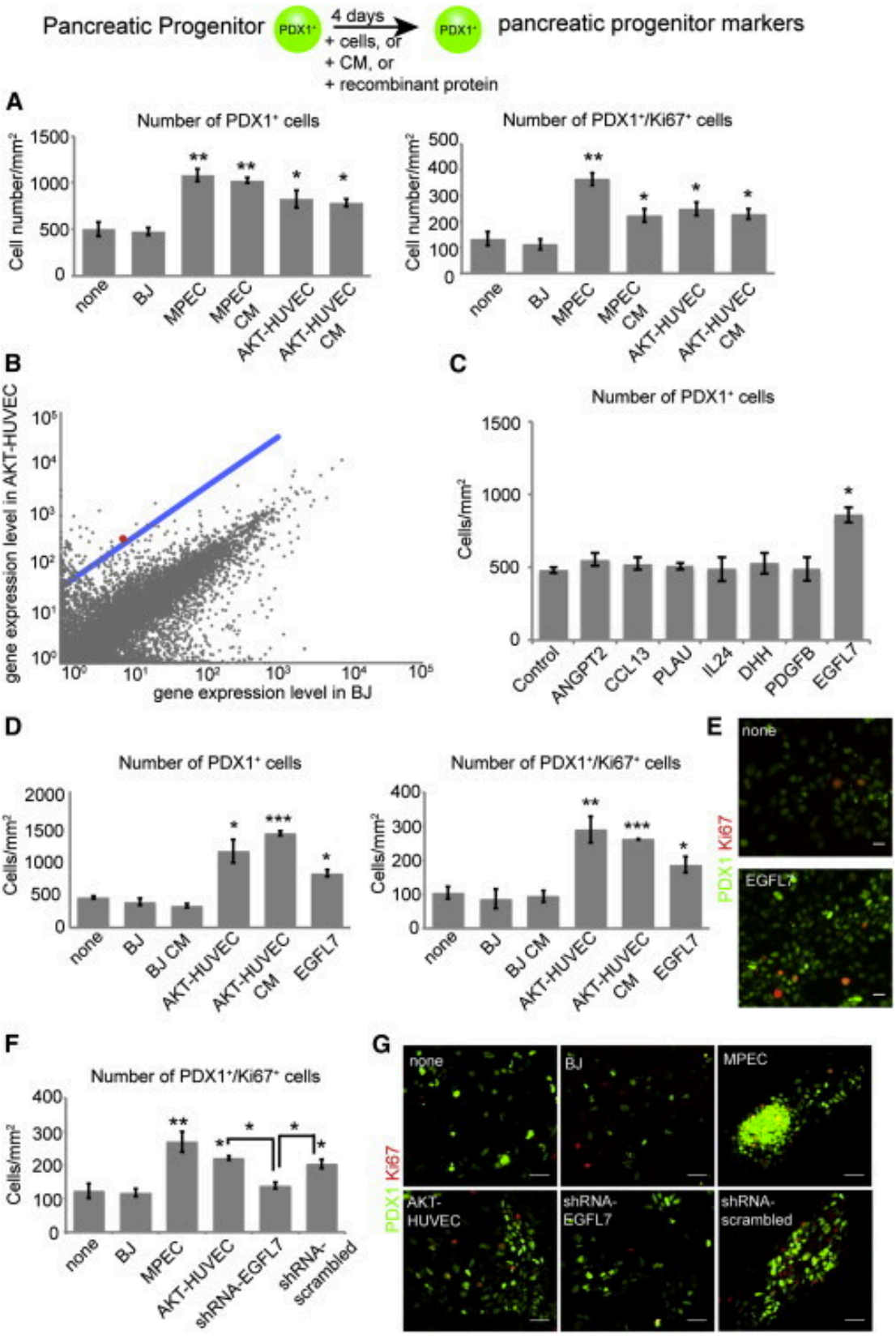
Pancreatic Progenitor
PDX1+
4 days
+ cells, or
+ CM, or
+ recombinant protein
PDX1+
pancreatic progenitor markers
A
Number of PDX1+ cells
Cell number/mm2
1500
1000
500
0
none
BJ
MPEC
MPEC CM
AKT-HUVEC
AKT-HUVEC CM
Number of PDX1+/Ki67+ cells
500
400
300
200
100
0
B
gene expression level in AKT-HUVEC
gene expression level in BJ
C
Number of PDX1+ cells
Cells/mm2
Control
ANGPT2
CCL13
PLAU
IL24
DHH
PDGFB
EGFL7
D
Number of PDX1+ cells
Cells/mm2
2000
1500
1000
500
0
none
BJ
BJ CM
AKT-HUVEC
AKT-HUVEC CM
EGFL7
Number of PDX1+/Ki67+ cells
400
300
200
100
E
none
PDX1 Ki67
EGFL7
F
Number of PDX1+/Ki67+ cells
Cells/mm2
shRNA-EGFL7
shRNA-scrambled
G
none
BJ
MPEC
PDX1 Ki67
AKT-HUVEC
shRNA-EGFL7
shRNA-scrambled

shRNA lentivirus as compared to a scrambled control lentivirus (**Supplemental Figure 2.3B**). When co-cultured with EGFL7-shRNA treated AKT-HUVECs, hESC-derived PPs showed significantly lower proliferation activity as compared to those co-cultured with untreated (P=0.0324) and scrambled-shRNA treated AKT-HUVECs (P= 0.0387, **Figure 2.3F, G**). These results indicate that EGFL7 is both sufficient and necessary for endothelial cells to maintain PP self-renewal.

Since EGFL7 has been shown to modulate the NOTCH pathway (*19*), we tested whether the NOTCH pathway is involved in endothelial cell-dependent PP expansion. HUES8-derived PP populations were treated with five different NOTCH inhibitors, including DAPT, XX, compound E, III-31-C, and Sulindac sulfide. The NOTCH inhibitors did not mimic the effect of EGFL7 to promote PP proliferation (**Supplemental Figure 2.3C**). In addition, qRT-PCR analysis showed that EGFL7 treatment did not alter the expression of NOTCH target genes, such as *Hes-1* and *Hey-1*, in *Pdx1*-GFP$^+$ cells (**Supplemental Figure 2.3D**).

Recent studies suggested that EGFL7 might also activate the EGF receptor pathway (*20, 21*). Several experiments were performed to determine whether EGF receptor is a downstream signal of EGFL7. Immunocytochemistry suggests that the EGF receptor is expressed in hESC-derived PDX1$^+$ PPs (**Supplemental Figure 2.3E**). In addition, microscale thermophoresis binding assay suggested that EGFL7 directly binds to the EGF receptor *in vitro* (K_d=384±76.5 nM, **Supplemental Figure 2.3F**). Furthermore, we found that

addition of an EGFR inhibitor (EGFRi) blocks the effect of endothelial cells and EGFL7 to expand PDX1$^+$ PPs (**Supplemental Figure 2.3G**). Finally, we found that mRNA expression level for EGF is much lower in AKT-HUVECs (0.09±0.02) and MPECs (0.09±0.02) than BJ fibroblasts (0.6±0.1), as determined by RNA-seq (**Supplemental Figure 2.3H**). Since endothelial cells, but not BJ fibroblasts, promote PP self-renewal, this suggests that endothelial cells do not promote PP proliferation by secreting EGF. Together, these results indicate that endothelial cells promote PP self-renewal through the secretion of EGFL7 and through activation of the EGF receptor signaling pathway.

To determine if EGFL7 treatment is capable to promote PP proliferation in long-term cultures, we tested the expansion and differentiation capacity of PDX1$^+$ PPs to the endocrine lineage following the pulsed expansion with recombinant EGFL7. HUES8-derived PP populations were treated with EGFL7 for different periods of time. One set of samples was fixed and stained with PDX1 and Ki67 antibodies to determine cell proliferation rates. The other set of samples were further differentiated in the absence of EGFL7 for additional 7 days and stained with antibodies against endocrine markers to determine the differentiation potential. The percentage of PDX1$^+$/Ki67$^+$ cells increased during the first week of EGFL7 treatment (**Supplemental Figure 2.3I**). After one week, the percentage of PDX1$^+$/Ki67$^+$ cells started decreasing in all conditions no matter whether EGFL7 was present or not. However, the percentages of PDX1$^+$/Ki67$^+$ cells treated with EGFL7 are higher than those of under control conditions at all time points (**Supplemental Figure 2.3I**). Consistent with the increase in cell proliferation, the percentage of insulin$^+$, C-peptide$^+$ and somatostatin$^+$ cells

increased in PPs cultured under EGFL7 treatment, and peaked at one week. The percentage of hormone-expressing cells under EGFL7-treated conditions is higher than that under control conditions at all time points (**Supplemental Figure 2.3J-L**). Together, these results suggest that one week of EGFL7 treatment can expand PDX1$^+$ PPs *in vitro*, resulting in significantly increased differentiation efficiency toward the endocrine cell lineages.

2.4.4 – Endothelial overexpression of Egfl7 in vivo increases proliferation of PPs.

To determine the effect of EGFL7 on the PP cell population *in vivo*, we analyzed pancreatic development in a transgenic mouse model, Tie2:Egfl7. In this strain, the *Egfl7* transgene is under the control of the endothelial specific *Tie2* promoter, resulting in a 2-3 fold overexpression of EGFL7 (*19*). Whole mount immunofluorescent staining was performed on E9.5 and E10.5 embryos from C57BL/6 wild type (WT) mice and Tie2:Egfl7-transgenic mice (TG) (**Figure 2.4A, D**). A CD31-positive capillary plexus surrounds the developing pancreatic bud *in vivo*, demonstrating the proximity of endothelial cells and implicating them as a potential source of EGFL7 to signal to the PDX1$^+$ PP population (**Supplemental Figure 2.4A**). Quantification of the vascular coverage at E10.5 demonstrated no significant difference in blood vessel density surrounding the developing pancreatic bud between WT and TG mice (**Supplemental Figure 2.4B**, P=0.299).

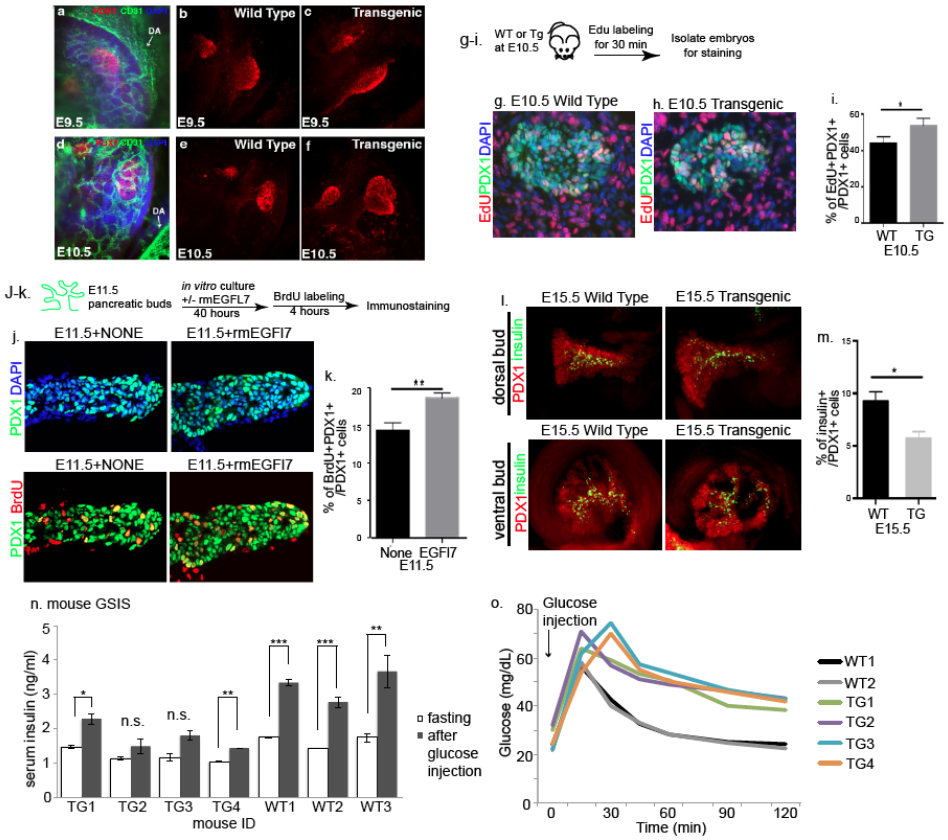

Figure 2.4 EGFL7 Increases Proliferation of PPs in Both TG and Explant Cultures. (A and D) Representative collapsed z stack confocal image of (A) E9.5 and (D) E10.5 mouse pancreatic buds costained for DAPI, PP marker PDX1, and endothelial cell marker, CD31. (B, C, E, and F) Representative collapsed z stack confocal images of E9.5 and E10.5 pancreatic buds from WT and TG mice stained for PDX1. (G and H) Representative Images of E10.5 mouse pancreatic bud sections from (G) WT and (H) TG mice, costained for PP marker, PDX1, and proliferation marker, EdU. (I) Quantification of the percentage of $EdU^+/PDX1^+$ cells of E10.5 WT and TG mice (n = 3). (J) Representative images of E11.5 WT pancreatic bud explants treated with or without 1 µg/ml recombinant mouse EGFL7 and costained for DAPI, Pdx1, and BrdU. (K) Quantification of the percentage of $BrdU^+/Pdx1^+$ cells of E11.5 WT pancreatic buds treated with or without recombinant EGFL7 (n = 6). (L) Representative images of E15.5 dorsal and ventral pancreatic buds from WT and TG mice, costained for PP marker, PDX1, and insulin. (M) Quantification of the ratio of $insulin^+$ cells over $PDX1^+$ cells of E15.5 pancreatic buds from WT and TG mice (n = 5). (N) Glucose-stimulated insulin secretion (GSIS) test of WT control (n = 3) and TG (n = 4) mice. (O) GTT of WT (n = 2) and TG (n = 4) mice. Data were presented as mean ± SEM.

At E9.5 and E10.5, the pancreatic buds of TG mice appear larger with less defined edges as compared to WT mice (**Figure 2.4B-F**). To determine if the larger pancreatic buds in the TG embryos resulted from increased proliferation of $PDX1^+$ cells, we performed EdU injections of pregnant E10.5 WT and TG mice (**Figure 2.4G, H**). We analyzed the percentage of EdU^+ PP ($PDX1^+$) cells in sections of pancreatic buds (**Figure 2.4I**). The percentage of proliferating PPs ($EdU^+/PDX1^+$) in TG mice is significantly higher than WT mice ($P^*<0.05$, **Figure 2.4I**). In addition, the $PDX1^+$ area in TG mice is significantly increased compared to WT mice ($P^*=0.031$ in **Supplemental Figure 2.4C** and $P^*=0.032$ in **Supplemental Figure 2.4D**). The number of $PDX1^+$ cells in TG mice shows the same trend toward increase as the $PDX1^+$ area, although it does not reach significance ($P=0.1144$ in **Supplemental Figure 2.4E**, $P=0.065$ in **Supplemental Figure 2.4F**). The increased of the number of $PDX1^+$ cells in TG mice is more pronounced at E15.5 (**Supplemental Figure 2.4G, H**, $P^{***}<0.001$). Together, these data suggest that PP proliferation was stimulated by endothelial-specific overexpression of EGFL7 *in vivo.*

In addition, WT E11.5 pancreatic buds were isolated from surrounding mesenchyme and cultured *in vitro* in the presence or absence of recombinant mouse EGFL7 for two days. The explants were pulsed for 4 hours with BrdU prior to fixation. The percentage of proliferating PPs ($BrdU^+/PDX1^+$ cells) out of the total number of PPs ($PDX1^+$ cells) was significantly increased in the presence of mouse recombinant EGFL7 ($P^{**}<0.01$, **Figure 2.4J, K**).

To determine the effect of EGFL7 *in vivo* on differentiation into hormonal-expressing cells, we analyzed the percentage of insulin$^+$ cells and PDX1$^+$ cells in E15.5 pancreatic buds (**Figure 2.4L**). The percentage of insulin$^+$ cells over PDX1$^+$ cells in E15.5 pancreatic buds is significantly decreased in TG mice (P*<0.05, **Figure 2.4M**). Consistently, the ratio of insulin$^+$ area over E-cadherin$^+$ area in E15.5 TG pancreatic buds shows a trend toward decrease compared with WT controls (**Supplemental Figure 2.4G, I**, P=0.396) although it does not reach significance. We also examined the total number of PDX1$^+$ cells and the percentages of PDX1$^+$/NKX6.1$^+$ cells, PDX1$^+$/SOX9$^+$ cells and PDX1$^+$/NKX6.1$^+$/SOX9$^+$ cells in total PDX1$^+$ cells at E15.5. Consistent with our results for E9.5 and E10.5 embryos, the total number of PDX1$^+$ cells in E15.5 TG pancreatic buds is significantly higher than that of WT controls (**Supplemental Figure 2.4H**, P***<0.001). The ratios of PDX1$^+$/NKX6.1$^+$ cells (P=0.385), PDX1$^+$/SOX9$^+$ cells (P=0.200) and PDX1$^+$/NKX6.1$^+$/SOX9$^+$ cells (P=0.495) in PDX1$^+$ cells did not differ significantly between TG and WT pancreatic buds (**Supplemental Figure 2.4J, K**). Importantly, less than 6% of total PDX1$^+$ cells coexpress NGN3 in both WT and TG pancreatic buds (**Supplemental Figure 2.4L, M**, P=0.053), suggesting that these PPs have not yet fully committed to endocrine progenitors. Together, these data suggest that EGFL7 suppresses PP differentiation into pancreatic endocrine cells, which is consistent with our results using hESC-derived cells (**Supplemental Figure 2.1D, E**).

To determine the effect of EGFL7 overexpression in adult beta cell function, we performed a glucose-stimulated insulin secretion (GSIS) test and a glucose

tolerance test (GTT) in 8-week old male TG and WT mice. Strikingly, all four TG mice showed significantly less insulin secretion at both fasting and after glucose stimulation, compared to WT controls (fasting: P*=0.048; after glucose stimulation: P*=0.027, **Figure 2.4N**). Furthermore, the TG mice showed consistently impaired glucose tolerance (**Figure 2.4O**). The data suggests that adult TG mice have less functional beta cells than WT control mice.

Stepwise differentiation of hESCs provides a useful platform to study human development. Using a stepwise pancreatic differentiation system, we found that an endothelial cell niche plays a stage-dependent role in human pancreatic development, promoting PP self-renewal and impairing differentiation from PPs towards hormone-expressing cells. Our finding could explain the results from previous animal studies: removing endothelial cells before the PP stage blocks pancreatic development (*1*), while forced hypervascularization at the PP stage negatively impacts the later endocrine differentiation (*8, 14, 15*). During pancreatic development, the endothelium pattern changes dramatically over time, which might affect the local concentration of paracrine factors, such as EGFL7, which will contribute to the cell fate decision. On the other hand, a recent study proposed that the endothelial cell niche could stimulate PPs to differentiate into insulin-secreting cells (*22*). In contrast to our co-culture conditions, in which MPECs and AKT-HUVECs survive well after 4 days of co-culture (**Supplemental Figure 2.4N**), the rat microvascular endothelial cells in that study do not survive well in differentiation conditions, and could not be detected after 6 days in culture (*22*). Although increased insulin expression was detected in the co-cultures, we can speculate that the rat microvascular

endothelial cells might provide a transient amplifying signal to expand PPs. If the endothelial cells start to die, the block on differentiation of PPs would be relieved. To test this hypothesis, we cultured hESC-derived PPs in endothelial cell CM for 4 days. The medium was then removed to induce spontaneous differentiation. Consistent with our hypothesis, the hESC-derived cells treated with CM show better differentiation toward insulin-expressing cells (**Supplemental Figure 2.4O**).

EGFL7 is a secreted protein that acts as a chemoattractant for endothelial cells, binds to the extracellular matrix, and promotes endothelial cell adhesion (*23*). Here, we identified the novel role of EGFL7 as the molecular handle involved in the crosstalk between endothelium and pancreatic epithelium, which plays as a gatekeeper to maintain PP self-renewal. In this context, it is interesting to note that the developmental stage of pancreatic bud formation (E9.0-E11.5) coincides with the peak in EGFL7 expression in the embryonic vasculature (*24*). Our data also suggested that EGFL7 might function through the EGF signaling pathway. Consistently, it has been shown that activation of EGF signaling facilitates the $PDX1^+$ cell expansion (*25*). Although our data strongly support our conclusion that EGFL7 promotes PP proliferation, we cannot exclude the possibility that EGFL7 may also promote foregut epithelium differentiation. In addition, recombinant EGFL7 protein was less efficient for expansion of $PDX1^+$ progenitors compared to co-culture with endothelial cells. To explain this discrepancy, we considered two possibilities. First, the recombinant EGFL7 protein may lack post-translational modifications and might not be as functionally active as native EGFL7 secreted by endothelial cells. Second, we

cannot exclude the possibility that endothelial cells secrete additional factors that boost the effect of EGFL7. Finally, since the *Egfl7* transgene is overexpressed in all endothelia, we cannot fully rule out the possibility of systemic effects.

Pancreatic development is a highly dynamic process controlled by multiple pathways. Additional work is needed to unravel the dynamic interaction of pancreatic endoderm with endothelial and mesenchymal cell niches. A complete understanding of the underlying mechanism may lead to the development of more efficient strategies to differentiate hESCs/iPSCs into mature glucose-responding cells *in vitro*.

Supplemental Figure 2.1 (Corresponds to Figure 2.1): Endothelial cells play a stage-dependent role in pancreatic development. (a) Cell number of SOX17+ cells, SOX17+/Ki67+ cells, or HNF4α+ cells per mm^2 after HUES8-dervied definitive endoderm (SOX17+) population were co-cultured with BJ cells, MPECs, or AKT-HUVECs at indicated ratios (1/10, 1/3 or 1/1) (n=3); (b) A majority of EGFP+ pancreatic progenitors derived from *Pdx1*-EGFP HUES8 remained PDX1+. Flow Cytometry of *Pdx1*-EGFP HUES8-derived pancreatic progenitors detected by secondary antibody only as a negative control (left) and in the presence of anti-GFP, anti-PDX1 and secondary antibody (right). Among 45.0% GFP+ cells, 40.6% of them were PDX1+. The data suggested that PDX1+ pancreatic progenitors can be enriched by sorting GFP+ cells in *Pdx1*-EGFP HUES8- derived pancreatic progenitors; (c) *Pdx1*-EGFP+ cells purified from *Pdx1*-EGFP HUES8 derived pancreatic progenitor population were cultured with BJ cells, MPECs or AKT-HUVECs for 4 days. Cell number of PDX1+ or PDX1+/Ki67+ cells per mm^2 was quantified after 4 days co-culture (n=3); (d) Cell number of hormone-expressing cells, Insulin+ (INS), Glucagon+ (GCG), c-peptide+ (CP), or Somatostatin+ (SST) cells per mm2, after HUES8-derived pancreatic progenitor (PDX1+) population were co-cultured with BJ cells, MPECs or AKT-HUVECs. Scale bar, 50 μm. Data represent the mean ± standard deviation (n=3); (e) HUES8-derived pancreatic progenitor population was co-cultured with mCherry labeled MPECs. 6 days later, HUES8-derived cells were purified by removing mCherry labeled MPECs with cell sorting and analyzed by qRT-PCR. The cells co-cultured with MPECs showed the decreased expression of insulin, glucagon and somatostatin (n=3); (f) The effect of endothelial cells on H1-derived pancreas progenitors. Cell number of PDX1+ or PDX1+/Ki67+ cells per mm^2 after H1-derived PDX1+ pancreatic progenitors were co-cultured with BJ cells, MPECs, or AKT-HUVECs at the indicated ratio comparing to pancreatic progenitors without co-culture (none) (n=3).

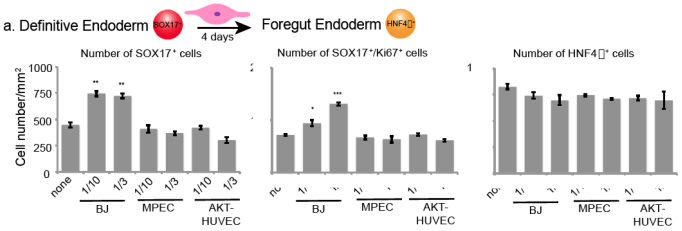
a. Definitive Endoderm
4 days
Foregut Endoderm
Number of SOX17⁺ cells
Number of SOX17⁺/Ki67⁺ cells
Number of HNF4⍺⁺ cells
Cell number/mm²
none
1/10
1/3
BJ
MPEC
AKT-HUVEC

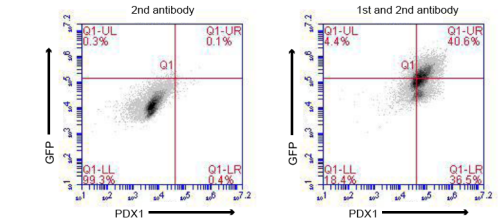
b.
2nd antibody
1st and 2nd antibody
Q1-UL
Q1-UR
Q1-LL
Q1-LR
GFP
PDX1

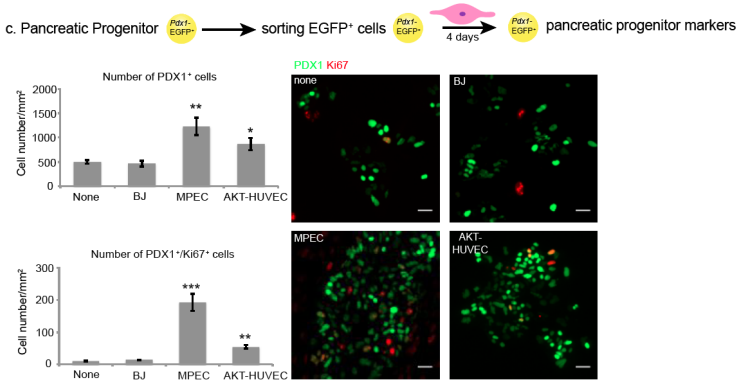
c. Pancreatic Progenitor
sorting EGFP⁺ cells
4 days
pancreatic progenitor markers
Number of PDX1⁺ cells
Number of PDX1⁺/Ki67⁺ cells
PDX1 Ki67
none
BJ
MPEC
AKT-HUVEC
None

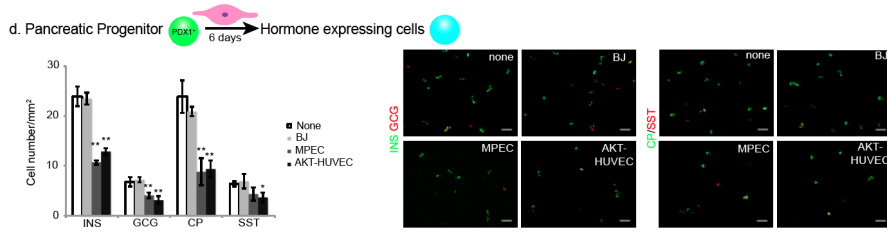
d. Pancreatic Progenitor
6 days
Hormone expressing cells
INS
GCG
CP
SST
INS GCG
CP/SST
none
BJ
MPEC
AKT-HUVEC

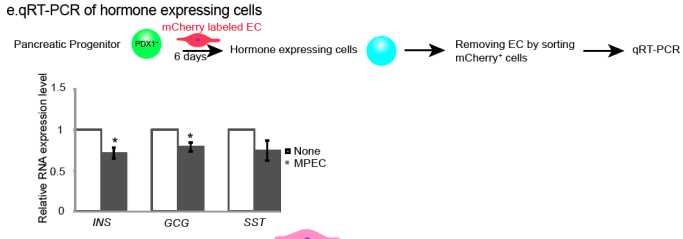
e.qRT-PCR of hormone expressing cells
Pancreatic Progenitor
mCherry labeled EC
6 days
Hormone expressing cells
Removing EC by sorting mCherry⁺ cells
qRT-PCR
Relative RNA expression level
None
MPEC

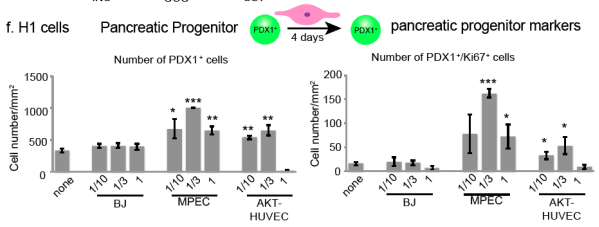
f. H1 cells
Pancreatic Progenitor
4 days
pancreatic progenitor markers
Number of PDX1⁺ cells
Number of PDX1⁺/Ki67⁺ cells
Cell number/mm²
none
BJ
MPEC
AKT-HUVEC

Supplemental Figure 2.2 (Corresponds to Figure 2.2): (a) Transcriptome analysis by RNA-seq. The scatter plot showed mRNA expression level in sorted *Pdx1*-EGFP+ cells before co-culture versus after co-cultured with MPECs. The red line indicated identical gene expression levels between two samples. The mRNA expression level is very similar in sorted *Pdx1*-EGFP+ cells before co-culture versus after co-culture with MPEC (R=0.9378). (b-g) qPCR of sorted *Pdx1*-EGFP+ pancreatic progenitors after 2 or 4 days of co-culture. RNA levels of (b) *FOXA2*, (c) *NKX6.1*, (d) *HNF6*, (e) *SOX9*, (f) *NGN3*, and (g) *NKX2.2* were measured by qPCR in sorted *Pdx1*-EGFP+ cells after 2 days or 4 days of co-culture in the absence (none) or presence of BJ cells and MPEC. All numbers were normalized to no co-culture of the same culture duration (in f, at day 4, P=0.1274 for none versus MPEC; P=0.8968 for BJ versus MPEC; Bonferroni). Data are presented as mean ± standard deviation (n=3). P*<0.05, P**<0.01, n.s. not significant.

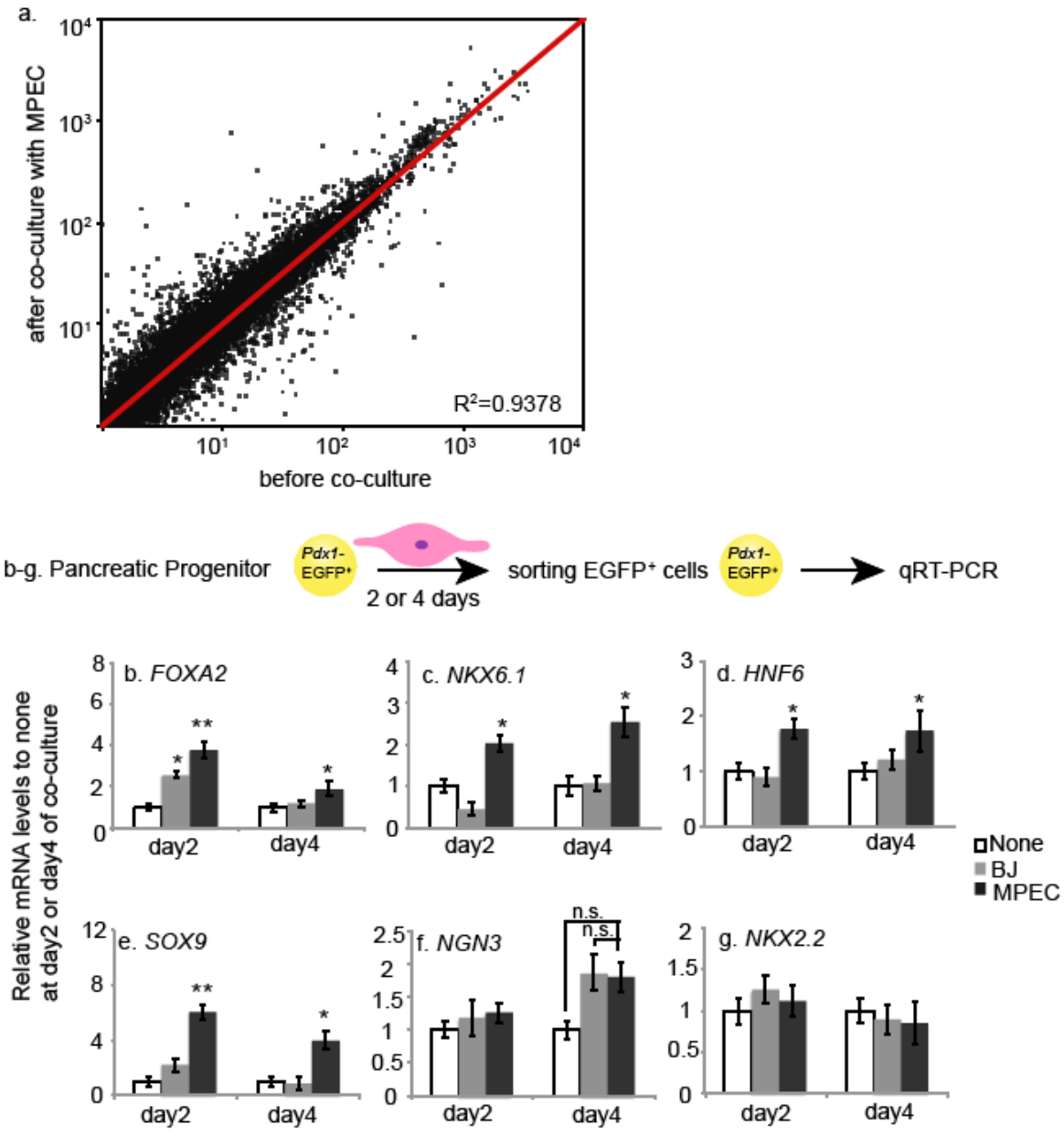
a.
after co-culture with MPEC
before co-culture
R²=0.9378
b-g. Pancreatic Progenitor
Pdx1-EGFP+
2 or 4 days
sorting EGFP+ cells
qRT-PCR
Relative mRNA levels to none at day2 or day4 of co-culture
b. FOXA2
c. NKX6.1
d. HNF6
e. SOX9
f. NGN3
g. NKX2.2
n.s.
day2
day4
None
BJ
MPEC

Supplemental Figure 2.3 (Corresponds to Figure 2.3): (a) Transcriptome analysis of gene expression in BJ cells and MPECs by RNA-seq (grey dots). Blue line indicates the cutoff line of a 30-fold increase in gene expression in MPECs as compared to BJ cells. Red dot indicates gene expression levels of EGFL7 in MPECs versus BJ cells; (b) Relative EGFL7 mRNA expression level in BJ cells, AKT-HUVECs expressing shRNA-EGFL7, or expressing scrambled shRNA comparing to AKT-HUVECs; (c) PDX1+ cell numbers per mm2 were measured after 4 days of treatment with DMSO or NOTCH inhibitors (DAPT, γ-Secretase Inhibitor XX, Compound E, III-31-C, and Sulindac sulfide) (n=3); (d) HUES8 *Pdx1*-GFP cell-derived pancreatic progenitors were cultured in the absence or presence of endothelial cells for four days. qRT-PCR for NOTCH target genes, *Hes-1* and *Hey-1*, was carried out on sorted *Pdx1*-EGFP+ cells; (e) Immunocytochemistry of EGF receptor (EGFR, green), PDX1 (red), and DAPI in HUES8 derived pancreatic progenitors; (f) Protein interaction between EGFR and EGFL7 was measured by microscale thermophoresis (MST). The dissociation constant (*Kd*= 387±76.5nM) of EGFL7 binding to EGFR was estimated by MST assay. (g) Effect of EGFRi on the relative number of PDX1+/Ki67+ HUES8-derived pancreatic progenitors after co-culture with MPECs, AKT-HUVECs, or treated with recombinant EGFL7 (n=3); (h) EGF mRNA expression levels in different cell types by RNA-seq; (i-l) proliferation (i, PDX1+/Ki67+) and differentiation ability of PDX1+ progenitors to endocrine lineage (j, Insulin; k, c-peptide; l, somatostatin) following pulsed expansion of progenitors with recombinant EGFL7 for 4 days, 1 week, 2 weeks or 4 weeks (n=3).

a.

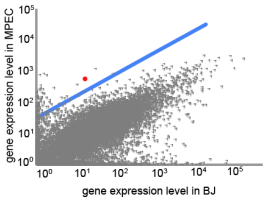

b.

sample	*EGFL7* expression level
AKT-HUVEC	1
BJ	5.13E-02
shRNA-EGFL7	0.365
shRAN-scrambled	1.58

c. Pancreatic Progenitor → 4 days, +/- inhibitors → PDX1⁺ cell number

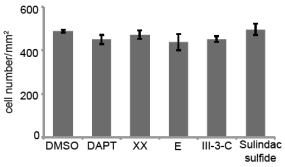

d. Pancreatic Progenitor → 4 days → sorting EGFP⁺ cells → qRT-PCR

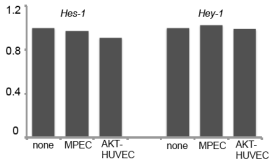

e.

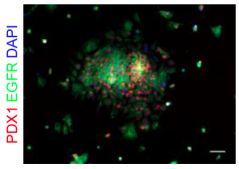

f. Microscale Thermophoresis (MST)

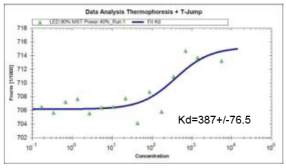

g. Pancreatic Progenitor → +/- EC or EGFL7, +/- inhibitors, 4 days → PDX1⁺/Ki67⁺ cell number

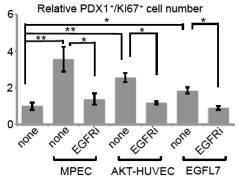

h. *EGF* mRNA expression levels in different cell types by RNA-seq

Cell types	EGF mRNA expression level
BJ	0.6±0.1
MPEC	0.09±0.02
AKT-HUVEC	0.09±0.02

i-l. Pancreatic Progenitor → + BSA or EGFL7, 4 days, 1 week, 2 weeks or 4 weeks → PDX1⁺/Ki67⁺ number → 7 days → Hormone expressing cells

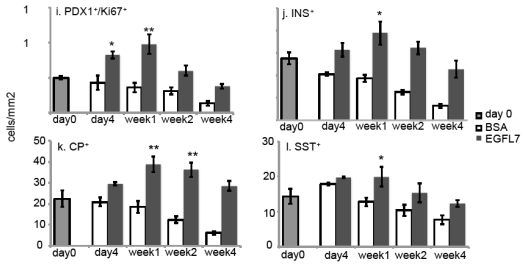

Supplemental Figure 2.4 (Corresponds to Figure 2.4 and discussion): (a,b) Representative collapsed z-stack confocal images and quantification of CD31+ area in E10.5 mouse pancreatic buds of C57BL/6 wild type and Tie2:Egfl7 Transgenic mice, co-stained for pancreatic progenitor marker, PDX1 (red), and CD31 (green), showing that overall vascular coverage around the developing pancreatic bud is unchanged (P=0.299). Quantification of PDX1+ area in (c) E9.5 and (d) E10.5 pancreatic buds (P*=0.031 in c and P*=0.032 in d); Quantification of the number of PDX1+ cells in (e) E9.5 and (f) E10.5 pancreatic buds (P=0.1144 in e and P=0.065 in f). (n=4-7) All data are represented as mean +/- SEM. (g) Immunocytochemistry analysis of E15.5 pancreatic buds using PDX1, E-cadherin, and insulin antibodies; (h) The total number of PDX1+ cells in E15.5 wild type (WT) and Tie2:Egfl7 transgenic (TG) pancreatic buds (P***<0.001); (i) The ratio of insulin+ area over E-cadherin+ area in E15.5 pancreatic buds (P=0.396, n=3 for each genotype); (j) Immunocytochemistry analysis of E15.5 pancreatic buds using PDX1, NKX6.1 and SOX9 antibodies; (k) The ratios of PDX1+/NKX6.1+ cells (P=0.385), PDX1+/SOX9+ cells (P=0.200), and PDX1+/NKX6.1+/SOX9+ (P=0.495) cells in total PDX1+ cells in E15.5 wild type (WT) and Tie2:Egfl7 transgenic (TG) pancreatic buds (n=3 for each genotype); (l) Immunocytochemistry analysis of E15.5 pancreatic buds using PDX1 and NGN3 antibodies; (m) The percentage of PDX1+/NGN3+ cells in total PDX1+ cells in E15.5 pancreatic buds (P=0.053, n=3 for each genotype); (n) Immunocytochemistry of CD31 (red) and PDX1 (green) in HUES8-derived pancreatic progenitors alone (none) or co-culturing with MPECs or AKT-HUVECs at day 0 or day 4. (o) The HUES8-derived pancreatic progenitors were treated with MPEC-CM (conditioned medium) or AKT-HUVEC-CM treatment or without treatment (none) for 4 days and followed by 6 days spontaneous differentiation after the removal of treatments (P**<0.01, n=3). Cell number of insulin+ cells per mm2 were quantified using a Molecular Devices high-content screening system and analyzed by MetaXpress. (n.s.= not significant).

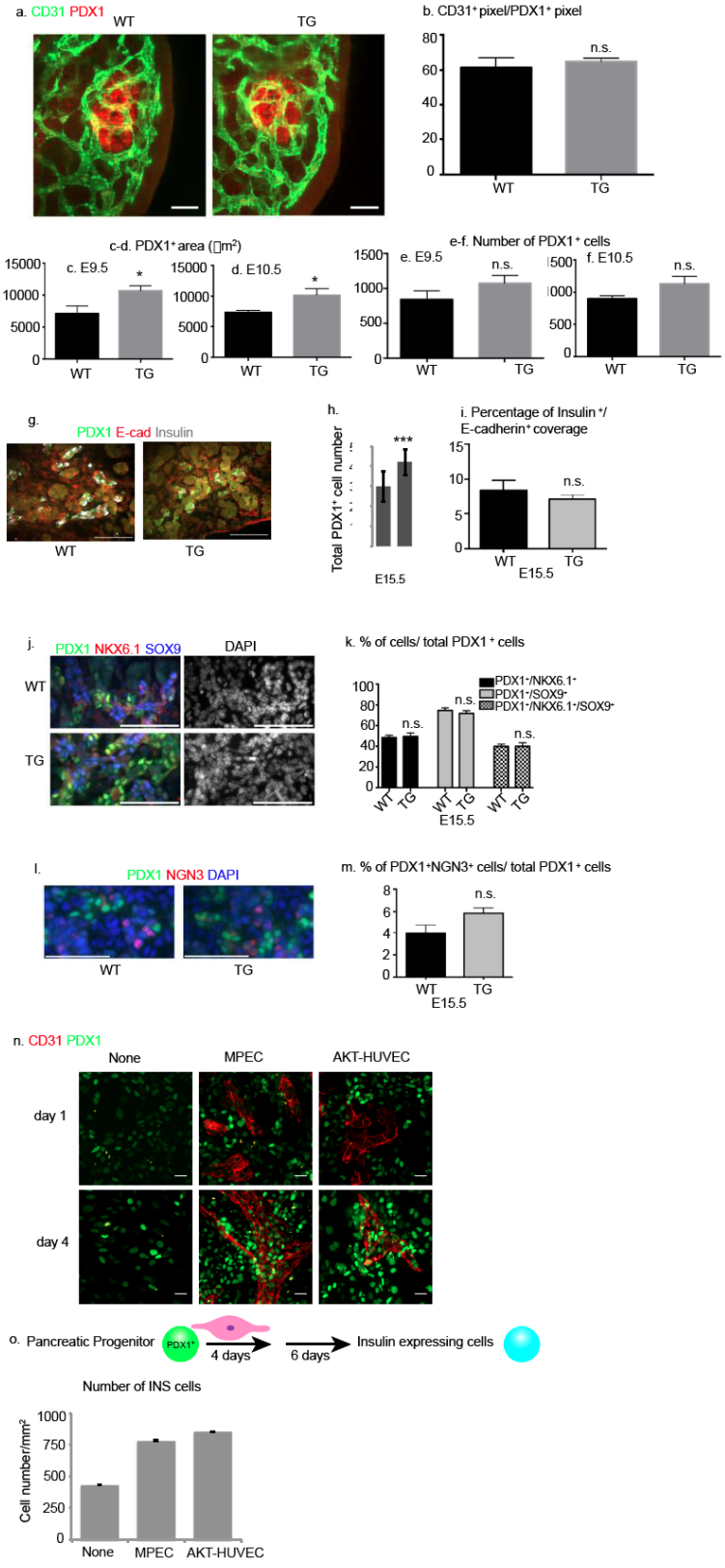
a. CD31 PDX1
WT
TG
b. CD31⁺ pixel/PDX1⁺ pixel
n.s.
c-d. PDX1⁺ area (μm²)
c. E9.5
d. E10.5
e-f. Number of PDX1⁺ cells
e. E9.5
f. E10.5
g.
PDX1 E-cad Insulin
h.
Total PDX1⁺ cell number
E15.5
i. Percentage of Insulin⁺/ E-cadherin⁺ coverage
j.
PDX1 NKX6.1 SOX9
DAPI
k. % of cells/ total PDX1⁺ cells
PDX1⁺/NKX6.1⁺
PDX1⁺/SOX9⁺
PDX1⁺/NKX6.1⁺/SOX9⁺
l.
PDX1 NGN3 DAPI
m. % of PDX1⁺NGN3⁺ cells/ total PDX1⁺ cells
n. CD31 PDX1
None
MPEC
AKT-HUVEC
day 1
day 4
o. Pancreatic Progenitor
PDX1⁺
4 days
6 days
Insulin expressing cells
Number of INS cells
Cell number/mm²
None
MPEC
AKT-HUVEC

Supplemental Table 2.1 (for Figure 2.3): The list of genes highly expressed in MPECs than in BJ cells (above the blue line in **Figure 2.3B**) and their subcellular protein localization (Olerud et al., 2009; Thorens, 2011).

Gene	Protein subcellular localization
PECAM1	plasma membrane
APLN	Secreted
CD34	plasma membrane
CDH5	plasma membrane
NPTX1	Cytoplasmic vesicle
NOS3	Nucleus; Plasma Membrane; cytoplasm; Golgi apparatus; cytoskeleton
CTSL2	Lysosome
PLVAP	Plasma Membrane
EMCN	Plasma Membrane
ANGPT2	Secreted
BST2	Golgi apparatus
AKR1B10	Lysosome. Secreted.
THBD	Plasma Membrane
TMEM176B	Nucleus membrane
ERG	nucleus
RAMP2	Cytoplasm
TTC9	
BCL6B	nucleus
MFNG	Golgi apparatus membrane
CH25H	Golgi Apparatus, Endoplasmic Reticulum
TIE1	Plasma Membrane
CGNL1	Cell junction
C15orf63	
PROCR	Plasma Membrane
F11R	Nucleus, Nucleolus
PROM1	Plasma Membrane
ROBO4	
GIMAP4	Mitochondria
MYCT1	Nucleus
ESAM	Plasma Membrane
STAB1	cytoplasm
MERTK	Plasma Membrane
EGFL7	Secreted
ACSL5	mitochondrion
KDR	Cell membrane
GIMAP6	
SLC25A4	mitochondrion
EGLN3	cytoplasm
LMO1	Nucleus
SPNS2	Membrane
LRRC32	Membrane
SELP	Secretory Vesicles, Plasma Membrane
DYSF	Plasma Membrane
EXOC3L1	Cytoplasmic vesicle
CYTH4	Cell membrane
ARHGEF15	Nucleus, Cytoplasm, Cytoplasmic Vesicles
KLHL4	Cytoplasm
N4BP3	cytoplasmic membrane-bound vesicle; Cytoplasm
NRARP	
HOXD8	Nucleus
CCL13	Secreted
RENBP	
NEFL	
CD93	Membrane
SH2D3C	Cytoplasm
GPR116	Cell membrane
SOX18	Nucleus
KRT80	
CXCR4	Cell membrane
RASIP1	Cytoplasm
TMEM176A	Membrane
IL24	Secreted
ICAM2	Membrane
KCNH2	Membrane
SFR1	Nucleus
PDE2A	Cell membrane
CPE	Nucleus
GRAP	
H3F3A	Nucleus
MEOX1	Nucleus
PRKCH	Cytoplasm
SPRR2G	Cytoplasm
EFNA1	Cell membrane
VCAM1	Membrane
ATRNL1	Membrane
CRLF2	Cell membrane
ICA1	Cytoplasm
NFIB	Nucleus
SEMA6B	Cell membrane
PLAU	Secreted
TMC6	Endoplasmic reticulum membrane
ARRB1	Cytoplasm
PAIP2B	
NPTXR	Membrane
DHH	Secreted
RAPGEF5	Nucleus
AIF1L	Cytoplasm
PDGFB	Secreted
ACADL	Mitochondrion matrix
LYVE1	Membrane
RNF39	Cytoplasm
VAMP8	Membrane
IRF8	Nucleus

Supplemental Table 2.2: Primer sequences used in this study were listed.

Gene	Forward Primer	Reverse Primer
INS	TGCGGGGAACGAGGCTTCTTCTA	AGGGACCCCTCCAGGGCCAAG
GCG	AAGCATTTACTTTGTGGCTGGATT	TGATCTGGATTTCTCCTCGTGTCT
SST	CCCCAGACTCCGTCAGTTTC	TCCGTCTGGTTGGGTTCAG
FOXA2	ATGCACTCGGCTTCCAGTAT	CATGTACGTGTTCATGCCGT
NKX6.1	GGGGATGACAGAGAGTCAGG	CGAGTCCTGCTTCTTCTTGG
HNF6	GGAGGATGTGGAAGTGGCT	TGTTGCCTCTATCCTTCCCA
SOX9	GTACCCGCACTTGCACAA	GTGGTCCTTCTTGTGCTGC
NGN3	GCTCATCGCTCTCTATTCTTTTGC	GGTTGAGGCGTCATCCTTTCT
NKX2.2	TCTACGACAGCAGCGACAAC	GGAGCTTGAGTCCTGAGGG

2.5 – Materials and Methods

hESC culture and differentiation. HUES8 and H1 cells were routinely cultured on irradiated MEF feeders in DMEM/F12 (Cellgro) supplemented with 20% KnockOut Serum Replacement, 2 mM GlutaMAX, 1 mM nonessential amino acids, 1.1 mM β-merceptoethanol, 10 ng/ml bFGF (Invitrogen), 50 ng/ml normacin (InvivoGen). Cells were passaged every 5 or 6 days using 0.05% trypsin (Invitrogen). To differentiate to the pancreatic progenitor population, hESCs were cultured on feeders to 80-90% confluency, then treated with 3 μM CHIR99021 (CHIR, Stem-RD) and 100 ng/ml activin A (R&D systems) in RPMI (Cellgro) supplemented with 2 mM GlutaMAX and 100 U/ml Pen/Strep for one day, and then 100 ng/ml activin A in RPMI supplemented with 0.2% fetal bovine serum (FBS), 2 mM GlutaMAX and 100 U/ml Pen/Strep. At this stage, hESC-derived cells containing a high percentage of $SOX17^+/FOXA2^+$ cells were defined as the hESC-derived definitive endoderm population. The medium was changed 2 days later to 50 ng/ml FGF7 (PeproTech) in RPMI supplemented with 2 mM GlutaMAX, 100 U/ml Pen/Strep and 2% FBS, and maintained for an additional 2 days. At this stage, hESC-derived cells containing a high percentage of $HNF4\alpha^+$ cells were defined as the hESC-derived foregut endoderm population. Cells were transferred to 300 nM LDN193189 (LDN, Axon), 2 μM retinoic acid (Sigma), and 0.25 μM SANT-1 (Sigma) for the first 4 days and then to 300 nM LDN193189 (LDN, Axon), 20 nM Phorbol 12,13-dibutyrate (PuBu, Sigma), and 1 μM ALK5i (Enzo) in DMEM supplemented with 2 mM GlutaMAX, 100 U/ml Pen/Strep, and 1x B27 (Invitrogen) for an additional 4 days. At this stage, hESCs-derived cells

containing a high percentage $PDX1^+$ cells are defined as the hESC-derived pancreatic progenitor population.

Co-culture experiments. MPECs (MS1, mouse pancreatic islet endothelial cell line, ATCC), AKT-HUVECs (AKT activated human umbilical vein endothelial cells (*16*)) and BJ cells (human foreskin fibroblasts, ATCC) were used in the co-culture experiments. hESC-derived populations were trypsinized by 0.25% trypsin (Invitrogen), resuspended in DMEM supplemented with 2 mM GlutaMAX, 100 U/ml Pen/Strep, and 1x B27, and plated at a density of $0.8*10^3$ cells/mm^2 in 96 well or 6 well plates. MPEC, AKT-HUVEC, or BJ cells were resuspended in the same medium and plated at a ratio of 1:1, 1:3 or 1:10 to hESC-derived pancreatic progenitors. One day after plating, medium was changed, and cells were maintained in the incubator for 4 days before fixation or further analysis.

Immunocytochemistry. Cells were fixed in 10% (v/v) formalin for 20 min at room temperature. Non-specific antigen and antibody association were blocked in 5% horse serum (Invitrogen), 0.3% Triton X in PBS for one hour at room temperature, followed by primary antibody incubation overnight. The following antibodies were used: goat anti-PDX1 (1:500, R&D systems, AF2419), rabbit anti-FOXA2 (1:1000, Millipore. 07-633), rabbit anti-HNF6 (1:200, Santa Cruz, sc-13050), mouse anti-NKX6.1 (1:500, U of Iowa Hybridoma bank, F55A12-c), guinea pig anti-insulin (1:1000, DAKO, A0564), mouse anti-C-peptide (1:1000, Millipore, 05-1109), rabbit anti-Amylase (1:1000, Sigma, A8273), rabbit anti-Ki67 (1:1000, Thermo, RM-9106-S1), mouse anti-Glucagon (1:2000, Sigma,

G2654), rabbit anti-Somatostatin (1:2000, DAKO, A0566), and rabbit anti-EGFR (1:50, Abcam, Ab2430). This was followed by incubation with species-appropriate secondary antibodies.

Data quantification. For cell number quantification, at least triplicates for each treatment in one experiment were carried out. Cells in the center 18 mm^2 of each well (with density of $2*10^3$ cells/mm^2 in average) were imaged using a Molecular Devices high-content screening system and images were analyzed by MetaXpress. Quantification was done for three independent experiments. Data presented mean ± standard deviation as cell number per mm^2 or relative cell number to none co-culture (none) in each independent experiment.

RNA extraction and quantitative RT-PCR. Total RNA was isolated using Qiagen RNeasy mini kit according to manufacture's instructions. RNA was reverse transcribed using superscript III reverse transcriptase and random primers (Invitrogen). Quantitative PCR with SYBR green detection was performed using LightCycler 480 system (Roche). Primer sequences were listed in supplementary material **Supplemental Table 2.2**.

RNA-seq. The quality of RNA samples was analyzed, and cDNA libraries were synthesized and sequenced by Weill Cornell Genomics Core facility. In brief, the quality of RNA samples was examined by Agilent bioanalyzer (Agilent). cDNA libraries were generated using TruSeq RNA Sample Preparation (Illumina). Each library was sequenced using single-read in HiSeq2000/1000

(Illumina). Gene expression levels were analyzed with TopHat and Cufflinks by the Genomic Core facility.

Accession numbers. RNA-seq data deposited in the GEO database can be accessed with GEO accession numbers GSE63840 and GSE63843.

Generation of Pdx1-EGFP HUES8 line. Pdx1-eGFP-Rex-Neo was constructed by replacing the aMHC promoter on aMHC-eGFP-Rex-Neo (Addgene 21229) with the mouse *Pdx1* promoter (Addgene 15085). To infect HUES8 cells, lentivirus carrying *Pdx1*-eGFP-Rex-Neo were generated in 293T cells. HUES8 cells were plated on matrigel after removal of feeders. Lentiviruses were added to HUES8 cells supplemented with bFGF. After two days infection, HUES8 were plated with Neo^R MEFs and selected by Geneticin (Invitrogen) for 4 days.

Mice. All animal protocols were approved by the Institutional Animal Care and Use Committee at Weill Cornell Medical College. Tie2:Egfl7 transgenic mice were from in-house colonies (*19*) and C57BL/6 mice were from Jackson Laboratories. For timed pregnancies, the date of visualization of a vaginal plug was designated as embryonic day 0.5 (E0.5). Mouse embryos (n=3-7 over 2-3 litters for each genotype per time point) were isolated and fixed in 4% paraformaldehyde overnight. Embryos were further dissected for whole mount staining, removing the body wall as previously described (*26*) to expose the pancreatic buds for imaging. Whole pancreatic and gut tissues were isolated from E15.5 embryos and processed for immunostaining. Whole pancreatic and gut tissue was isolated from E15.5 embryos and either fixed in 4%

paraformaldehyde overnight or fresh frozen in (2:1) OCT:30% sucrose mixture. Fixed pancreatic tissues were used for whole mount immunostaining or cryopreserved and embedded in (2:1) OCT:30% sucrose mixture for sectioning.

Whole Mount Immunostaining. Processed embryos were washed and permeablized in PBS-0.4% Triton-X, then blocked in 10% donkey serum/0.4% Triton-X/PBS overnight at 4°C. Embryos were then incubated in primary antibodies in 5% donkey serum/0.4% Triton-X/PBS overnight at 4°C (PDX1, R&D Systems AF2419, 1:100 or 1:200; CD31, BD Biosciences #553370, 1:500; Insulin, DAKO A0564, 1:750; NKX6.1, U of Iowa Hybridoma bank F55A12, 1:350; Sox9, Millipore AB5535, 1:2000; E-cadherin, BD 610181, 1:150), washed overnight, and incubated in secondary antibodies (594-donkey-anti-goat, 1:500; 488-donkey-anti-rat, 1:200; 488-donkey-anti-guinea pig, 1:500; 488-donkey-anti-goat, 1:1000; 647-donkey-anti-guinea pig, 1:500, Cy3-donkey-anti-mouse, 1:500; Cy5-donkey-anti-rabbit, 1:500; Jackson Immunoresearch) overnight at 4°C. Embryos were washed, incubated in DAPI (1 μg/ml, Invitrogen), and mounted in Prolong Gold (Invitrogen) using Fastwell Spacers (Sigma-Aldrich). Images were acquired using an LSM Live 5 line scanner confocal microscope (Carl Zeiss) or Nikon TE200 microscope. Volume and total cell number quantifications were performed on z-stack confocal images, while area quantification was performed on collapsed z-stack confocal images (n=3-7). Four to five sections every 100μm were used for quantifications per embryo, and analyzed using Metamorph and Prism Software.

For NGN3 immunostaining, fresh frozen sections were dried on a heat block for 20min and post-fixed in 4% paraformaldehyde for 15min. Sections were then washed and permeablized in 0.1%triton-X/0.1%tween-20 for 15min and blocked in 0.1%tween-20/1%BSA/0.5%donkey serum for 45min. Primary antibodies (PDX1, Abcam#Ab47308,1:1000; Ngn3, Abcam#Ab47383, 1:1000**)** were incubated in block overnight at 4°C. Sections were then washed, incubated with secondary antibodies (594-donkey-anti-goat at 1:1000 Jackson Immunoresearch) in block, and mounted with Prolong Gold + DAPI (Invitrogen). Four to five sections every 100μm were used for quantifications per embryo (n=3 per genotype), and analyzed using Metamorph and Prism software.

Using EdU to monitor the pancreatic progenitor proliferation in vivo.
Proliferating cells were labeled using the Click-iT EdU Imaging Kit (Life Technologies, C10339). Female C57BL/6 and Tie2:Egfl7-Transgenic mice were subject to intraperitoneal injection of EdU at 50 μg per gram of body weight at E10.5 of pregnancy. After 30 minutes, mice were euthanized and embryos were isolated, dissected to expose pancreatic buds as above, and fixed in 4% paraformaldehyde overnight. Tissue was cryopreserved, embedded in a 2:1 OCT:30% sucrose mixture, and sectioned for further processing. Sections were permeablized and EdU detection was carried out according to the manufacturer's protocol. Antibody staining was then performed. Sections were blocked for 30 mins in 5% donkey serum/0.3% Triton-X/PBS, incubated in primary antibody (PDX1, R&D Systems AF2419, 1:500) in block overnight at 4°C. Sections were washed and incubated in secondary antibody (488-donkey-anti-goat, 1:1000; Jackson Immunoresearch). Sections were then washed,

incubated in DAPI (1 μg/ml, Invitrogen), and mounted in Prolong Gold (Invitrogen). Images were acquired using Axioplan 2 imaging microscope (Carl Zeiss). Approximately every 10^{th} section was used, for a total of five sections per embryo (n=3 per genotype), and analyzed using ImageJ and Prism software.

FACS (Fluorescence activated cell sorting). Cells were dissociated by accutase (Innovative Cell Technologies) and resuspended in sorting buffer (1% Fetal bovine serum, 1mM EDTA, 25mM HEPES in DMEM without phenol red). Cell sorting was performed using BD FASCvantage by the flow cytometry core facility at the Hospital of Special Surgery.

Explant culture. Mouse embryonic bud cultures largely followed published protocols (*27*). Briefly, E11.5 pancreatic buds were dissected to strip most of the surrounding mesenchymal tissue and cultured on Millicell filters (*Millipore*) in DMEM supplemented with 2 mM GlutaMAX, 100 U/ml Pen/Strep, and 1x B27 with or without recombinant mouse EGFL7 protein (1 μg/ml). After 40-hour culture, fresh media with BrdU (50ng/ml) were utilized to label mitotic cells. Tissues were harvested 4 hours later for processing and staining. Guinea pig anti-Pdx1 is a gift from Dr. Chris Wright. Mouse anti-BrdU (G3G4) is from the Developmental Studies Hybridoma Bank.

Chemicals. Recombinant mouse EGFL7 and human EGFL7 proteins were purchased from Sino Biological Inc. Recombinant Human Angiopoietin-2 (ANGPT2), CCL13, u-Plasminogen Activator/Urokinase (PLAU), IL24, Desert

Hedgehog (DHH), and PDGF-BB (PDGFB) were purchased from R&D system. EGFRi (EGFR/ErbB-2/ErbB-4 Inhibitor) was purchased from Calbiochem.

Microscale thermophoresis (MST). EGF receptor and EGFL7 were purchased from Sino biologics, 10001-H08H and 11979-H07B. EGF receptor (20mM) was labeled by L001 Monolith protein labeling kit RED-NHS. Labeled EGF receptor was diluted to about 67.7 nM in the binding reaction to optimize the intensity and stability of fluorescence signal. In each binding reaction, EGFL7 was reconstituted and diluted in a titration series from 5500 nM to 0.17 nM. The interaction between EGF receptor and EGFL7 was performed in PBST buffer (DPBS, Corning 21-031-CM, plus 0.05% tween 20). MST was monitored by NanoTemper MST monolith 115 in High-Throughput and Spectroscopy Resource Center at Rockefeller University.

Glucose stimulated insulin secretion. Glucose stimulated insulin secretion (GSIS) test of C57BL/6 control (WT, n=3) and Tie2:Egfl7-transgenic (TG, n=4) mice. Mice were starved for about 20 hours before the test. Blood samples were collected from mouse tail veins as the measurement of serum insulin level under fasting condition. 3g/kg glucose solution (300g/L) by mouse weight was injected. 15 minutes after injection, blood samples were collected again as the measurement of serum insulin level after glucose injection.

Glucose tolerance test. Glucose tolerance test was tested in C57BL/6 wild type (WT, n=2) and Tie2:Egfl7-transgenic (TG, n=4) mice. Blood glucose level (mg/dL) in each animal was measured before and every 15 minutes in the first

hour, and every 30 minutes in the second hour after glucose injection using AlphaTrak2.

Statistical Analysis. Unless otherwise stated in figure legends, P-values given are from *t* tests. Bonferroni correction was performed as a multiple comparison test. In all figures, data were presented as mean ± SD if not otherwise stated, and $P^* < 0.05$, $P^{**} < 0.01$, $P^{***} < 0.001$. N represents the number of independent experiments.

REFERENCES

1. E. Lammert, O. Cleaver, D. Melton, Induction of pancreatic differentiation by signals from blood vessels. *Science* **294**, 564-567 (2001).
2. S. K. Kim, M. Hebrok, D. A. Melton, Notochord to endoderm signaling is required for pancreas development. *Development* **124**, 4243-4252 (1997).
3. M. F. Offield, T. L. Jetton, P. A. Labosky, M. Ray, R. W. Stein, M. A. Magnuson, B. L. Hogan, C. V. Wright, PDX-1 is required for pancreatic outgrowth and differentiation of the rostral duodenum. *Development* **122**, 983-995 (1996).
4. J. Jonsson, L. Carlsson, T. Edlund, H. Edlund, Insulin-promoter-factor 1 is required for pancreas development in mice. *Nature* **371**, 606-609 (1994).
5. F. C. Pan, C. Wright, Pancreas organogenesis: from bud to plexus to gland. *Dev Dyn* **240**, 530-565 (2011).
6. D. Eberhard, M. Kragl, E. Lammert, 'Giving and taking': endothelial and beta-cells in the islets of Langerhans. *Trends Endocrinol Metab* **21**, 457-463 (2010).
7. H. Yoshitomi, K. S. Zaret, Endothelial cell interactions initiate dorsal pancreas development by selectively inducing the transcription factor Ptf1a. *Development* **131**, 807-817 (2004).
8. J. Magenheim, O. Ilovich, A. Lazarus, A. Klochendler, O. Ziv, R. Werman, A. Hija, O. Cleaver, E. Mishani, E. Keshet, Y. Dor, Blood vessels restrain pancreas branching, differentiation and growth. *Development* **138**, 4743-4752 (2011).
9. A. D. Association, Diagnosis and classification of diabetes mellitus. *Diabetes Care* **32 Suppl 1**, S62-67 (2009).
10. S. Wild, G. Roglic, A. Green, R. Sicree, H. King, Global prevalence of diabetes: estimates for the year 2000 and projections for 2030. *Diabetes Care* **27**, 1047-1053 (2004).
11. D. I. Kao, S. Chen, Pluripotent stem cell-derived pancreatic β-cells: potential for regenerative medicine in diabetes. *Regen Med* **7**, 583-593 (2012).
12. D. I. Kao, L. A. Lacko, B. S. Ding, C. Huang, K. Phung, G. Gu, S. Rafii, H. Stuhlmann, S. Chen, Endothelial Cells Control Pancreatic Cell Fate at Defined Stages through EGFL7 Signaling. *Stem Cell Reports* **4**, 181-189 (2015).
13. P. Jacquemin, H. Yoshitomi, Y. Kashima, G. G. Rousseau, F. P. Lemaigre, K. S. Zaret, An endothelial-mesenchymal relay pathway

regulates early phases of pancreas development. *Dev Biol* **290**, 189-199 (2006).
14. F. W. Sand, A. Hörnblad, J. K. Johansson, C. Lorén, J. Edsbagge, A. Ståhlberg, J. Magenheim, O. Ilovich, E. Mishani, Y. Dor, U. Ahlgren, H. Semb, Growth-limiting role of endothelial cells in endoderm development. *Dev Biol* **352**, 267-277 (2011).
15. Q. Cai, M. Brissova, R. B. Reinert, F. C. Pan, P. Brahmachary, M. Jeansson, A. Shostak, A. Radhika, G. Poffenberger, S. E. Quaggin, W. G. Jerome, D. J. Dumont, A. C. Powers, Enhanced expression of VEGF-A in β cells increases endothelial cell number but impairs islet morphogenesis and β cell proliferation. *Dev Biol* **367**, 40-54 (2012).
16. H. Kobayashi, J. M. Butler, R. O'Donnell, M. Kobayashi, B. S. Ding, B. Bonner, V. K. Chiu, D. J. Nolan, K. Shido, L. Benjamin, S. Rafii, Angiocrine factors from Akt-activated endothelial cells balance self-renewal and differentiation of haematopoietic stem cells. *Nat Cell Biol* **12**, 1046-1056 (2010).
17. S. Chen, M. Borowiak, J. L. Fox, R. Maehr, K. Osafune, L. Davidow, K. Lam, L. F. Peng, S. L. Schreiber, L. L. Rubin, D. Melton, A small molecule that directs differentiation of human ESCs into the pancreatic lineage. *Nat Chem Biol* **5**, 258-265 (2009).
18. M. Hebrok, S. K. Kim, B. St Jacques, A. P. McMahon, D. A. Melton, Regulation of pancreas development by hedgehog signaling. *Development* **127**, 4905-4913 (2000).
19. D. Nichol, C. Shawber, M. J. Fitch, K. Bambino, A. Sharma, J. Kitajewski, H. Stuhlmann, Impaired angiogenesis and altered Notch signaling in mice overexpressing endothelial Egfl7. *Blood* **116**, 6133-6143 (2010).
20. B. H. Luo, F. Xiong, J. P. Wang, J. H. Li, M. Zhong, Q. L. Liu, G. Q. Luo, X. J. Yang, N. Xiao, B. Xie, H. Xiao, R. J. Liu, C. S. Dong, K. S. Wang, J. F. Wen, Epidermal growth factor-like domain-containing protein 7 (EGFL7) enhances EGF receptor-AKT signaling, epithelial-mesenchymal transition, and metastasis of gastric cancer cells. *PLoS One* **9**, e99922 (2014).
21. F. Wu, L. Y. Yang, Y. F. Li, D. P. Ou, D. P. Chen, C. Fan, Novel role for epidermal growth factor-like domain 7 in metastasis of human hepatocellular carcinoma. *Hepatology* **50**, 1839-1850 (2009).
22. M. Jaramillo, I. Banerjee, Endothelial cell co-culture mediates maturation of human embryonic stem cell to pancreatic insulin producing cells in a directed differentiation approach. *J Vis Exp*, (2012).
23. M. Schmidt, K. Paes, A. De Mazière, T. Smyczek, S. Yang, A. Gray, D. French, I. Kasman, J. Klumperman, D. S. Rice, W. Ye, EGFL7 regulates the collective migration of endothelial cells by restricting their spatial distribution. *Development* **134**, 2913-2923 (2007).

24. M. J. Fitch, L. Campagnolo, F. Kuhnert, H. Stuhlmann, Egfl7, a novel epidermal growth factor-domain gene expressed in endothelial cells. *Dev Dyn* **230**, 316-324 (2004).
25. D. Zhang, W. Jiang, M. Liu, X. Sui, X. Yin, S. Chen, Y. Shi, H. Deng, Highly efficient differentiation of human ES cells and iPS cells into mature pancreatic insulin-producing cells. *Cell Res* **19**, 429-438 (2009).
26. T. Yokomizo, T. Yamada-Inagawa, A. D. Yzaguirre, M. J. Chen, N. A. Speck, E. Dzierzak, Whole-mount three-dimensional imaging of internally localized immunostained cells within mouse embryos. *Nat Protoc* **7**, 421-431 (2012).
27. K. A. Johansson, U. Dursun, N. Jordan, G. Gu, F. Beermann, G. Gradwohl, A. Grapin-Botton, Temporal control of neurogenin3 activity in pancreas progenitors reveals competence windows for the generation of different endocrine cell types. *Dev Cell* **12**, 457-465 (2007).

Chapter 3 – Novel expression of EGFL7 in placental trophoblast and endothelial cells and its implication in preeclampsia[*†]

3.1 – Rationale

The mammalian placenta is responsible for exchange of nutrients and gases between the mother and the fetus. It is a highly vascularized, transient organ that requires coordinated signaling to complete maternal vascular remodeling and fetal vasculogenesis and angiogenesis. Dysregulated placental development can result in placental pathologies, such as preeclampsia (PE), a disease that affects 2-8% of all pregnancies and accounts for 10-15% of maternal deaths each year (*1*). PE is characterized by the sudden onset of maternal hypertension and proteinuria after 20 weeks gestation. Despite being a leading cause of maternal and fetal morbidity and mortality, the only treatment for PE remains to be delivery of the placenta and fetus (*2*). Importantly, the resolution of maternal signs of PE after delivery of the placenta implicates this organ in the cause of the disease.

The American College of Obstetrics and Gynecology diagnoses PE when a patient presents with blood pressure greater than 140/90 mm Hg occurring more than once, combined with urinary protein greater than 300 mg/day (*3*), however many studies show that these criteria are inadequate as patient symptom presentation is variable. Work is underway to improve the diagnostic criteria for the disease (*4, 5*). Global endothelial dysfunction underlies the maternal signs of hypertension and proteinuria in PE (*6*). Hypertension results

---

[*] **Lacko LA**, Massimiani M, Sones JL, Hurtado R, Salvi S, Ferazzani S, Davisson RL, Campagnolo L, and Stuhlmann H. Novel expression of EGFL7 in placental trophoblast and endothelial cells and its implication in preeclampsia. Mechanisms of Development, 133, 163-176 (2014).

[†] **NOTE:* Human studies were performed by M. Massimiani, S. Salvi, S. Ferazzani and L. Campagnolo

from peripheral vasoconstriction, while proteinuria results from glomerular endotheliosis. Despite a great deal of research and advancements into the cause of PE, the pathophysiology of the disease remains largely unknown and early predictive diagnostics are lacking (*5, 7*).

PE is a multifactorial, multisystem disorder. Although the maternal signs present after 20-weeks, PE is thought to begin much earlier in gestation (*8, 9*). Furthermore, inadequate trophoblast cell invasion, dysregulated placental vascularization, and an altered immune response have been implicated in the pathophysiology of PE (*2, 6, 10*). Several groups have shown that an imbalance of pro- and anti- angiogenic growth factors underlies the cause of PE (*2, 6*). Under-perfused and under-vascularized placentas are predominantly seen in PE patients, which may result from dysregulated angiogenic signaling. Dysregulation of pro-angiogenic molecules Vascular Endothelial Growth Factor (VEGF), Placental Growth Factor (PlGF), and Transforming Growth Factor beta (TGFβ), as well as anti-angiogenic molecules soluble fms-like tyrosine kinase1 (sFlt1) and soluble Endoglin (sEng), have been associated with PE (*6*). It will be critical to understand the pathophysiology of PE and to develop novel predictive markers to better treat and diagnose patients with PE. Thus far, the most promising predictive measurement in PE has been the ratio of sFlt1 and PlGF, however, much work is still needed (*6, 11*).

Studies of placentation and placental pathologies have been limited by the lack of both the availability of human tissues early in gestation and animal models that faithfully recapitulate human placental development. Rodents and humans both exhibit hemochorial placentation, in which maternal blood comes in direct contact with the chorion. Primates are hemomonochorial and rodents are hemotrichorial, with one and three trophoblast cell layers separating maternal blood from the fetal endothelium (*12*). Mouse placentas are similar to humans

in their morphology, structure, and gene expression, and are also amenable to powerful genetic technologies, making them an attractive animal model for studying placentation (*12-14*). In this chapter, I will present a novel angiogenic factor that is dysregulated in preeclampsia in both the mouse and human, and define its spatiotemporal expression profile during placental development.

3.2 – Abstract

The mammalian placenta is the site of nutrient and gas exchange between the mother and fetus, and is comprised of two principal cell types, trophoblasts and endothelial cells. Proper placental development requires invasion and differentiation of trophoblast cells, together with coordinated fetal vasculogenesis and maternal vascular remodeling. Disruption in these processes can result in placental pathologies such as preeclampsia (PE), a disease characterized by late gestational hypertension and proteinuria. Epidermal Growth Factor Like Domain 7 (EGFL7) is a largely endothelial-restricted secreted factor that is critical for embryonic vascular development, and functions by modulating the Notch signaling pathway. However, the role of EGFL7 in placental development remains unknown. In this study, we use mouse models and human placentas to begin to understand the role of EGFL7 during normal and pathological placentation. We show that Egfl7 is expressed by the endothelium of both the maternal and fetal vasculature throughout placental development. Importantly, we uncovered a previously unknown site of EGFL7 expression in the trophoblast cell lineage, including the trophectoderm, trophoblast stem cells, and placental trophoblasts. Our results demonstrate significantly reduced Egfl7 expression in human PE placentas, concurrent with

a downregulation of Notch target genes. Moreover, using the BPH/5 mouse model of PE, we show that the downregulation of Egfl7 in compromised placentas occurs prior to the onset of characteristic maternal signs of PE. Together, our results implicate Egfl7 as a possible factor in normal placental development and in the etiology of PE.

3.3 – Introduction

The placenta serves as the site of contact for the maternal and embryonic circulatory systems to enable nutrient and gas exchange, and contains two primary functional cell types, trophoblasts and endothelial cells. Proper placental development requires invasion and differentiation of trophoblast cells, as well as coordinated maternal vascular remodeling and fetal vasculogenesis (*15*). Any disruption in these processes can result in placental pathologies, including preeclampsia (PE). PE is a leading cause of maternal and fetal morbidity and mortality worldwide, and the only resolutive treatment is delivery of the baby and placenta. Although the pathophysiology of PE remains largely unknown, inadequate trophoblast cell invasion, endothelial cell dysfunction, dysregulated uteroplacental vascularization, and an imbalance of pro- and anti-angiogenic growth factors have been implicated in the disease (*2*).

Recent studies have implicated Notch signaling, an evolutionarily conserved pathway that is important for cell fate specification, proliferation, and patterning (*16*), in placental development and the pathogenesis of PE. Targeted mutations of Notch signaling components in the mouse result in placental defects, demonstrating their vital roles for proper placental development (*17-20*). In

addition, Notch pathway proteins are downregulated in trophoblast cells, endothelial cells, and stromal cells of third trimester placentas from human preeclamptic patients as compared to normal patients (*21*).

Epidermal Growth Factor Like Domain 7 (EGFL7) is a secreted factor that is present in both soluble and extracellular matrix-bound forms (*22*). Egfl7 expression in the developing embryo is largely restricted to endothelial progenitors and actively proliferating endothelium (*22-24*). However, it is also found in embryonic stem cells, pre- and peri-implantation embryos, primordial germ cells, and some CNS neurons (*22, 24-27*). EGFL7 is largely downregulated during late embryogenesis and in the quiescent endothelium of the adult mouse, and is upregulated during pathological and physiological angiogenesis, such as in the uterus (*22-24*). Egfl7 is upregulated in response to, and has a protective effect against, hypoxia (*28-30*). It acts as a chemoattractant for endothelial cells and plays an important role in their proliferation and migration (*23, 31, 32*). EGFL7 functions in vascular patterning, stratification, and tubulogenesis *in vitro* and in the mouse and zebrafish (*23, 26, 32, 33*). EGFL7 has been shown to modulate the Notch signaling cascade by acting either as a Notch agonist, such as in the developing embryo, or as a Notch antagonist, such as in the postnatal retina and neural stem cells (*27, 33*).

Despite its key role in early embryogenesis, vascular development, and modulation of Notch signaling, the expression pattern and function of EGFL7 in normal and PE placentas is poorly understood. In this study, we investigated the expression pattern of EGFL7 in normal murine and human placentas. Rodents and primates both undergo hemochorial placentation (*34*). Despite some structural differences, the trophoblast cell types and the molecular

pathways driving placental development are highly conserved between mouse and human (*13, 14, 34, 35*). Importantly, the labyrinth in the mouse placenta is analogous to the chorionic villi in human placentas, whereas the junctional zone in mice is analogous to the cytotrophoblast cell columns (*14*) or the basal plate in humans (*13*).

In addition to examining the expression profile of Egfl7 during normal placental development, this study investigates a potential role for EGFL7 in preeclampsia by analyzing human PE placentas and compromised placentas from the BPH/5 murine PE model. The BPH/5 mouse strain exhibits the characteristic PE signs of late-gestational hypertension, proteinuria, and endothelial dysfunction (*36, 37*). BPH/5 mice also show fetoplacental defects such as impaired endothelial cell branching, maternal spiral artery remodeling, and reduced fetal labyrinth depth (*37*). Here we have described the spatiotemporal expression profile of Egfl7 in placental endothelial cells in the mouse and human. We uncovered a previously unknown site of EGFL7 localization in the non-endothelial trophoblast lineage, beginning at the blastocyst stage and becoming restricted to a subset of differentiated trophoblast cells. Furthermore, we provide evidence that a downregulation of EGFL7 is associated with human PE and the BPH/5 mouse model of PE, and this downregulation is concomitant with a decrease in Notch target gene expression.

3.4 – Results

3.4.1 – EGFL7 is expressed by maternal and fetal endothelial cells in the mouse placenta throughout gestation

To obtain a temporal and spatial expression profile for Egfl7 throughout pregnancy, we used the mouse as a model system. To localize expression of Egfl7 transcripts in the maternal and fetal placental vasculature, RNA in situ hybridization (ISH) was performed on 100μm thick vibratome sections of C57BL/6 mouse placentas using an Egfl7 specific riboprobe. Egfl7 transcripts were highly expressed at E10.5, and were localized to maternal vessels, including the spiral arteries of the decidua (**Figure 3.1A,B**), and the branching vascular structures in the fetal labyrinth (**Figure 3.1A,C**). Following ISH, specimens were embedded in paraffin, sectioned, and counterstained to analyze the cellular morphology of Egfl7 mRNA expression in the placenta. Results revealed Egfl7 transcript expression in cells lining the large lumen of maternal vessels in the decidua (**Figure 3.1D**) and in the narrow and highly branched capillaries of the fetal labyrinth (**Figure 3.1E**). Egfl7 transcript levels were dramatically reduced at E12.5 and nearly undetectable at E18.5 (**Supplemental Figure 3.1**). Egfl7 sense controls (insets of **Figure 3.1A, Supplemental Figure 3.1A,C**) demonstrate specificity of the Egfl7 riboprobe.

To determine the spatiotemporal expression profile of EGFL7 protein, we performed double immunofluorescent staining for EGFL7 and the pan-endothelial marker, CD31, on C57BL/6 mouse placentas (**Figure 3.1-F-M**, **Supplemental Figure 3.2**). EGFL7 colocalized with CD31 in the maternal

decidua and the fetal labyrinth at every stage examined, confirming that EGFL7 localized to maternal and fetal endothelial cells in the placenta.

Together, the results demonstrate that Egfl7 transcript and protein expression was dynamic throughout gestation. Egfl7 expression is high during early stages of vascular development in the placenta, with transcript expression peaking at E10.5 (**Figure 3.1A-E**), as well as high protein expression at E10.5 and E12.5 (**Figure 3.1F-M, Supplemental Figure 3.2A**). At E18.5, a time point with fewer newly forming nascent vessels, Egfl7 transcript expression is dramatically lower (**Supplemental Figure 3.1D**), while the protein expression persists (**Supplemental Figure 3.2B**). Our data are consistent with previously reported Egfl7 expression data during vascular development and physiological angiogenesis, where the highest expression levels of Egfl7 are detected in actively proliferating endothelial cells, such as during formation of the initial vascular plexus during early embryogenesis (*22, 23, 25, 26, 31-33*).

3.4.2 – Novel EGFL7 expression in placental trophoblast cells and the trophoblast cell lineage

In addition to demonstrating dynamic expression of EGFL7 in the placental endothelium, our in situ hybridization images at high magnification also uncovered a novel expression domain for Egfl7 in non-endothelial cells of the junctional zone of the mouse placenta, albeit at reduced levels (**Figure 3.2A-B**). Images of Egfl7 ISH paraffin sections revealed clusters of EGFL7 positive

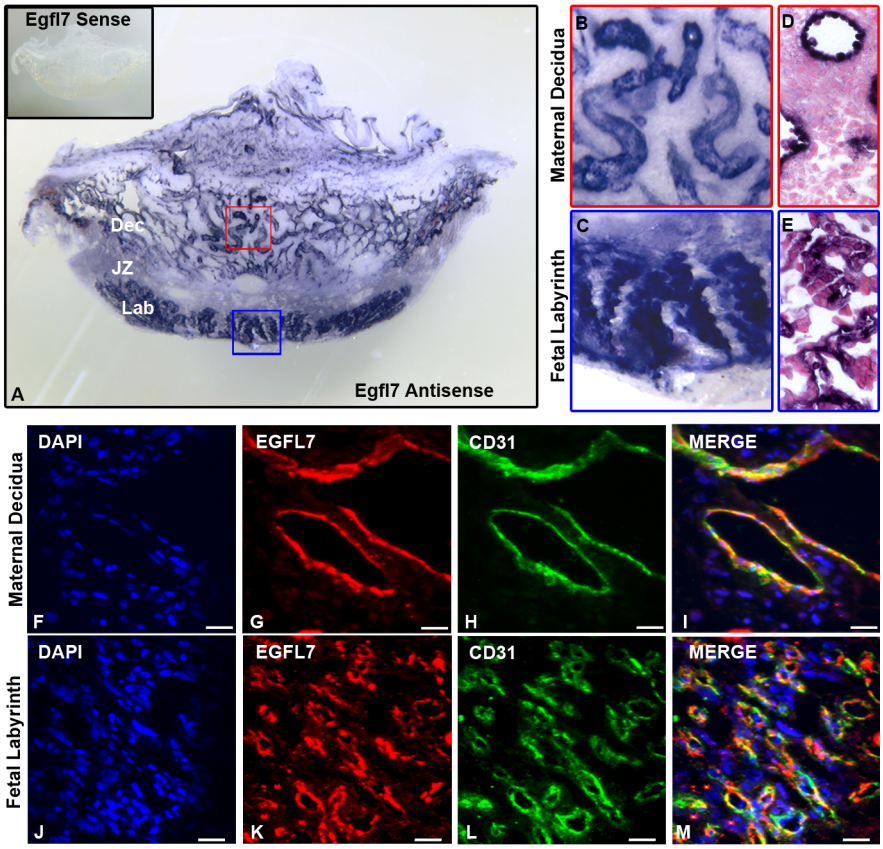

Figure 3.1 EGFL7 is expressed by maternal and fetal endothelial cells in the mouse placenta. In situ hybridization was performed to determine Egfl7 mRNA localization, using an Egfl7 riboprobe on 100μm thick vibratome sections of E10.5 C57BL/6 placentas **(A-E)**. Higher magnification images of boxes in **(A)** demonstrating Egfl7 transcript is highly expressed in the maternal decidua **(B)** and fetal labyrinth **(C)**. Egfl7 sense controls **(A** inset**)** show specificity of Egfl7 riboprobe. Paraffin sections of the vibratome sections showing cellular morphology after Egfl7 riboprobe staining in the maternal decidua **(D)** and fetal labyrinth **(E)**. To determine the cell types expressing EGFL7 protein in the placenta, double immunofluorescent staining was performed on E12.5 C57BL/6 placentas for EGFL7 (red), CD31 (green) and nuclear DAPI (blue) **(F-M)**. EGFL7 colocalizes with the endothelial cell marker, CD31, in the maternal decidua **(F-I)** and the fetal labyrinth **(J-M)**. Dec-Maternal Decidua, JZ-Junctional Zone, Lab-Fetal Labyrinth. Scale bar (F-M) = 20μm.

cells located in the junctional zone, between the fetal labyrinth and trophoblast giant cells (**Figure 3.2B**). Double immunofluorescent staining for EGFL7 and the pan-trophoblast marker CYTOKERATIN (CK), performed on mid-gestation mouse placentas confirmed EGFL7 localization to the trophoblast lineage (**Figure 3.2C-F**). This is the first evidence that EGFL7 localizes to trophoblast cells of the placenta. The newly uncovered expression of EGFL7 in placental trophoblast cells prompted us to examine its temporal expression pattern during trophoblast lineage development in mice. Differentiated trophoblast cells are derived from the outer cell layer of blastocysts, the trophectoderm (*38*). We have previously shown that Egfl7 mRNA was expressed by blastocysts and embryonic stem cells, however its spatial expression in pre-implantation embryos was not defined (*23, 25*). Here, we isolated embryos from C57BL/6 mice at the blastocyst stage of development and performed whole-mount immunofluorescent staining for EGFL7 and the trophectoderm marker, CDX2. Both inner cell mass cells and trophectoderm cells expressed EGFL7 (**Figure 3.2G-J**). Therefore, Egfl7 is expressed at the first step of trophoblast lineage development.

To further establish EGFL7 expression in the trophoblast lineage, we assayed trophoblast stem cells (TSC), a model of *in vitro* trophoblast cell differentiation. Multipotent TSC are derived from the trophectoderm of blastocysts, and upon removal of exogenous Fibroblast Growth Factor, they recapitulate the defining characteristics of *in vivo* trophoblast cell differentiation (*39*). Semi-quantitative and Real Time RT-PCR analysis showed that TSC express Egfl7 mRNA at significantly higher levels than embryonic stem cells (ESC), whereas primary mouse embryonic fibroblasts (MEF) express very low levels of Egfl7 (**Figure**

Figure 3.2 EGFL7 is expressed in the trophoblast cell lineage of the mouse. In situ hybridization was performed to determine Egfl7 mRNA localization, using an Egfl7 riboprobe on 100μm thick vibratome sections of E10.5 C57BL/6 placentas **(A)**. Shown is the junctional zone of the placenta **(A)**. Paraffin sections of the vibratome section showing cellular morphology of Egfl7 riboprobe staining in the junctional zone of the placenta **(B)**. Arrows indicate positive Egfl7 transcript signal in the junctional zone trophoblast cells. (TGC=Trophoblast Giant Cell). To determine the cell type expressing EGFL7 protein in the placenta, double immunofluorescent staining was performed on E10.5 C57BL/6 placentas **(C-F)** for the pan-trophoblast marker, CYTOKERATIN (CK, red), EGFL7 (green), and nuclear DAPI (blue). Cross-section of E10.5 placenta showing the fetal labyrinth (Lab), junctional zone (JZ, demarked by white lines) and maternal decidua (Dec). High magnification images **(D-F)** of the junctional zone demonstrating colocalization of EGFL7 with CK in the JZ trophoblast cells (arrows). Whole mount immunofluorescent staining of blastocyst-stage C57BL/6 embryos **(G-J)** for DAPI (blue), EGFL7 (red), and trophectoderm cell marker, CDX2 (green) reveals EGFL7 protein localization to both inner cell mass (ICM) cells and trophectoderm cells (arrowheads). Real Time RT-PCR data for Egfl7 transcript expression in trophoblast stem cells (TSC), embryonic stem cells (ESC), and mouse embryonic fibroblasts (MEF), shows a significantly higher level of Egfl7 expression in TSC, ***P<0.01* **(K**, top**)**. Agarose gel with products of semi-quantitative RT-PCR for TSC, ESC and MEFs are shown, using *Egfl7* and *β-actin* specific primers **(K**, bottom**)**. RNA in situ hybridization analysis of Egfl7 mRNA in TSC **(L-O)** defines Egfl7 transcript expression in TSC. Phase-contrast and bright-field images of TSC incubated with an Egfl7 sense control probe **(L-M)**, and an Egfl7 antisense probe **(N-O)**. Double immunofluorescent staining of TSC **(P-T)** for DAPI, EGFL7, and CDX2 demonstrating EGFL7 protein localization to TSC. Phase-contrast image of TSC colony is shown in **(P)**. Scale bars in D-F=25μm, G-J=20μm, C and L-T=100μm.

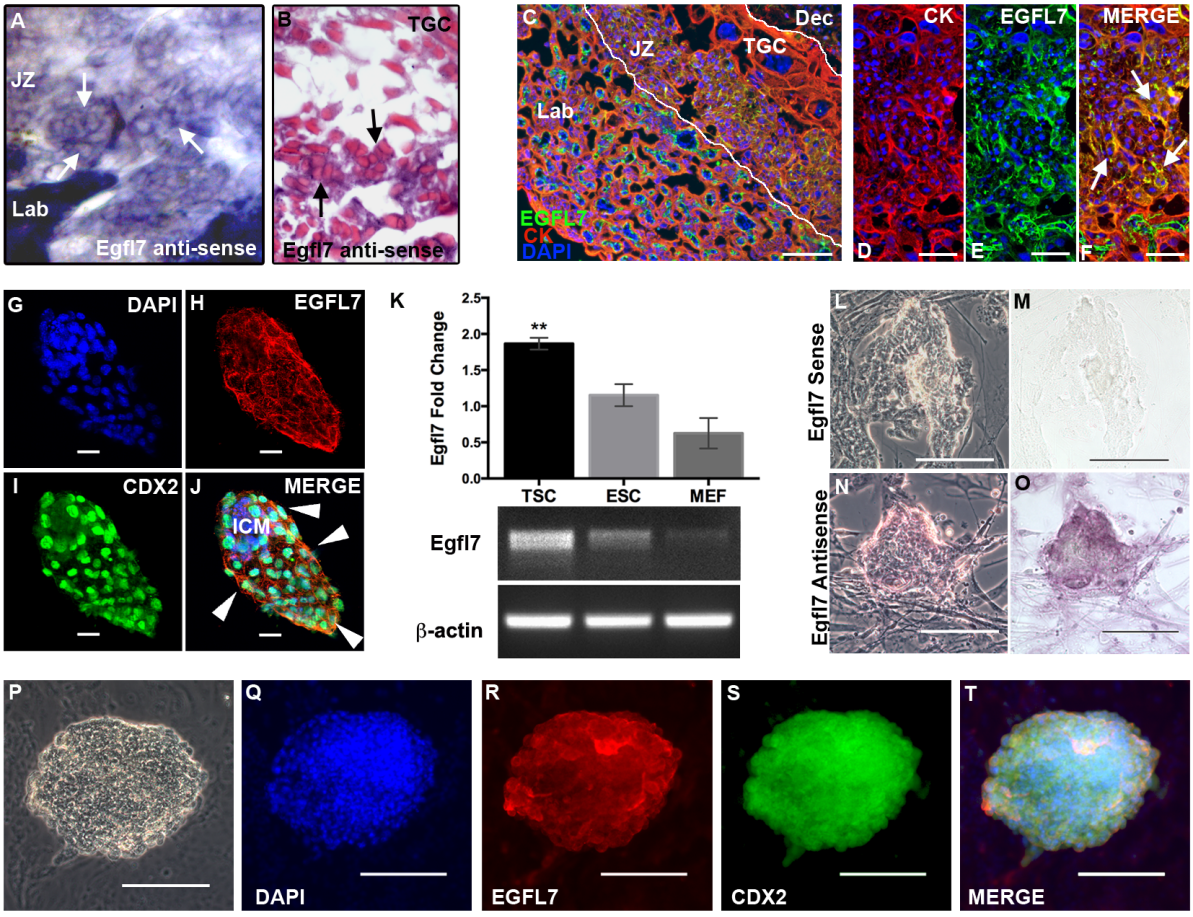
A
JZ
Lab
Egfl7 anti-sense
B
TGC
Egfl7 anti-sense
C
Dec
JZ
TGC
Lab
EGFL7
CK
DAPI
CK
EGFL7
MERGE
D
E
F
G
DAPI
H
EGFL7
I
CDX2
J
MERGE
ICM
K
Egfl7 Fold Change
2.5
2.0
1.5
1.0
0.5
0.0
**
TSC
ESC
MEF
Egfl7
β-actin
L
M
Egfl7 Sense
N
O
Egfl7 Antisense
P
Q
DAPI
R
EGFL7
S
CDX2
T
MERGE

3.2K, *P<0.01*). RNA in situ hybridization on TSC revealed specific localization of Egfl7 mRNA in TSC (**Figure 3.2L-O**). EGFL7 protein was detected on cultured TSC, as shown by colocalization of EGFL7 and CDX2 using double immunofluorescent staining (**Figure 3.2P-T**). Two additional antibodies that are directed against different regions of the EGFL7 protein gave comparable results (data not shown). Together, our results show that EGFL7 is expressed by the trophectoderm of blastocysts, in trophoblast stem cells, and a subset of differentiated trophoblast cells in the mid-gestation mouse placenta.

3.4.3 – EGFL7 is expressed by fetal endothelial cells and trophoblast cells of human chorionic villi

To determine if EGFL7 expression in endothelial and trophoblast cells is conserved in human placentas, chorionic villi samples were obtained from normal pregnant women with an average pregnancy duration of 39 weeks. Double immunofluorescent staining analysis revealed that EGFL7 was expressed on fetal vessels, where it colocalized with the pan-endothelial marker, CD31 (**Figure 3.3A-D**). Importantly, EGFL7 was also expressed on the syncytiotrophoblast layer of the villi, where it colocalized with the pan-trophoblast marker CYTOKERATIN (**Figure 3.3E-H**). To confirm this observation, EGFL7 staining was performed using two antibodies directed against different regions of the EGFL7 protein, and both gave comparable results (**Supplemental Figure 3.3**). Of note, expression of Egfl7 was not detected in the analogous mouse syncytiotrophoblasts. To further determine if EGFL7 localized to trophoblast cells of the human placenta, we isolated

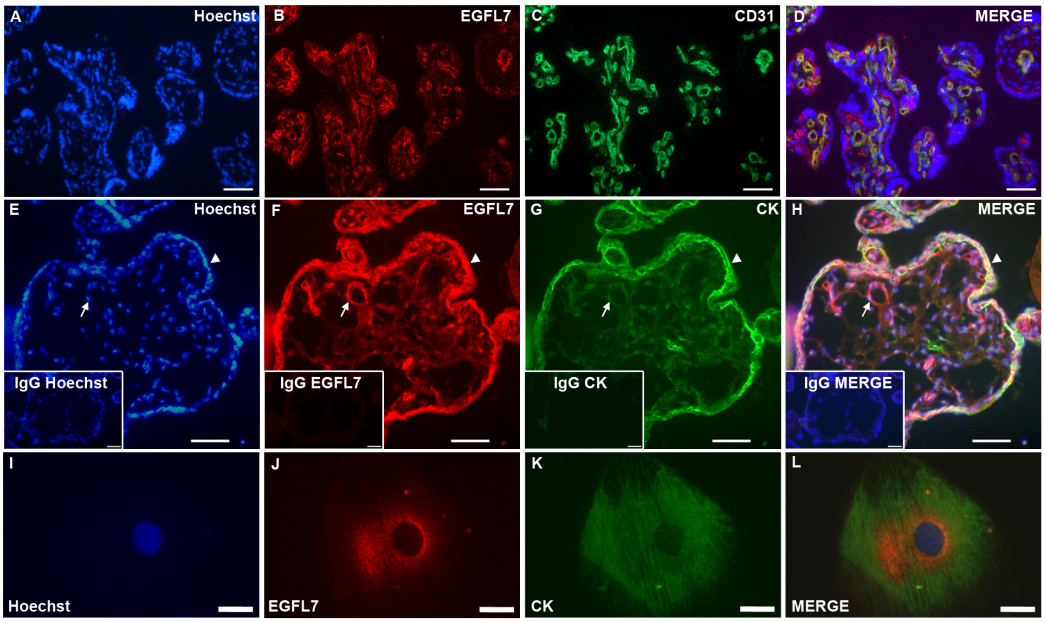

Figure 3.3 EGFL7 is expressed in endothelial cells and trophoblast cells of the human placenta. Double immunofluorescent staining of normal human placentas **(A-D)** for EGFL7 (red), CD31 (green), and nuclear DAPI (blue) showing localization of EGFL7 protein on endothelial cells. Double immunofluorescent staining of human chorionic villi from placentas at 40-weeks of gestation **(E-H)** for nuclear DAPI (blue), EGFL7 (red), and pan-trophoblast marker CYTOKERATIN (CK) (green) demonstrates EGFL7 protein localization to trophoblast cells (arrows-fetal vessels, arrowheads-trophoblasts). Control staining of a close-by section **(insets, E-H)** using IgG and secondary antibodies only and nuclear Hoechst (blue) shows specificity of the antibodies. Expression of EGFL7 protein is found in human cytotrophoblast cells isolated from term placentas **(I-L)**. Cells were stained for Hoechst (blue), EGFL7 (red) and CYTOKERATIN (green) **(I-L)**. Scale bars in E-H and insets =100μm, and I-L=30μm.

cytotrophoblast cells from term placentas as previously described (*40*). Double immunofluorescent staining showed that EGFL7 and CYTOKERATIN colocalized to the isolated cytotrophoblast cell (**Figure 3.3I-L**). Thus, our data demonstrate that EGFL7 is expressed in endothelial cells and trophoblast cells in both mouse and human placentas.

3.4.4 – EGFL7 is downregulated in placentas of the BPH/5 mouse model of PE, prior to the onset of maternal signs of PE

To examine potential variations in the expression and spatial distribution of EGFL7 in PE, we first utilized the BPH/5 mouse model of preeclampsia. E10.5 placentas from control C57BL/6 and compromised BPH/5 fetoplacental units (see Materials and Methods) were subjected to immunofluorescent staining for EGFL7 and CD31 (**Figure 3.4B-I**). Importantly, this time point is prior to the onset of the late-gestational signs of PE in BPH/5 mice (*36*). EGFL7 protein expression was reduced in the fetal labyrinth zone of the BPH/5 placentas compared to C57BL/6 (**Figure 3.4C,G**). Total levels of CD31 appear unchanged (**Figure 3.4D-E,H-I**), suggesting no overall reduction in placental vascular density. The pattern of the vessels, however, appears irregular in BPH/5 placentas. In fact, a previous study reported the anatomical appearance of attenuated and irregularly branched fetal vessels in isolectin B4-stained BPH/5 placentas (*37*). To provide quantitative evidence, we performed Real Time RT-PCR analysis of E10.5 placentas from C57BL/6 and affected BPH/5 fetoplacental units for Egfl7. Results demonstrated that Egfl7 mRNA levels were significantly downregulated in BPH/5 placentas compared to C57BL/6 (**Figure 3.4A,** **P<0.05*).

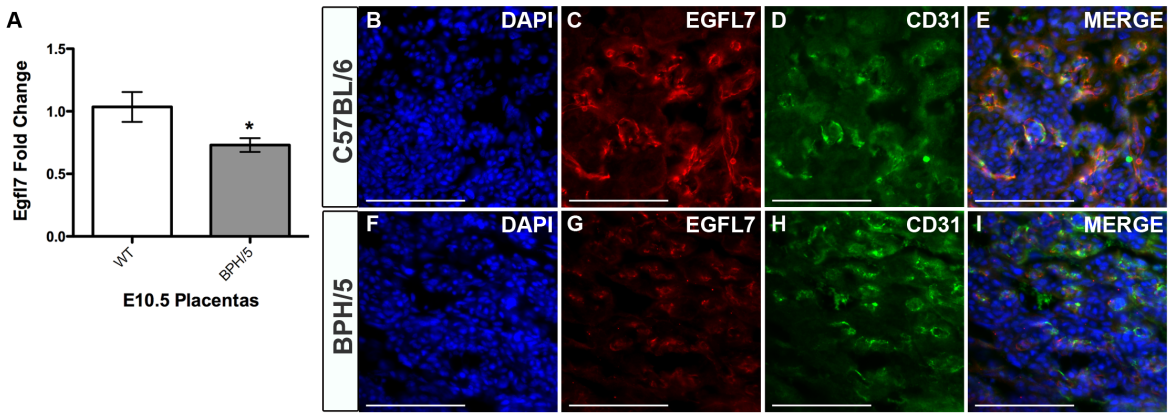

Figure 3.4 EGFL7 is downregulated in the placentas of the BPH/5 mouse model of preeclampsia. Real Time RT-PCR data for Egfl7 transcript levels in E10.5 placentas from C57BL/6 (WT) and BPH/5 mice reveal a significant decrease in Egfl7 in BPH/5 mice *$P<0.05$ **(A)**. Immunofluorescent staining for EGFL7 protein (red), CD31 (green), and nuclear DAPI (blue) on the fetal labyrinth of E10.5 placentas from C57BL/6 **(B-E)** and BPH/5 mice **(F-I)** demonstrating a decrease in EGFL7 in BPH/5 placentas. Scale bar=100μm.

3.4.5 – EGFL7 expression is significantly reduced in human preeclamptic placentas

Our results in the mouse model of PE prompted us to investigate potential variations in the expression of EGFL7 in human PE placentas. Biopsies from normal and PE human placentas were obtained and analyzed. Clinical characteristics of patients in this study are shown in **Table 3.1** (*41*). The study group consisted of ten early-onset preeclamptic patients with average pregnancy duration of 32 weeks. The control group consisted of ten healthy pregnant women with average pregnancy duration of 39 weeks. All patients underwent Caesarean sections. There were no differences in patient age at delivery, gravidity, or parity between the study and control groups. However, the study group exhibited lower neonatal birth weight and placental weight, higher systolic and diastolic pressure, and earlier gestational age, all of which are characteristic of PE patients.

To examine the EGFL7 protein expression profile of normal and PE placentas, we performed immunofluorescent staining for EGFL7 and CD31 on human placental biopsies (**Figure 3.5A-F**). EGFL7 was immunodetected on the endothelium and trophoblast cells of the human placenta. When comparing immunofluorescent staining of normal and PE placentas, EGFL7 appeared lower in both endothelial and trophoblast cells of PE placentas (**Figure 3.5A-B**)**,** whereas no major differences were observed for CD31 (**Figure 3.5C-D**).

To quantify this observation, we performed Real-Time RT-PCR analysis on normal and PE samples for EGFL7 (**Figure 3.5G**) and CD31 (**Figure 3.5H**).

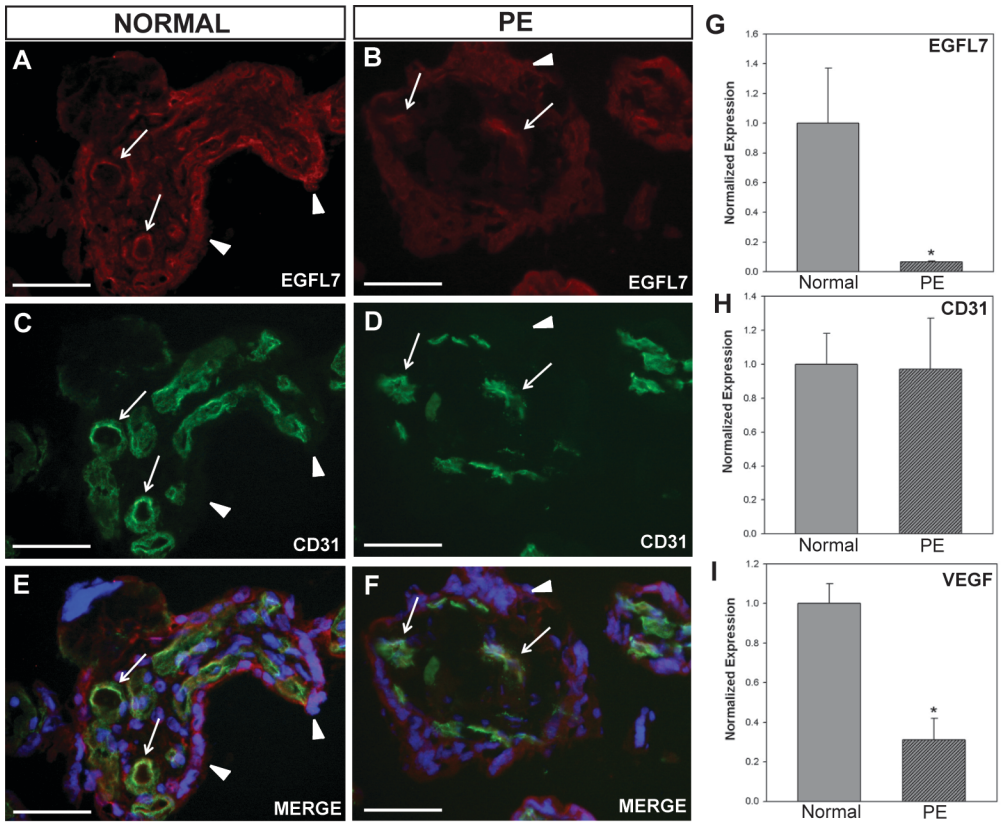

<u>Figure 3.5</u> EGFL7 is significantly reduced in human preeclamptic placentas. Double immunofluorescent staining of normal and preeclamptic (PE) human placentas **(A-F)** for EGFL7 protein (red), CD31 (green), and nuclear Hoechst (blue) revealing a decrease in EGFL7 protein in PE placentas (arrows-fetal vessels, arrowheads-trophoblasts). Real Time RT-PCR data for EGFL7 **(G)**, CD31 **(H)**, and VEGF **(I)** on normal and preeclamptic (PE) human placentas demonstrating a significant decrease in EGFL7 transcript levels in PE placentas, even further than the known angiogenic factor, VEGF (n=10, **P<0.05*). Scale bars = 50μm.

EGFL7 mRNA expression was significantly decreased by more than 10-fold in PE when compared to normal placentas (*$P<0.05$). In contrast, no significant difference in the level of CD31 mRNA was detected, suggesting the difference in EGFL7 transcript levels was not due to an overall reduced expression of endothelial-specific genes or a reduction in vascular density (*33, 42-44*). In our study, the reduction in EGFL7 levels in PE was more pronounced as compared to VEGF levels (**Figure 3.5I**), a growth factor whose implication in PE has been extensively studied by others, and found to be either decreased (*45-47*) or increased (*48-50*) in PE placentas. Thus, EGFL7 expression is significantly downregulated in both a mouse model of PE and human PE placentas.

3.4.6 – EGFL7 expression correlates with NOTCH signaling in normal and PE placentas

Previous studies demonstrated that EGFL7 interacts with and modulates NOTCH signaling *in vitro* and *in vivo* (*27, 33*). To examine if EGFL7 and the Notch signaling pathway are concomitantly dysregulated in PE, we performed Real-Time RT-PCR analysis of normal and human PE placentas for NOTCH pathway members and NOTCH target genes. Our results demonstrated a significant decrease in NOTCH1, NOTCH4, HEY2, HEY1, and HES1 mRNA expression ($P<0.05$), and a downward trend in NOTCH2 expression in PE samples when compared to normal placentas (**Figure 3.6 A-F**). In contrast, transcript levels for the Notch ligands DLL4 and JAGGED1 were unchanged (**Figure 3.6 G-H**). Additionally, double immunofluorescent staining of human placentas revealed that EGFL7 colocalized with NOTCH4 on the syncytiotrophoblast cells (**Figure 3.6 I-K**). Thus, downregulation of NOTCH

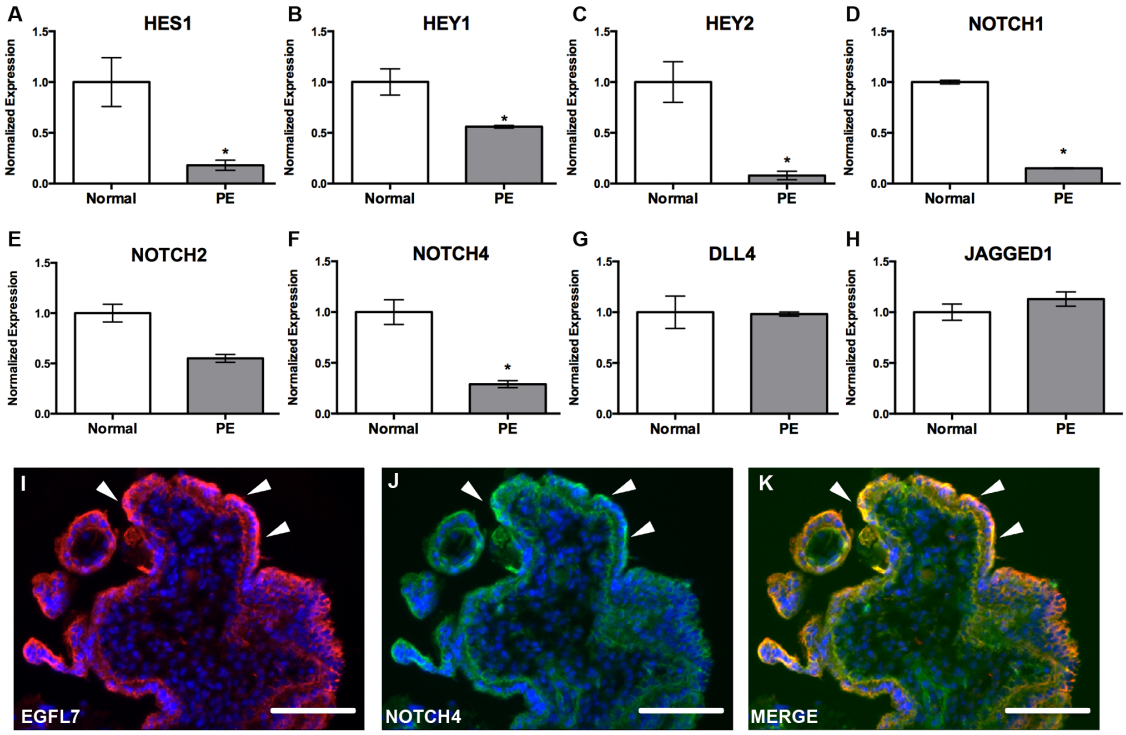

<u>Figure 3.6</u> Expression of NOTCH target genes and NOTCH receptors are downregulated in PE, concomitant with EGFL7. Real Time RT-PCR data for NOTCH pathway members on normal and preeclamptic (PE) human placentas **(A-H)**. Gene expression analysis for HES1 **(A)**, HEY1 **(B)**, and HEY2 **(C)** demonstrating a significant decrease in all NOTCH target gene transcripts in PE. Gene expression analysis for NOTCH receptors NOTCH1 **(D)**, NOTCH2 **(E)**, and NOTCH4 **(F)** demonstrating a significant downregulation in NOTCH1 and NOTCH4, and a downward trend in NOTCH2 in PE patients. Gene expression analysis indicating no change in NOTCH ligands DLL4 **(G)** and JAGGED1 **(H)**. (n=3-7, **P<0.05*). Immunofluorescent staining of a cross section of human villi **(I-K)** for EGFL7 (red), NOTCH4 (green), and Hoechst (blue) (arrowheads-trophoblasts) shows colocalization of EGFL7 protein and NOTCH4. (**P<0.05*) Scale bars = 50μm.

signaling members and NOTCH target gene expression correlate with a downregulation of EGFL7 in PE placentas, suggesting that EGFL7 may possibly function through the Notch signaling pathway.

3.5 – Discussion

PE is a complex placental disease that occurs in approximately 2-7.5% of pregnancies worldwide (*51, 52*), yet the etiology of the disease remains unknown and early predictive biomarkers are lacking. Research on the human placenta has mostly been limited to studying the organ at late gestation and full term. To fully understand the early causes and progression of this placental disease, it is crucial to employ appropriate animal and *in vitro* models. Our results show that expression of EGFL7 is significantly reduced in compromised placentas from the BPH/5 mouse model of PE compared to control mice. These findings are corroborated by our results from human PE samples. Importantly, reduced EGFL7 expression in PE placentas did not correlate with reduced expression of the pan-endothelial marker CD31 or reduced density of CD31-positive vessels. This suggests that the change in EGFL7 was not a consequence of reduced vascular density. However, as a caveat, CD31 transcript expression is an indirect indicator for endothelial cell content and therefore may vary from the total vascular density in the placenta.

Of interest to this study, EGFL7 was identified in two recent microarray studies as one of the genes significantly reduced in human PE placentas compared to normal placentas, consistent with our data (*53, 54*). Importantly, PE is thought to begin much earlier in gestation than when the late-stage human placental

biopsies used in most studies are obtained (*8, 9*). Our results describe changes in EGFL7 expression in phenotypically abnormal placentas of a PE mouse model, prior to the onset of characteristic maternal signs of PE, suggesting EGFL7 may be an early biomarker for the disease. It would be of interest to determine whether EGFL7 is altered in phenotypically abnormal placentas of other placental pathologies.

Moreover, we have shown that EGFL7 is downregulated in human placentas of early-onset PE patients. Formally, we cannot rule out the possibility that the difference in EGFL7 expression is due to a difference in gestational age (PE: week-32 versus Normal: average of 39-week gestation). However, analysis of a single placenta at week-34 of gestation from a normal pregnancy indicated that EGFL7 expression levels were similar to those in normal term placentas (data not shown). Furthermore, both early onset PE and intrauterine growth restriction (IUGR) are associated with abnormal placentation and changes in plasma levels of placental angiogenic factors, but IUGR does not present with the maternal signs of hypertension and proteinuria. A recent study demonstrated that isolated IUGR with no maternal disease is associated with the same changes in placental angiogenic factors and subclinical endothelial dysfunction as in PE (*55*), suggesting the only difference between these two diseases may be maternal manifestations of the disease. Early-onset PE, which manifests by maternal hypertension and proteinuria, and progresses to a systemic hypoperfusion of multiple maternal organs, is often accompanied by abnormal fetal growth (*56*), as in the cases of our study (9/10; 90%). Therefore, reduced EGFL7 expression correlates with abnormal placentation that may be associated with either early-onset PE or isolated IUGR. Contribution of

additional facilitating factors, possibly at the level of maternal predisposition, may influence the manifestation of maternal hypertension and proteinuria.

Previously, EGFL7 expression was thought to be restricted to actively proliferating vascular endothelium and to embryonic stem cells (*22, 25, 27*). Our study has used multiple methods to uncover a novel and dynamic expression pattern for Egfl7 during murine placental development. Egfl7 is expressed highly in the fetal and maternal vasculature of the placenta. Its highly regulated expression pattern that correlates with expression during embryonic development suggests a potential angiogenic role in placental angiogenesis. Notably, in addition to its expression in the fetal and maternal vessels of the placenta, we showed, for the first time, that Egfl7 was also expressed in the trophoblast cell lineage, beginning at the blastocyst stage and becoming restricted to a subset of differentiated trophoblast cells in the mature placenta. Trophoblast cells are the principal non-endothelial cell populations at the fetal-maternal interface. Targeted mutations in genes important for trophoblast cell differentiation result in placental defects or complete loss of placenta formation (*38*). Interestingly, knockdown of Egfl7 in ESC decreases the proliferation rate of undifferentiated ESC and impairs endothelial cord formation in an embryoid body model of ESC differentiation (*32*). Determining the role of Egfl7 in TSC and trophoblasts will be crucial for understanding the molecular mechanisms that control trophoblast lineage development and formation of the placenta.

EGFL7 has previously been shown to colocalize and functionally interact with NOTCH to modulate Notch signaling (*27, 33*). Notch signaling is a crucial

pathway for placental development that affects both trophoblast and vascular cell function. For example, mouse strains with targeted deletions in the Notch receptors *Notch1/4*, their ligand *Dll4,* Notch target genes *Hey1/2*, or the Notch nuclear co-activator *RBPJ*κ show defects in chorioallantoic branching and fetal placental angiogenesis (*17-19, 57-61*). *Mash2*, a basic helix-loop-helix transcription factor that is thought to be repressed by the Notch target *Hes1* (*61*), is critical for trophoblast cell fate specification in the mouse (*62*). *Notch2* receptor function is crucial for formation of maternal blood sinuses and maternal spiral artery and arterial canal remodeling (*20, 63*). A recent study demonstrated that the Notch2 receptor is prominently expressed in the junctional zone trophoblast cells at E10.5 (*64*), as is EGFL7. It would be of interest to determine if EGFL7 functionally interacts with NOTCH2 in the placental junctional zone. Here we showed that NOTCH4 colocalized with EGFL7 in the placenta, and that downregulation of EGFL7 coincided with a reduction in Notch target gene expression in human PE placentas. Together, our results suggest EGFL7 may act, at least in part, as a NOTCH agonist in the placenta. Interestingly, whereas Egfl7 was found to act as an antagonist of Notch postnatally and in HUVECs (*27, 33*), embryonic overexpression of Egfl7 significantly increased Hey1 and Hey2 transcript levels, consistent with acting as a Notch agonist during embryogenesis (*33*). It will be important to further explore the functional relationship between EGFL7 and the Notch signaling pathway during placental development, in addition to other pathways through which EGFL7 may be functioning.

EGFL7 gain- and loss-of-function approaches will help to fully understand the role of EGFL7 in the placenta and in placentopathies, and to dissect the

underlying mechanism in both trophoblast cells and endothelial cells. It will be important to examine if endothelial and/or trophoblast-derived EGFL7 acts as an angiogenic factor in the placenta and if secreted EGFL7 acts in an autocrine or paracrine fashion, as has been suggested (*65*). Of interest, partial embryonic lethality at mid-gestation was reported in the EGFL7 mutant mice that either overexpress EGFL7 or are EGFL7 deficient (*31, 33*). It is plausible that the partial lethality is, at least in part, due to a dysfunction in placental development.

In conclusion, our study has uncovered a novel expression domain for EGFL7 in non-endothelial trophoblast cell types. Its novel and dynamic expression pattern suggests a potential role in the molecular mechanisms that regulate trophoblast cell proliferation, differentiation, and invasion during placental development. Our study also links a significant downregulation of EGFL7 expression to PE placentas. We demonstrate that, in a PE mouse model, the change occurs in phenotypically abnormal placentas before the onset of the characteristic maternal signs of preeclampsia. It is tempting to speculate that EGFL7 could play a functional role in the pathophysiology of PE, and that EGFL7 could be an early biomarker of PE.

Table 3.1: Clinical characteristics of pregnancies for placentas studied. Data are presented as median ± standard deviation and analyzed using a student's t-test.

Table 3.1			
	Clinical Characteristics of Pregnancies for Placentas Studied		
Parameter	**Preeclampsia (n=10)**	**Control (n=10)**	**Significance**
Parity	0 ± 0.3	0	
Gestational age (weeks)	32 ± 2	39 ± 0	<0.0001
Maternal age (years)	34 ± 4	35 ± 6	0.54
Gravidity	2 ± 1	2 ± 1	0.59
Birth Weight (grams)	1235 ± 359	3372 ± 354	<0.001
Birth Weight Percentile	9 ± 3	63 ± 18	<0.001
Placental Weight (grams)	236 ± 65	550 ± 55	<0.001
Systolic blood pressure at delivery (mm Hg)	161 ± 11	130 ± 5	<0.001
Diastolic blood pressure at delivery (mm Hg)	109 ± 8	82 ± 3	<0.001

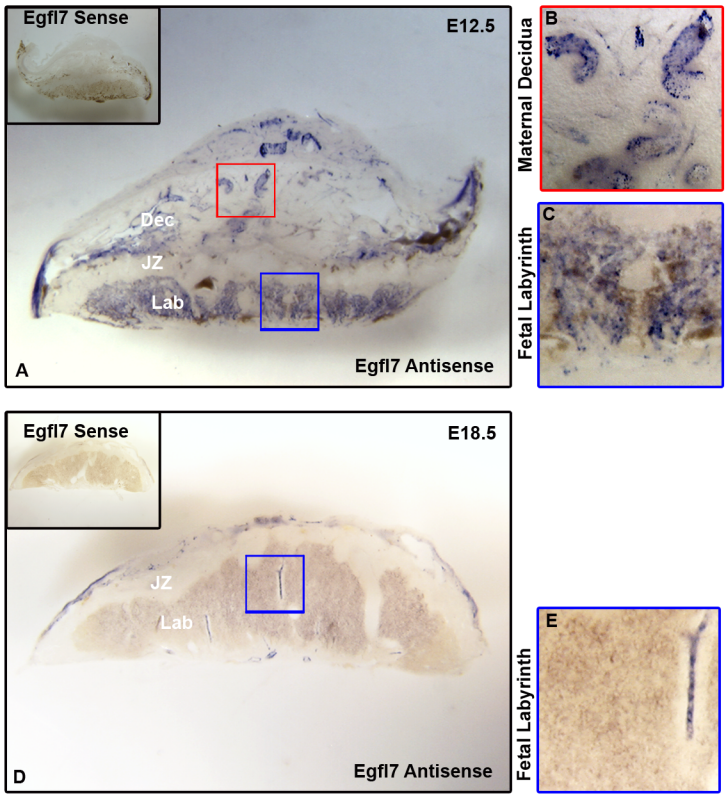

<u>Supplemental Figure 3.1</u> Egfl7 transcript expression in E12.5 and E18.5 mouse placentas. In situ hybridization was performed using an Egfl7 riboprobe on 100μm thick vibratome sections of E12.5 **(A-C)** and E18.5 **(D-E)** C57BL/6 placentas. Higher magnification images of boxes in **(A)** demonstrating that Egfl7 transcript is expressed in the maternal decidua **(B)** and fetal labyrinth **(C)**. Egfl7 transcript is largely downregulated at E18.5 **(D)**, except in a few vascular structures resembling arterioles in the fetal labyrinth **(E)**. Egfl7 sense controls **(A, D** insets**)** show specificity of Egfl7 riboprobe. Dec-Maternal Decidua, JZ-Junctional Zone, Lab-Fetal Labyrinth.

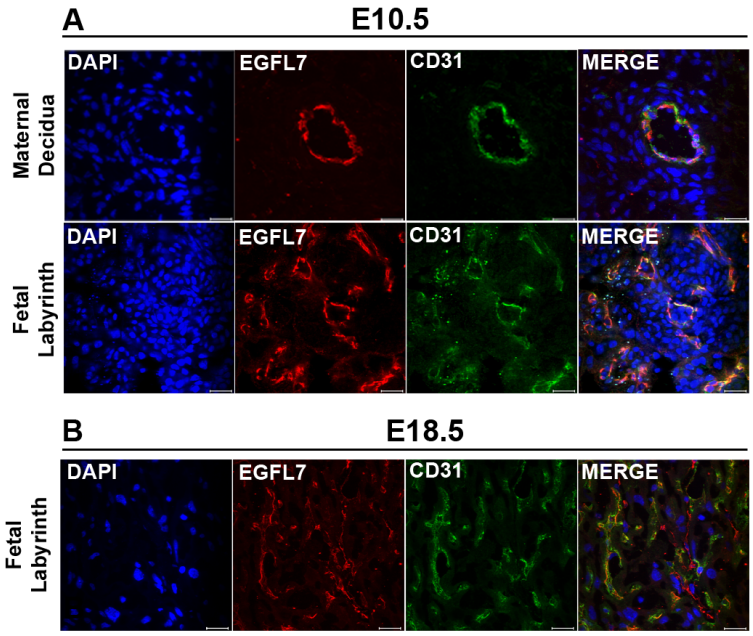

Supplemental Figure 3.2 EGFL7 localizes to endothelial cells of E10.5 and E18.5 mouse placentas. Double immunofluorescent staining was performed on E10.5 **(A)** and E18.5 **(B)** C57BL/6 placentas for EGFL7 (red), CD31 (green) and nuclear DAPI (blue). Images are collapsed z-stack confocal images of the maternal decidua and fetal labyrinth placental zones. EGFL7 colocalizes with the endothelial cell marker, CD31, in the maternal decidua and the fetal labyrinth. Scale bar=20μm.

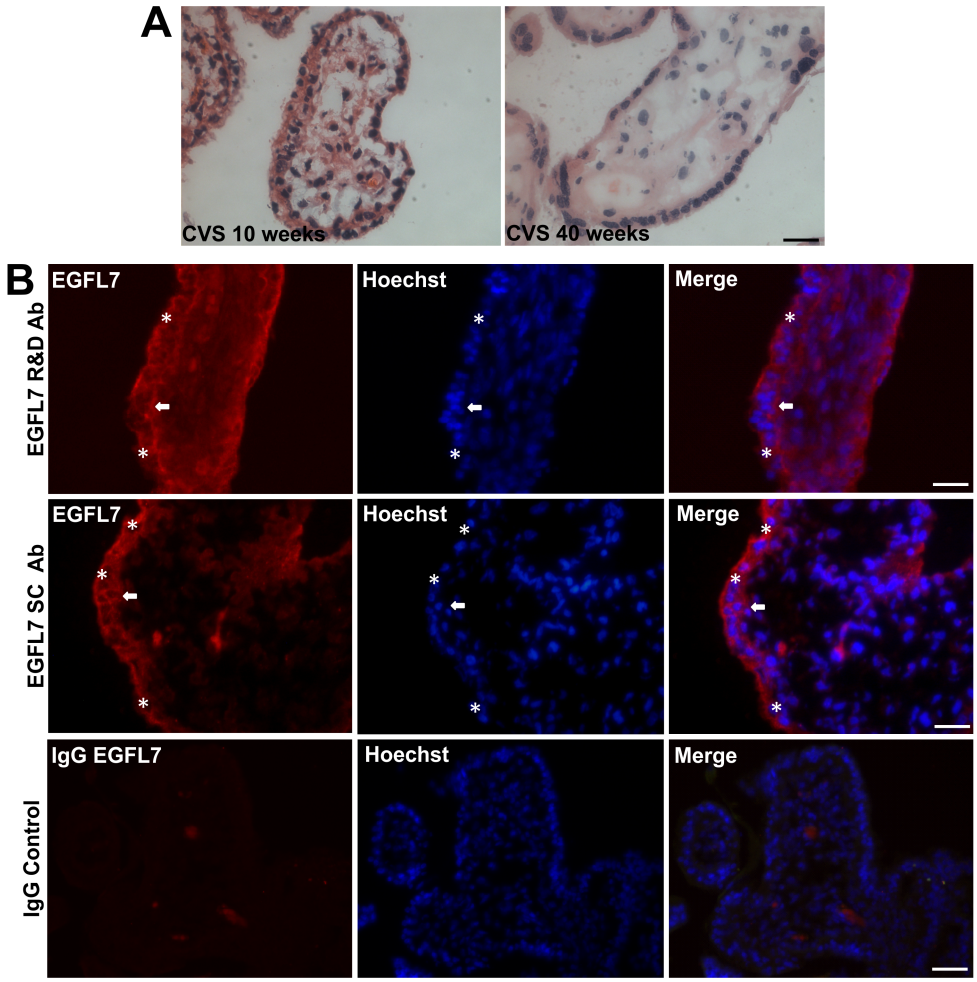

Supplemental Figure 3.3 EGFL7 expression in human placentas. **(A)** H&E staining of week-10 chorionic villi (left), and of week-40 chorionic villi (right) demonstrating morphology. Scale bars=50mm. **(B)** EGFL7 antibodies from different sources show similar staining patterns in trophoblasts. Depicted are staining of chorionic villi from placentas at week-10 of gestation for Hoechst (blue) and EGFL7 (red). Top row: EGFL7 antibody from R&D; middle row: Egfl7 antibody from Santa Cruz; bottom row: IgG control on the same chorionic villi specimen. (*-syncytiotrophoblast cell layer; arrow-inner trophoblast cell layer). Scale bar=50mm.

3.6 – Materials and methods

Mice and placental sampling

All animal protocols were approved by the Institutional Animal Care and Use Committee at Weill Cornell Medical College and Cornell University. BPH/5 mice were from in-house colonies. C57BL/6 mice were obtained from Jackson Laboratories and served as a control for the BPH/5 strain (*36*). For timed pregnancies, the day of visualization of a vaginal plug was designated embryonic day 0.5 (E0.5). Fetoplacental units of BPH/5 pregnancies are of varying status as assessed by ultrasonography *in utero*, ranging from normal to compromised to resorbed (*36*). A subset of placentas were dissected only from E10.5 BPH/5 fetoplacental units that were compromised, i.e. with reduced fetal size, heart rate, and blood flow as determined by ultrasound as described (*36, 37*). Placentas from normal or resorbed BPH/5 fetoplacental units were not sampled.

Human placenta sampling

Biopsies of placentas from normal (n=10) and early-onset PE pregnancies (n=10) were obtained from the Catholic University of Rome. The study respected the principles expressed in the Declaration of Helsinki and was approved by the Bioethical Committee of the Catholic University of Rome. For the collection of samples, all patients provided written informed consent. Clinical criteria used to define preeclampsia in our study were in accordance with the definition of the International Society for the Study of Hypertension in Pregnancy (ISSHP). In short, a patient (previously normotensive) was defined as being affected by PE if she had at least two diastolic blood pressure

measurements of 90mmHg in 24 hours (≥4 hours apart), accompanied by proteinuria of at least 300 mg in a 24-hour collection of urine. Early-onset PE diagnosis was defined as the development of PE before the 34th week of gestation. All 10 PE patients displayed abnormal uterine artery Doppler velocimetry. Among PE patients, two had a normal umbilical artery Doppler velocimetry, and five patients showed altered umbilical artery Doppler data (two of which were associated with a brain sparing effect). No Doppler data were available for three PE patients. Nine out of ten (90%) of the early-onset PE pregnancies were associated with intrauterine growth restriction, defined as an estimated fetal weight below the 10th percentile for gestational age.

Chorionic villus samples were obtained from 3 healthy patients during prenatal diagnosis on the 10th week of gestation, following standard biopsy procedures. Placental villi from the third trimester of gestation were collected from 10 normotensive, healthy patients during cesarean section by multiple biopsies in the parasagittal plane with respect to the umbilical cord insertion. Similar procedures were followed for the collection of PE samples. Portions of all placental sample types were immediately frozen in liquid nitrogen or embedded in OCT. Clinical characteristics of patients in this study are shown in **Table 3.1** (*41*).

Cell Culture

Mouse trophoblast stem cells (TSC) were gifts from Dr. Kat Hadjantonakis (Memorial Sloan Kettering Institute, New York, NY) and Dr. Janet Rossant (Hospital for Sick Children, Toronto, Canada). TSC were cultured and maintained using published methods (*39*), on mouse embryonic fibroblasts

(MEF) or with 50% MEF preconditioned medium. Primary human cytotrophoblasts were isolated from term placentas of normal patients, using a published protocol (*40*). Cytotrophoblast cells were cultured on Matrigel-coated dishes in DMEM/H-21 medium (Gibco) supplemented with 2% Nutridoma (Roche).

RT-PCR

Placentas from C57BL/6 and BPH/5 mice were dissected and flash frozen in liquid nitrogen. TSC were grown on 60-mm plates for RNA extraction. For mouse and cell culture studies, RNA was isolated using Trizol (Invitrogen) and reverse transcribed using qScript cDNA Supermix (Quanta Biosciences). Gene expression was measured quantitatively using SYBR Green (Applied Biosciences) and specific primer sets for *β-actin*, *Egfl7*, *CD31*, *Hes1*, and *Hey1*/*2* as described (*33*). Differences among target expression were quantified using the ΔΔCT method with normalization to *β-actin*. For semi-quantitative RT-PCR, cDNA was amplified using the following primers:

Egfl7 (forward) 5'-CCACAAAAAGAAGAAGGCTACCC-3'

Egfl7 (reverse) 5'-TCCAAGAAGGACCCTGCTCACTC-3'

β-actin (forward) 5'-GTGGGCCGCTCTAGGCACCAA-3'

β-actin (reverse) 5'-CTCTTTGATGTCACGCACGATTTC-3'

Products were analyzed on agarose gels.

DNAse-free RNA from human placental tissue was prepared using the RNeasy Mini Kit (Qiagen). RNA quality was examined by determining the presence of ribosomal RNA bands in agarose gels. RNA was reverse transcribed using

random primers and the Superscript First Strand Synthesis System (Invitrogen) following the manufacturer's protocol. Specific intron-spanning primers for *EGFL7*, *CD31* and *VEGF* were designed using Primer Express software (Applied Biosystems, sequences are listed below). Gene expression was measured using Real Master Mix SYBR ROX (Eppendorf) and normalized to *GAPDH*.

EGFL7: 5'-TCGTGCAGCGTGTGTACCAG-3'

5'-GCGGTAGGCGGTCCTATAGATG-3'

CD31: 5'-TAGCGCATGGCCTGGTTAGAG-3'

5'-GGCGGTGCTCCCAAGTAGTCT-3'

VEGF: 5'-ATGACGAGGGCCTGGAGTGTG-3'

5'-CCTATGTGCTGGCCTTGGTGAG-3'

GAPDH: 5'-TCGGAGTCAACGGATTTGGT-3'

5'-GAATTTGCCATGGGTGGAAT-3'

NOTCH1: 5'- GCGGGATCCACTGTGAGAA-3'

5'-CCGTTGAAGCAGGAGCTCTCT-3'

NOTCH2: 5'- AAAAATGGGGCCAACCGAGAC-3'

5'-TTCATCCAGAAGGCGCACAA-3'

NOTCH4: 5'- CGGGCCTCTCTGCAACCT-3'

5'-GACGTCTATGCCTTGGCTCAGT-3'

HES1: 5'-AAAGATAGCTCGCGGCATTC-3'

5'-AGGTGCTTCACTGTCATTTCCA-3'

HEY1: 5'- CATCGAGGTGGAGAAGGAGAGT-3'

5'-GACATGGAACCTAGAGCCGAACT-*3'*

HEY2: 5'- CGACCTCCGAGAGCGACAT-3'

5'-CTTTGCCCCGAGTAATTGTTCT-3'

JAGGED1: 5'-GGAGGCGTGGGATTCCA-3'

5'-CCGAGTGAGAAGCCTTTTCAATAAT-3'

DLL-4: 5'-CCAGCCAGATGGCAACTTGT-3'

5'-CCCGAAAGACAGATAGGCTGTT-3'

RNA in situ hybridization

Egfl7 cDNA probes were generated by RT-PCR using the following primers: *Egfl7* forward 5'-AGTTACTGGTGCCAGGGATG-3' and *Egfl7* reverse 5'-TCCTCCAAGAAGGACACCTG-3'. Amplicons were subcloned into pCR-2.1 or pCRII-Topo-TA vectors (Invitrogen) and linearized with SpeI or EcoRV. All probes were synthesized using DIG-labeling mix (Roche) according to manufacturer's instructions.

In situ hybridization (ISH) was performed by modification of the protocol described by Hurtado *et al* (*66*). C57BL/6 placentas were isolated, fixed in 4% paraformaldehyde, and methanol dehydrated. Placentas were rehydrated, incubated in 5% low melt agarose (BioRad) at 42°C for 2hours, and embedded in 5% low melt agarose through solidification at room temperature. Blocks were cut at 100μm thickness. Agarose was removed; sections were washed in PBT (PBS-0.01%Tween20), and treated with Proteinase K (10μg/ml, Roche) for 20min. After terminating proteinase K reaction with Glycine (2mg/ml) and postfixation with 4% paraformaldehyde-0.1% gluteraldehyde (40min), samples were washed with PBT, pre-incubated with hybridization buffer (50% Formamide, 200μg/ml Yeast RNA, 0.5% Chaps, 1.3X SSC, 5mM EDTA,

100μg/ml Heparin, 0.2% Tween20 in DEPC-H_2O) for 1hour at 60°C, and incubated overnight with DIG-labeled RNA probes (1μg/ml) at 60°C. Samples were washed and blocked with 2% Boehringer Blocking Reagent (BBR) (Roche) in MABT for 1hour and 2%BBR-20%NGS in MABT for 1hour, then incubated with alkaline phosphatase conjugated anti-DIG (Roche) at 1:2000 overnight at 4°C. Samples were washed with MABT then NTMT (100mM NaCl, 100mM Tris-HCl pH9.5, 50mM MgCl2, 1% Tween20, 20μM Levamisole, in H_2O). Signals were detected with NBT-BCIP (Roche) chromogenic substrate in NTMT at 4°C. Samples were post-fixed in 4% paraformaldehyde and imaged using a DKC-5000 (Sony) Digital Photo Camera.

Specimens were processed for paraffin sectioning as described by Hurtado, *et al* (*66*). Briefly, after ISH specimens were post-fixed with 4% paraformaldehyde in PBS, rocking for 48 hours at room temperature, and then overnight at 4°C. Specimens were then dehydrated stepwise in ethanol/double distilled H_2O solutions as follows: 70% ethanol for 10 min, 90% ethanol for 10 min, 95% ethanol for 10 min, 3 × 100% ethanol for 10 min, 1:1 of ethanol/Citrisolv (Sigma) for 15 min. Specimens were then incubated in paraffin at 65°C as follows: 1:1 of Citrisolv/paraffin for 15 min, 3 × paraffin for 1hour, paraffin overnight, 2 × paraffin for 1hour. Specimens were then embedded in paraffin in a sagittal orientation and sectioned at 10μm thickness. Sections were rehydrated through a series of ethanol washes (100%, 90%, 85%, 70%), counterstained with Nuclear Fast Red (Sigma-Aldrich), dehydrated through a series of ethanol washes (70%, 85%, 90%, 100%), and mounted with Permount (Fisher Scientific).

For TSC, in situ hybridization was performed as above with the following modifications: TSC were cultured on 8-chamber slides (BD Biosciences) for 2 days prior to fixation and proteinase K incubation was carried out for 3min.

Antibodies

The following primary antibodies were used for all immunostaining: EGFL7 (Santa Cruz, SC-34416, 2μg/ml; R&D Systems AF3089; 2μg/ml, In-house EGFL7 (*22*), 1:100), CD31 (BD Biosciences, 553370; 5μg/ml (mouse studies) or 0.78mg/ml (human studies)), CDX2 (Biogenex; CDX2-88; 25mg/ml), Cytokeratin (DakoCytomation; 53.5μg/ml (human studies)), Cytokeratin (DAKO Z0622; 12μg/ml (mouse studies)), and NOTCH4 (Santa Cruz, SC-5594; 2mg/ml). The following secondary antibodies were used: Dylight 594-donkey-α-goat (Jackson Immunoresearch, 1.5μg/ml), Alexa 488-donkey-α-goat (Jackson Immunoresearch, 1.5μg/ml) or Cy3-donkey-α-goat (Chemicon, 4μg/ml), Alexa488 donkey-α-rabbit (Jackson Immunoresearch, 1.5μg/ml) or FITC-donkey-α-rabbit (Chemicon, 4μg/ml), Alexa488 donkey-α-mouse (Jackson Immunoresearch, 1.5μg/ml (mouse studies) or Invitrogen, 4μg/ml (human studies)).

Immunofluorescence

Mouse whole fetoplacental units or placentas alone were isolated and embedded in an OCT:30% sucrose (2:1) mixture. Sections were permeablized in 0.5% Triton-X/0.1% Saponin/PBS (TSP) and blocked with 1% donkey serum in 0.1% TSP/PBS (PBS-TSP). Primary antibodies (EGFL7, CD31, CYTOKERATIN) were incubated for 3 hours at 37°C in block, then secondary antibodies in block, and mounted with Prolong Gold +DAPI (Invitrogen).

TSC were grown on 8-chamber slides (BD Biosciences) for 2-4 days and fixed with cold methanol for 5 minutes. TSC were washed in PBS-TSP and blocked with 1% donkey serum in PBS. Primary antibodies (EGFL7, CDX2) were incubated overnight at 4°C or 2hrs at RT in block, then secondary antibodies in block, and mounted as above.

For the human studies, sections were fixed in methanol for 5 minutes at -20°C and blocked in 10% donkey serum/PBS. Sections were incubated with primary antibodies (EGFL7, CD31, CYTOKERATIN, NOTCH4) in 0.1%BSA/PBS overnight at 4°C. Sections were incubated in secondary antibodies, stained with Hoechst33342 (Sigma-Aldrich), and mounted with Möwiol (Sigma-Aldrich).

Primary human cytotrophoblasts were cultured overnight, fixed with ice-cold methanol for 5 min at -20^{o}C, and immunostained with EGFL7 and CYTOKERATIN antibodies.

All images were acquired using an Axioplan 2 imaging microscope (Carl Zeiss) or a LSM Live 5 line scanner confocal microscope (Carl Zeiss).

Whole Mount Immunostaining

Blastocyst-stage embryos were isolated by flushing uteri with M2 Medium (Sigma). Embryos were collected between E3.5 and E4.0, washed with M2 medium, fixed in 2% paraformaldehyde, and permeablized with 0.25%Triton-X/PBS. Embryos were blocked with 2.5% donkey serum/0.5%PBS-TSP/PBS, and incubated with primary antibodies (EGFL7, CDX2) overnight at 37°C in

block. Blastocysts were incubated with secondary antibodies and mounted with Prolong Gold+DAPI using Fastwell spacers (Sigma-Aldrich).

Statistics

Data are represented as mean ± SEM. The data were analyzed using a student's t-test with statistical significance defined as $P < 0.05$.

REFERENCES

1. L. Duley, The global impact of pre-eclampsia and eclampsia. *Semin Perinatol* **33**, 130-137 (2009).
2. B. C. Young, R. J. Levine, S. A. Karumanchi, Pathogenesis of preeclampsia. *Annu Rev Pathol* **5**, 173-192 (2010).
3. A. C. o. O. Practice, Practice bulletin #33: diagnosis and management of preeclampsia and eclampsia. *Obstetrics & Gynecology* **99**, 159-167 (2002).
4. P. von Dadelszen, L. A. Magee, Pre-eclampsia: an update. *Curr Hypertens Rep* **16**, 454 (2014).
5. J. A. Turner, Diagnosis and management of pre-eclampsia: an update. *Int J Womens Health* **2**, 327-337 (2010).
6. C. E. Powe, R. J. Levine, S. A. Karumanchi, Preeclampsia, a disease of the maternal endothelium: the role of antiangiogenic factors and implications for later cardiovascular disease. *Circulation* **123**, 2856-2869 (2011).
7. M. Kar, Role of biomarkers in early detection of preeclampsia. *J Clin Diagn Res* **8**, BE01-04 (2014).
8. L. L. Waite, A. K. Atwood, R. N. Taylor, Preeclampsia, an implantation disorder. *Rev Endocr Metab Disord* **3**, 151-158 (2002).
9. P. Merviel, L. Carbillon, J. C. Challier, M. Rabreau, M. Beaufils, S. Uzan, Pathophysiology of preeclampsia: links with implantation disorders. *Eur J Obstet Gynecol Reprod Biol* **115**, 134-147 (2004).
10. S. Saito, A. Shiozaki, A. Nakashima, M. Sakai, Y. Sasaki, The role of the immune system in preeclampsia. *Mol Aspects Med* **28**, 192-209 (2007).
11. M. Hund, D. Allegranza, M. Schoedl, P. Dilba, W. Verhagen-Kamerbeek, H. Stepan, Multicenter prospective clinical study to evaluate the prediction of short-term outcome in pregnant women with suspected preeclampsia (PROGNOSIS): study protocol. *BMC Pregnancy Childbirth* **14**, 324 (2014).
12. S. Furukawa, Y. Kuroda, A. Sugiyama, A comparison of the histological structure of the placenta in experimental animals. *J Toxicol Pathol* **27**, 11-18 (2014).
13. P. Georgiades, A. C. Ferguson-Smith, G. J. Burton, Comparative developmental anatomy of the murine and human definitive placentae. *Placenta* **23**, 3-19 (2002).
14. J. Rossant, J. C. Cross, Placental development: lessons from mouse mutants. *Nat Rev Genet* **2**, 538-548 (2001).
15. E. R. Norwitz, D. J. Schust, S. J. Fisher, Implantation and the survival of early pregnancy. *N Engl J Med* **345**, 1400-1408 (2001).
16. L. K. Phng, H. Gerhardt, Angiogenesis: a team effort coordinated by notch. *Dev Cell* **16**, 196-208 (2009).

17. L. T. Krebs, Y. Xue, C. R. Norton, J. R. Shutter, M. Maguire, J. P. Sundberg, D. Gallahan, V. Closson, J. Kitajewski, R. Callahan, G. H. Smith, K. L. Stark, T. Gridley, Notch signaling is essential for vascular morphogenesis in mice. *Genes Dev* **14**, 1343-1352 (2000).
18. A. Duarte, M. Hirashima, R. Benedito, A. Trindade, P. Diniz, E. Bekman, L. Costa, D. Henrique, J. Rossant, Dosage-sensitive requirement for mouse Dll4 in artery development. *Genes Dev* **18**, 2474-2478 (2004).
19. A. Fischer, N. Schumacher, M. Maier, M. Sendtner, M. Gessler, The Notch target genes Hey1 and Hey2 are required for embryonic vascular development. *Genes Dev* **18**, 901-911 (2004).
20. N. M. Hunkapiller, M. Gasperowicz, M. Kapidzic, V. Plaks, E. Maltepe, J. Kitajewski, J. C. Cross, S. J. Fisher, A role for Notch signaling in trophoblast endovascular invasion and in the pathogenesis of pre-eclampsia. *Development* **138**, 2987-2998 (2011).
21. L. Cobellis, A. Mastrogiacomo, E. Federico, M. T. Schettino, M. De Falco, L. Manente, G. Coppola, M. Torella, N. Colacurci, A. De Luca, Distribution of Notch protein members in normal and preeclampsia-complicated placentas. *Cell Tissue Res* **330**, 527-534 (2007).
22. M. J. Fitch, L. Campagnolo, F. Kuhnert, H. Stuhlmann, Egfl7, a novel epidermal growth factor-domain gene expressed in endothelial cells. *Dev Dyn* **230**, 316-324 (2004).
23. L. Campagnolo, A. Leahy, S. Chitnis, S. Koschnick, M. J. Fitch, J. T. Fallon, D. Loskutoff, M. B. Taubman, H. Stuhlmann, EGFL7 is a chemoattractant for endothelial cells and is up-regulated in angiogenesis and arterial injury. *Am J Pathol* **167**, 275-284 (2005).
24. F. Soncin, V. Mattot, F. Lionneton, N. Spruyt, F. Lepretre, A. Begue, D. Stehelin, VE-statin, an endothelial repressor of smooth muscle cell migration. *EMBO J* **22**, 5700-5711 (2003).
25. L. Campagnolo, I. Moscatelli, M. Pellegrini, G. Siracusa, H. Stuhlmann, Expression of EGFL7 in primordial germ cells and in adult ovaries and testes. *Gene Expr Patterns* **8**, 389-396 (2008).
26. L. H. Parker, M. Schmidt, S. W. Jin, A. M. Gray, D. Beis, T. Pham, G. Frantz, S. Palmieri, K. Hillan, D. Y. Stainier, F. J. De Sauvage, W. Ye, The endothelial-cell-derived secreted factor Egfl7 regulates vascular tube formation. *Nature* **428**, 754-758 (2004).
27. M. H. Schmidt, F. Bicker, I. Nikolic, J. Meister, T. Babuke, S. Picuric, W. Müller-Esterl, K. H. Plate, I. Dikic, Epidermal growth factor-like domain 7 (EGFL7) modulates Notch signalling and affects neural stem cell renewal. *Nat Cell Biol* **11**, 873-880 (2009).
28. M. V. Badiwala, L. C. Tumiati, J. M. Joseph, R. Sheshgiri, H. J. Ross, D. H. Delgado, V. Rao, Epidermal growth factor-like domain 7 suppresses intercellular adhesion molecule 1 expression in response to

hypoxia/reoxygenation injury in human coronary artery endothelial cells. *Circulation* **122**, S156-161 (2010).
29. M. Gustavsson, C. Mallard, S. J. Vannucci, M. A. Wilson, M. V. Johnston, H. Hagberg, Vascular response to hypoxic preconditioning in the immature brain. *J Cereb Blood Flow Metab* **27**, 928-938 (2007).
30. D. Xu, R. E. Perez, I. I. Ekekezie, A. Navarro, W. E. Truog, Epidermal growth factor-like domain 7 protects endothelial cells from hyperoxia-induced cell death. *Am J Physiol Lung Cell Mol Physiol* **294**, L17-23 (2008).
31. M. Schmidt, K. Paes, A. De Mazière, T. Smyczek, S. Yang, A. Gray, D. French, I. Kasman, J. Klumperman, D. S. Rice, W. Ye, EGFL7 regulates the collective migration of endothelial cells by restricting their spatial distribution. *Development* **134**, 2913-2923 (2007).
32. A. Durrans, H. Stuhlmann, A role for Egfl7 during endothelial organization in the embryoid body model system. *J Angiogenes Res* **2**, 4 (2010).
33. D. Nichol, C. Shawber, M. J. Fitch, K. Bambino, A. Sharma, J. Kitajewski, H. Stuhlmann, Impaired angiogenesis and altered Notch signaling in mice overexpressing endothelial Egfl7. *Blood* **116**, 6133-6143 (2010).
34. J. C. Cross, D. Baczyk, N. Dobric, M. Hemberger, M. Hughes, D. G. Simmons, H. Yamamoto, J. C. Kingdom, Genes, development and evolution of the placenta. *Placenta* **24**, 123-130 (2003).
35. D. Hu, J. C. Cross, Development and function of trophoblast giant cells in the rodent placenta. *Int J Dev Biol* **54**, 341-354 (2010).
36. R. L. Davisson, D. S. Hoffmann, G. M. Butz, G. Aldape, G. Schlager, D. C. Merrill, S. Sethi, R. M. Weiss, J. N. Bates, Discovery of a spontaneous genetic mouse model of preeclampsia. *Hypertension* **39**, 337-342 (2002).
37. A. Dokras, D. S. Hoffmann, J. S. Eastvold, M. F. Kienzle, L. M. Gruman, P. A. Kirby, R. M. Weiss, R. L. Davisson, Severe feto-placental abnormalities precede the onset of hypertension and proteinuria in a mouse model of preeclampsia. *Biol Reprod* **75**, 899-907 (2006).
38. J. C. Cross, How to make a placenta: mechanisms of trophoblast cell differentiation in mice--a review. *Placenta* **26 Suppl A**, S3-9 (2005).
39. S. Tanaka, T. Kunath, A. K. Hadjantonakis, A. Nagy, J. Rossant, Promotion of trophoblast stem cell proliferation by FGF4. *Science* **282**, 2072-2075 (1998).
40. N. M. Hunkapiller, S. J. Fisher, Chapter 12. Placental remodeling of the uterine vasculature. *Methods Enzymol* **445**, 281-302 (2008).
41. D. Nelson, G. Burton, A technical note to improve the reporting of studies of the human placenta. *Placenta* **32**, 195-196 (2010).

42. M. van Tuyl, J. Liu, J. Wang, M. Kuliszewski, D. Tibboel, M. Post, Role of oxygen and vascular development in epithelial branching morphogenesis of the developing mouse lung. *Am J Physiol Lung Cell Mol Physiol* **288**, L167-178 (2005).
43. M. J. Costa, X. Wu, H. Cuervo, R. Srinivasan, S. K. Bechis, E. Cheang, O. Marjanovic, T. Gridley, C. A. Cvetic, R. A. Wang, Notch4 is required for tumor onset and perfusion. *Vasc Cell* **5**, 7 (2013).
44. K. Nadra, L. Quignodon, C. Sardella, E. Joye, A. Mucciolo, R. Chrast, B. Desvergne, PPARgamma in placental angiogenesis. *Endocrinology* **151**, 4969-4981 (2010).
45. J. C. Cooper, A. M. Sharkey, D. S. Charnock-Jones, C. R. Palmer, S. K. Smith, VEGF mRNA levels in placentae from pregnancies complicated by pre-eclampsia. *Br J Obstet Gynaecol* **103**, 1191-1196 (1996).
46. F. Lyall, A. Young, F. Boswell, J. C. Kingdom, I. A. Greer, Placental expression of vascular endothelial growth factor in placentae from pregnancies complicated by pre-eclampsia and intrauterine growth restriction does not support placental hypoxia at delivery. *Placenta* **18**, 269-276 (1997).
47. J. S. Park, H. W. Baik, S. K. Lee, W. S. Na, Y. R. Song, Y. S. Yang, M. H. Park, I. T. Hwang, K. Y. Oh, Vascular endothelial growth factor, fms-like tyrosine kinase-1 (Flt-1) and soluble Flt-1 gene expressions in Korean pre-eclamptic placentas. *J Obstet Gynaecol Res* **36**, 726-732 (2010).
48. F. Akercan, T. Cirpan, M. C. Terek, H. T. Ozcakir, G. Giray, S. Sagol, N. Karadadas, The immunohistochemical evaluation of VEGF in placenta biopsies of pregnancies complicated by preeclampsia. *Arch Gynecol Obstet* **277**, 109-114 (2008).
49. J. Y. Chung, Y. Song, Y. Wang, R. R. Magness, J. Zheng, Differential expression of vascular endothelial growth factor (VEGF), endocrine gland derived-VEGF, and VEGF receptors in human placentas from normal and preeclamptic pregnancies. *J Clin Endocrinol Metab* **89**, 2484-2490 (2004).
50. E. Geva, D. G. Ginzinger, C. J. Zaloudek, D. H. Moore, A. Byrne, R. B. Jaffe, Human placental vascular development: vasculogenic and angiogenic (branching and nonbranching) transformation is regulated by vascular endothelial growth factor-A, angiopoietin-1, and angiopoietin-2. *J Clin Endocrinol Metab* **87**, 4213-4224 (2002).
51. A. B. Wallis, A. F. Saftlas, J. Hsia, H. K. Atrash, Secular trends in the rates of preeclampsia, eclampsia, and gestational hypertension, United States, 1987-2004. *Am J Hypertens* **21**, 521-526 (2008).
52. C. Dolea, C. AbouZahr, in *Evidence and Information for Policy (EIP)*. (World Health Organization, Geneva, 2003).

53. A. Johansson, M. Løset, S. B. Mundal, M. P. Johnson, K. A. Freed, M. H. Fenstad, E. K. Moses, R. Austgulen, J. Blangero, Partial correlation network analyses to detect altered gene interactions in human disease: using preeclampsia as a model. *Hum Genet* **129**, 25-34 (2011).
54. K. Junus, M. Centlow, A. K. Wikström, I. Larsson, S. R. Hansson, M. Olovsson, Gene expression profiling of placentae from women with early- and late-onset pre-eclampsia: down-regulation of the angiogenesis-related genes ACVRL1 and EGFL7 in early-onset disease. *Mol Hum Reprod* **18**, 146-155 (2012).
55. F. Crispi, C. Domínguez, E. Llurba, P. Martín-Gallán, L. Cabero, E. Gratacós, Placental angiogenic growth factors and uterine artery Doppler findings for characterization of different subsets in preeclampsia and in isolated intrauterine growth restriction. *Am J Obstet Gynecol* **195**, 201-207 (2006).
56. R. B. Ness, B. M. Sibai, Shared and disparate components of the pathophysiologies of fetal growth restriction and preeclampsia. *Am J Obstet Gynecol* **195**, 40-49 (2006).
57. L. T. Krebs, J. R. Shutter, K. Tanigaki, T. Honjo, K. L. Stark, T. Gridley, Haploinsufficient lethality and formation of arteriovenous malformations in Notch pathway mutants. *Genes Dev* **18**, 2469-2473 (2004).
58. F. P. Limbourg, K. Takeshita, F. Radtke, R. T. Bronson, M. T. Chin, J. K. Liao, Essential role of endothelial Notch1 in angiogenesis. *Circulation* **111**, 1826-1832 (2005).
59. N. W. Gale, M. G. Dominguez, I. Noguera, L. Pan, V. Hughes, D. M. Valenzuela, A. J. Murphy, N. C. Adams, H. C. Lin, J. Holash, G. Thurston, G. D. Yancopoulos, Haploinsufficiency of delta-like 4 ligand results in embryonic lethality due to major defects in arterial and vascular development. *Proc Natl Acad Sci U S A* **101**, 15949-15954 (2004).
60. C. Oka, T. Nakano, A. Wakeham, J. L. de la Pompa, C. Mori, T. Sakai, S. Okazaki, M. Kawaichi, K. Shiota, T. W. Mak, T. Honjo, Disruption of the mouse RBP-J kappa gene results in early embryonic death. *Development* **121**, 3291-3301 (1995).
61. M. Gasperowicz, F. Otto, The notch signalling pathway in the development of the mouse placenta. *Placenta* **29**, 651-659 (2008).
62. F. Guillemot, A. Nagy, A. Auerbach, J. Rossant, A. L. Joyner, Essential role of Mash-2 in extraembryonic development. *Nature* **371**, 333-336 (1994).
63. Y. Hamada, T. Hiroe, Y. Suzuki, M. Oda, Y. Tsujimoto, J. R. Coleman, S. Tanaka, Notch2 is required for formation of the placental circulatory system, but not for cell-type specification in the developing mouse placenta. *Differentiation* **75**, 268-278 (2007).

64. M. Gasperowicz, A. Rai, J. C. Cross, Spatiotemporal expression of Notch receptors and ligands in developing mouse placenta. *Gene Expr Patterns*, (2013).
65. D. Nichol, H. Stuhlmann, EGFL7: a unique angiogenic signaling factor in vascular development and disease. *Blood* **119**, 1345-1352 (2012).
66. R. Hurtado, T. Mikawa, Enhanced sensitivity and stability in two-color in situ hybridization by means of a novel chromagenic substrate combination. *Dev Dyn* **235**, 2811-2816 (2006).

Chapter 4 – Fetal vascular patterning defects in placentas with Egfl7 loss-of-function[*]

4.1 – Rationale

The pathophysiology of preeclampsia (PE) is believed to begin early during pregnancy, despite the presentation of symptoms in late gestation (*1, 2*). The resolution of symptoms upon delivery of the placenta, as well as the vascular defects and dysregulated pro- and anti-angiogenic signaling common to most PE pregnancies, point to defects in placental vascularization and development as a major contributing factor underlying the disease (*3-5*). It is important to dissect the tightly regulated molecular mechanisms controlling normal placental development to begin to understand the diseased state and to elucidate diagnostic and therapeutic treatments.

Formation of the placenta begins when the blastocyst-staged embryo implants into the receptive uterus. Fetal trophoblast cells invade the uterine decidua and commence a series of events to form the fetal-maternal interface, a site in which the fetal and maternal circulatory systems come in close contact. The first step in fetal labyrinth development is chorioallantoic fusion, when the allantois makes contact with the chorionic trophoblast cells (*6-8*). One molecule implicated in this process, for example, is cell adhesion molecule VCAM-1. *VCAM-1* mutant mice display defects in chorioallantoic fusion and subsequent embryonic lethality (*9, 10*). Following chorioallantoic fusion, branching morphogenesis is initiated at sites along the chorion where Gcm1 is upregulated (*7, 8, 11*). Indeed, chorions of *Gcm1*-null mice remain flat and fail to initiate branching (*11*). Invaginations form within the chorion into which blood vessels grow from the allantois (*6*). Branching morphogenesis continues to

[*] **Lacko LA**, Hurtado R, Hinds SG, Gale NW, Stuhlmann H. Fetal vascular patterning defects in placentas with *Egfl7* loss-of-function. Developmental Biology. *To be submitted*. 2015

form a dense, arborized vascular network. The maternal blood is brought through large central arteries where their endothelial cells are replaced by specialized trophoblast cells. The maternal blood bathes the fetal vessels in the fetal labyrinth compartment of the placenta for efficient fetal-maternal exchange of nutrients, gases, and wastes (*6*).

It is important to dissect the primary defect when analyzing abnormal placental vascularization, as it has been shown that many are caused by a primary defect in the trophoblast compartment (*7, 8*). In fact, several mouse mutants with a small, underdeveloped labyrinth are of genes primarily expressed in the trophoblast compartment, including *Fgf2* and *Fzd5* (*6*). Determining factors with primary vascular defects will allow for insights into disease states and therapeutics that can be used.

In the previous chapter, I have described a novel, secreted angiogenic factor dysregulated in human term PE placentas and in a mouse model of PE early in gestation. The spatiotemporal expression profile of EGFL7 in trophoblast and endothelial cells of the developing placenta, and the downregulation prior to the onset of maternal signs of the disease, suggest that EGFL7 may play a causative role in the pathophysiology of PE. In this chapter, I will describe the functional role of *Egfl7* during placental development using a global *Egfl7* loss-of-function mouse. Mice and humans exhibit strong similarities in the vascular development and remodeling events that occur in the placenta (*12*), making it an excellent model to study fetal labyrinth formation.

4.2 – Abstract

The placenta provides an interface between the maternal and fetal circulatory systems during mammalian development. Proper placental development requires branching morphogenesis to form the arborized vascular network of fetal blood vessels. The fetal labyrinth vessels are bathed by maternal blood brought to the fetal compartment of the placenta through remodeling of maternal spiral arteries. Defects in fetoplacental vascularization can result in placental pathologies such as preeclampsia (PE) and/or intrauterine growth restriction. Angiogenic signaling plays an important role in normal placental development, and has been implicated in the pathophysiology of PE. We have recently shown that the secreted angiogenic factor, Epidermal Growth Factor Like Domain 7 (Egfl7) is expressed in the endothelium of the fetal labyrinth and in spongiotrophoblasts of the junctional zone. Egfl7 expression is downregulated in human PE placentas and in placentas of the BPH/5 mouse model of PE. In this study, we investigated the role of Egfl7 during placental vascularization using mice with global Egfl7 loss-of-function (Egfl7 KO). At midgestion, Egfl7 KO placentas have reduced weight and exhibit irregular vascular patterning in the fetal labyrinth, resulting in reduced fetal blood space and reduced placental perfusion. Transcriptome profiling of mutant placentas implicates a role for Egfl7 in inflammatory signaling and extracellular matrix formation. Results of this study demonstrate that Egfl7 plays an important role in normal placental development and suggest that it could be a potential novel diagnostic tool and/or therapeutic target for treating placentopathies, including PE.

4.3 – Introduction

The placenta is a critical, transient organ, which provides an interface between the maternal and fetal circulatory systems during pregnancy. The placenta performs gas and nutrient exchange as well as immunological and endocrine functions necessary for proper development of the mammalian embryo. The site of exchange occurs in the chorionic villi in humans and the analogous fetal labyrinth zone in mice, where the maternal and fetal circulations are brought in close contact. Proper development of the fetal labyrinth requires a series of morphogenetic events, including chorionic branching morphogenesis and subsequent blood vessel development (*6*). At embryonic day (E)8.5 in the mouse, chorioallantoic fusion occurs when the allantois, arising from the posterior embryonic mesoderm, makes contact with the chorionic trophoblast cells, which arise from the extraembryonic ectoderm (*6, 7*). Upregulation of Glial cells missing-1 (Gcm1) in clusters of trophoblast cells in the chorion marks the sites of initiation of branching morphogenesis (*11, 13*). Chorion trophoblast differentiation and morphogenesis develop extensive folds of chorionic villi, into which blood vessels from the allantois invade and interdigitate (*6, 7*), resulting in the highly branched vascular network of the fetal labyrinth of the placenta.

Defects in fetoplacental vascularization can result in intrauterine growth restriction or placental pathologies such as preeclampsia (PE), a disease clinically diagnosed by late gestational hypertension and proteinuria. Despite intense research, the only treatment for PE is to induce labor and deliver the fetus and placenta. A number of factors have been implicated in the

pathogenesis of PE. These include an imbalance in pro- and anti-angiogenic factors, including dysregulation of soluble Flt1 (sFlt1), Placental Growth Factor (PlGF), and soluble Endoglin (sEng) (reviewed in (*3, 4, 14, 15*). We and others have shown that Epidermal growth factor like domain 7 (Egfl7) encodes an angiogenic factor that functions during vascular development in mouse and zebrafish embryos. Egfl7 expression is downregulated in human preeclamptic placentas (*16, 17*), placentas of a mouse model of PE prior to the onset of clinical signs (*16*), and in sera of PE patients (*18*).

EGFL7 is a partially secreted protein that is predominantly localized to the extracellular matrix. Egfl7 is expressed in pre- and peri-implantation embryos, in both the inner cell mass and trophectoderm, and later becomes restricted to actively proliferating endothelium of the developing embryo proper, as well as placental endothelial cells and spongiotrophoblast cells (*16, 19-22*). *Egfl7* regulates vascular patterning and tubulogenesis in mouse, zebrafish, and Xenopus embryos (*21, 23, 24*), and has been shown to be important for the migration of endothelial and trophoblast cells (*24-26*). Furthermore, endothelial-specific overexpression of Egfl7 in mice results in partial embryonic lethality at mid-gestation (*24*).

To understand the functional role of *Egfl7* during placental development and to determine if *Egfl7* may functionally contribute to the development of PE-like symptoms, we analyzed placental development and fetal labyrinth formation in mice with a global *Egfl7* loss-of-function. Although the mouse placenta differs from the human placenta in some aspects, the key signaling and developmental pathways are conserved between the two species, making the

mouse a good model of placental development and disease (*6, 27*). We show here that placentas with global Egfl7 knockout exhibit vascular patterning defects resulting in poor placental perfusion. Transcriptome profiling of mutant placentas uncovered dysregulation of genes involved in a number of biological processes important during placentation and pregnancy. The results of this study demonstrate that *Egfl7* plays an important role in regulating fetal labyrinth formation in the placenta.

4.4 – Results

4.4.1 – Egfl7 loss-of-function results in reduced placental weights and embryonic lengths

Previous *Egfl7* loss-of-function studies in mice have been complicated by the presence of an intronic microRNA, miR-126 (*28*). Original analysis of knockout mice suggested a role for *Egfl7* in vascular morphogenesis, however, later studies demonstrated that exclusive loss of miR-126 phenocopied the original *Egfl7* knockout (Egfl7 KO) (*21, 28*). These results suggested the mutant phenotype could be attributed to the loss of miR-126 rather than loss of *Egfl7*.

To determine *Egfl7* function during placental development, we generated global *Egfl7* loss-of-function in mice that did not affect expression of miR-126 (Egfl7 KO). An embryonic stem cell clone, Velocigene #1501 (Regeneron) that contains a targeted Egfl7 allele with a 12-base pair deletion of the N-terminal MQTM sequence of its coding sequence, including the two predicted 5' ATG start codons and an insertion of a hygromycin cassette flanked by loxP sites

(**Figure 4.1A**) was used for blastocyst injections. Founder mice were backcrossed ten generations into the C57BL/6 congenic background and then crossed to global Cre-expressing mice (CAG-Cre) for excision of the hygromycin cassette. Egfl7 transcript expression was measured by Real Time RT-PCR using two sets of primers, one complimentary to sequences in exons 8 and 9, and a second pair with one primer complimentary to a sequence in exon 4 and the other containing the 12bp sequence targeted for deletion in the Egfl7 KO mice. Results demonstrate that Egfl7 mRNA containing exon 8 and 9 sequences is transcribed in both C57BL/6 control and Egfl7 KO placentas. However the Egfl7 transcript that was amplified with the primer complimentary to the sequence encoding the two translational start sites is detected at high levels in C57BL/6 control mice, but not in Egfl7 KO mice (**Figure 4.1B**). The specific deletion of the translational start sites of *Egfl7* is predicted to not affect production of miR-126, which is embedded in intron 7. Indeed, Real Time RT-PCR of E12.5 C57BL/6 control and Egfl7 KO placentas demonstrate no significant difference in miR-126 expression levels (**Figure 4.1C**). Egfl7 KO mice are fertile, however, *Egfl7-/-* newborn pups are detected at a slightly lower than expected Mendelian ratio (**Table 4.1**). In addition, approximately 10-12% of Egfl7 KO mice die within the first two weeks of life.

To analyze the effect of *Egfl7* loss-of-function on placental development, we first analyzed the placental and embryonic weights at E12.5 from *Egfl7* heterozygous (*Egfl7*+/-) intercrosses. At E12.5, all three layers of the mature mouse placenta are formed, including the maternal decidua, junctional zone, and the fetal labyrinth. At approximately E13.5, a global molecular switch from placental-expressed genes with functions in developmental processes to a

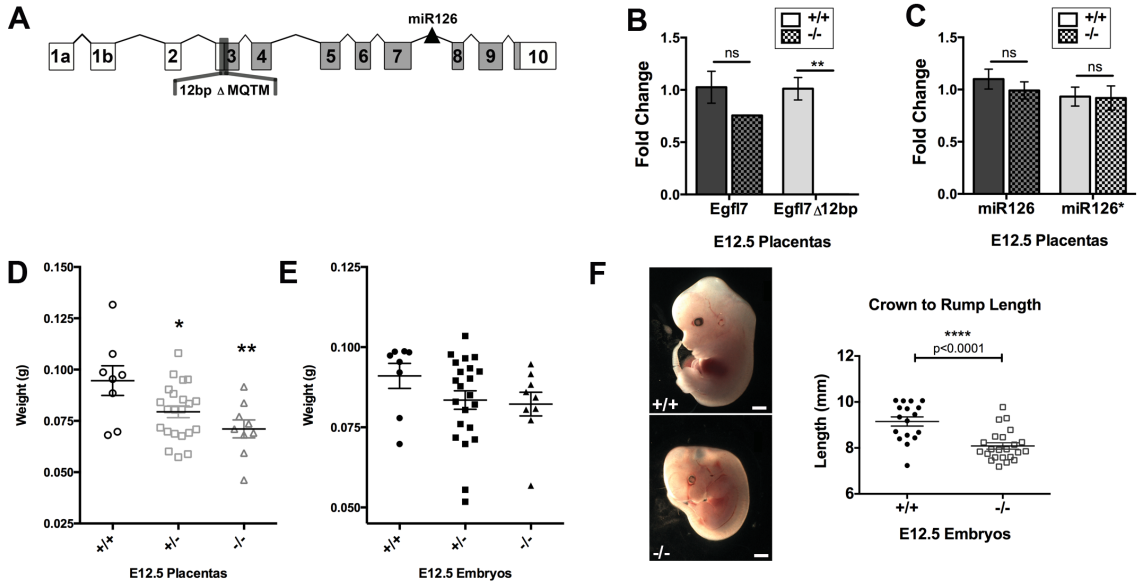

FIGURE 4.1 Egfl7 KO mice exhibit reduced placental weights and embryonic crown-to-rump lengths at E12.5. (A) Schematic representation of the *Egfl7* gene structure. Shaded regions represent protein coding exons. The positions of the microRNA miR-126 embedded in intron 7 and the 12-bp deletion in the mutant Egfl7 allele including the two ATG codons in exon 3 are depicted (not drawn to scale). (B) Real Time RT-PCR for unmodified Egfl7 mRNA and modified Egfl7 mRNA containing the 12-bp deletion in E12.5 placentas from C57BL/6 control (+/+) and Egfl7 KO (-/-) mice. (C) Real Time RT-PCR for miR-126 and miR-126* in E12.5 placentas from C57BL/6 (+/+) and Egfl7 KO (-/-) mice. (D-E) E12.5 placenta (D) and embryo (E) weights from Egfl7+/- intercrosses demonstrating a significant decrease in Egfl7+/- and Egfl7-/- placentas. (F) Representative images of an E12.5 C57BL/6 control (+/+) embryo and Egfl7 KO (-/-) embryo. Quantification of the crown-to-rump length of E12.5 embryos showing a significant reduction in Egfl7 KO (-/-) embryo lengths.

TABLE 4.1 Observed Mendelien ratios of Egfl7 intercross matings.

+/+	+/-	-/-
25/88	42/88	20/88
28.4%	47.7%	22.7%

mature phase requiring genes that stimulate increased metabolic functions occurs (*29*). Coincidentally, endothelial-specific overexpression of Egfl7 results in partial embryonic lethality at E12.5 (*24*).

Egfl7+/- and *Egfl7-/-* placentas exhibit significantly reduced placental weights at E12.5 (**Figure 4.1D**). *Egfl7+/-* and *Egfl7-/-* embryonic weights trend downward but do not reach significance at this stage, when compared to *Egfl7+/+* embryos (**Figure 4.1E**). To determine if *Egfl7* knockout affects the size of midgestation embryos, crown-to-rump measurements were taken at E12.5 of embryos from C57BL/6 control and Egfl7 KO matings. The lengths of Egfl7 KO embryos were approximately 1mm shorter than C57BL/6 control embryos (**Figure 4.1E**). The results reveal a significant growth restriction at midgestation of Egfl7 KO embryos.

Together, *Egfl7* loss-of-function while maintaining normal miR-126 expression results in reduced placental weights and embryonic lengths, suggesting a functional role for Egfl7 in placental development.

4.4.2 – Egfl7 loss-of-function results in vascular patterning defects and reduced fetal blood space in the fetal labyrinth

To examine the morphology of *Egfl7-/-* placentas, hematoxylin and eosin staining was performed on cross-sections of paraffin-embedded E12.5 C57BL/6 control and Egfl7 KO placentas. No gross abnormalities of placental zone formation, including the maternal decidua, junctional zone, and fetal labyrinth were found (**Supplemental Figure 4.1A-B**). At higher magnification,

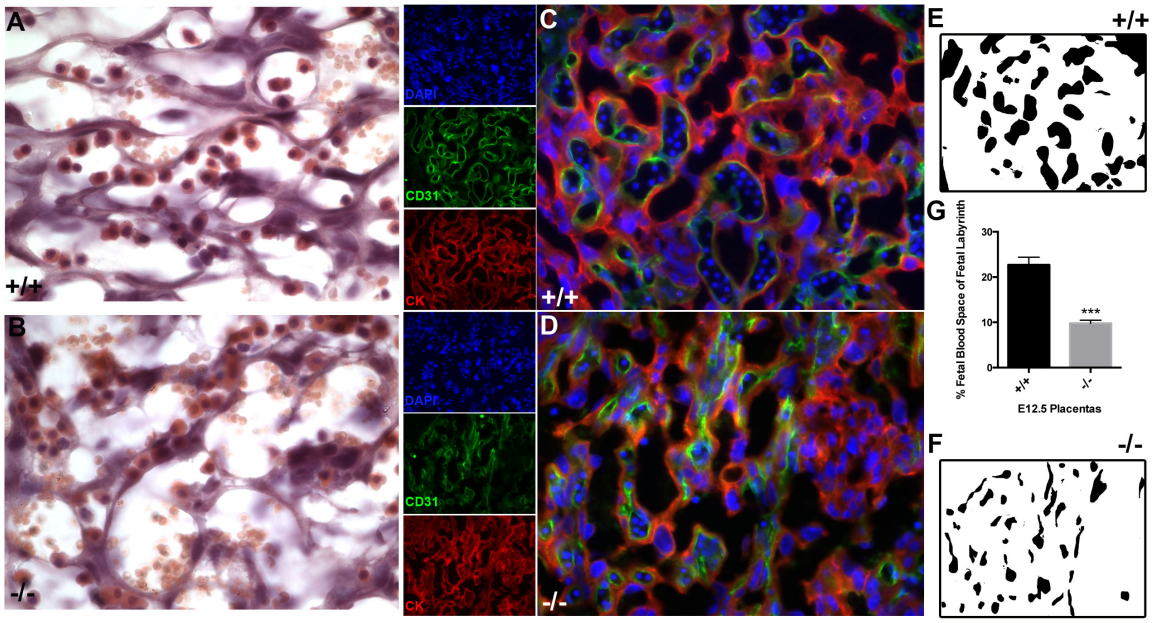

FIGURE 4.2 Egfl7 KO placentas exhibit fetal labyrinth patterning defects and reduced fetal capillary blood space. (A-B) Hematoxylin and eosin stained fetal labyrinth sections of E12.5 C57BL/6 control (+/+) (A) and Egfl7 KO (-/-) (B) placentas. (C-D) Double immunofluorescence staining for pan-endothelial marker, CD31 (green) and pan-trophoblast marker, CYTOKERATIN (red), on placenta sections from E12.5 C57BL/6 (+/+; C) and Egfl7 KO (-/-; D) conceptuses. (E-G) Quantification of the area of fetal blood space in the fetal labyrinth of C57BL/6 (+/+; E) and Egfl7 KO (-/-; F) mice, demonstrating a significant decrease in the percentage of area (G) covered by fetal capillaries in the fetal labyrinth zone of Egfl7 KO placentas.

the fetal capillaries of the Egfl7 KO placentas displayed vascular patterning defects, including decreased fetal blood space area (**Figure 4.2A-B**). The maternal decidua and junctional zone of Egfl7 KO placentas displayed no abnormalities at high magnification (**Supplemental Figure 4.1C-D**). To further characterize the placental morphology, double immunofluorescent staining was performed on frozen sections of E12.5 placentas for the pan-endothelial marker, CD31, and the pan-trophoblast marker, CYTOKERATIN. Results revealed that endothelial cells surround the irregularly patterned and narrowed fetal capillaries, while trophoblast cells line the maternal blood spaces (**Figure 4.2C-D**). To determine if the fetal blood space area was reduced in *Egfl7-/-* placentas, the area of fetal capillary lumens was quantified. Results reveal a significant reduction in fetal capillary blood space in the fetal labyrinth of Egfl7 KO placentas (**Figure 4.2E-G**).

To determine if the reduced placental weights and altered vascular patterning observed in the Egfl7 KO placentas was due to an alteration in the proliferation rates of placental cells, EdU was injected intraperitoneally into E12.5 pregnant females. Placentas were isolated after 45 minutes, processed for EdU detection and stained for endothelial and trophoblast markers, CD31 and CYTOKERATIN (**Supplemental Figure 4.2A-B**). To quantify the number of proliferating endothelial cells, placentas were processed for EdU detection and immunostained for nuclear ERG (**Supplemental Figure 4.2E-F**). In the fetal labyrinth zone of E12.5 placentas from C57BL/6 control and Egfl7 KO mice, ERG is an endothelial specific marker that colocalizes with CD31 (**Supplemental Figure 4.2C-D**). No significant difference in the number and

percentage of proliferating endothelial and non-endothelial cells was observed between Egfl7 KO and C57BL/6 control placentas (**Supplemental Figure 4.2G-H**).

Thus, our data demonstrate that *Egfl7* loss-of-function results in abnormal vascularization of the placental fetal labyrinth, and this defect cannot be attributed to altered proliferation.

4.4.3 – Altered vascular patterning results in reduced placental perfusion in Egfl7 loss-of-function placentas

To determine if the reduced fetal capillary blood space in mutant placentas affects placental perfusion with fetal blood, C57BL/6 control and Egfl7 KO whole conceptuses were isolated at gestation day 12.5. Microangiography of each conceptus was performed by injecting a fluorescent-lectin solution into the umbilical artery in order to mark endothelial cells of perfused vessels in the fetal labyrinth. Vibratome sections (100μm) of perfused C57BL/6 control placentas revealed a dense, arborized vascular network. Large chorionic vessels at the base of the placenta branched into smaller vessels of the fetal labyrinth, and further into the dense capillary network that covers a large surface area. Perfusion was restricted to the fetal labyrinth zone of the control placentas (**Figure 4.3A**). In contrast, Egfl7 KO placentas exhibited locally restricted and reduced placental perfusion. The large chorionic vessels were well perfused in the Egfl7 KO placentas. However, sporadic areas of well-perfused, smaller branched vessels were surrounded by areas of poorly perfused vessels (**Figure 4.3B**).

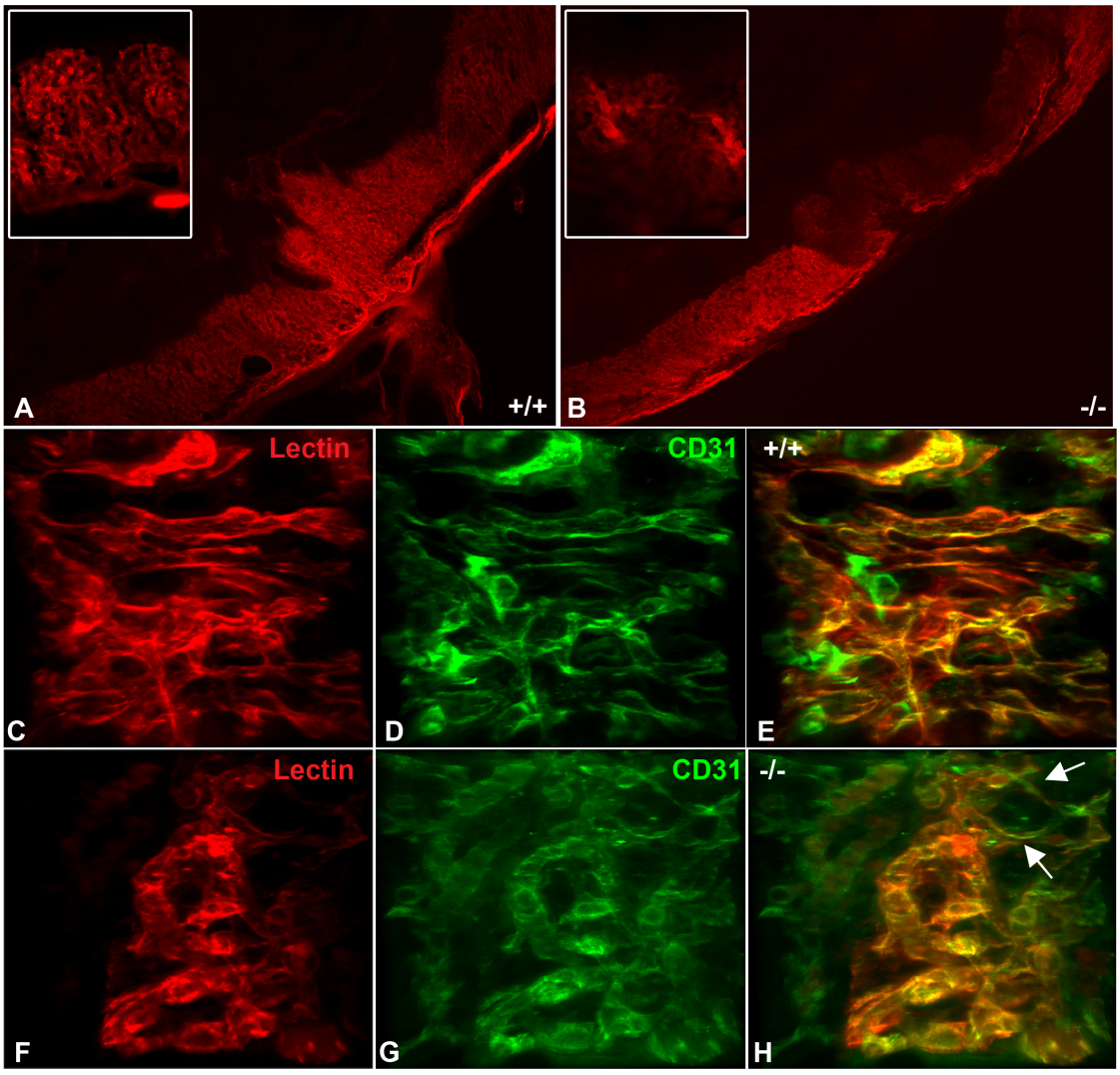

FIGURE 4.3 Egfl7 KO mice exhibit reduced perfusion of the placental fetal labyrinth. (A-B) Microangiography of placentas from E12.5 C57BL/6 (+/+; A) and Egfl7 KO (-/-; B) mice. Insets: high magnification of representative images of 100μm thick vibratome cross-section of placentas perfused with tomato-lectin showing areas of reduced placental perfusion in Egfl7 KO mice as compared to controls. (C-H) Three-dimensional reconstruction of z-stack confocal images of placentas perfused with tomato-lectin (red) and co-stained with CD31 (green). (C-E) C57BL/6 placentas exhibit evenly perfused vessels lined by CD31-positive endothelial cells, while (F-H) Egfl7 KO placentas exhibit areas with well-perfused vessels lined by CD31-positive endothelial cells adjacent to poorly perfused CD31-positive vessels. Arrows demarcate narrowed fetal capillaries and demonstrate areas where reduction in perfusion begins.

Immunofluoresence staining for CD31 was performed on vibratome sections to determine if the reduced perfusion resulted from narrowed fetal capillaries lined by endothelial cells and vascular patterning defects. Confocal imaging of the fetal labyrinth revealed a well-patterned, perfused fetal capillary network lined by CD31-positive endothelial cells in C57BL/6 control placentas (**Figure 4.3C-E**). In contrast, Egfl7 KO fetal labyrinth capillaries were tortuous, and subsets of vessels were poorly perfused (**Figure 4.3F-H**). Microangiography results revealed that perfusion was reduced at the sites of small, narrowed or constricted fetal capillaries in Egfl7 KO placentas (**Figure 4.3H**).

To determine if the observed reduced placental perfusion had a functional consequence and affected embryonic growth at term, we analyzed the weights of embryos from *Egfl7+/-* X *Egfl7+/-* intercrosses at E18.5. Results demonstrated a trend toward decreased embryonic weight in *Egfl7-/-* embryos (**Supplemental Figure 4.3**). Thus, *Egfl7* loss-of-function results in poor placental perfusion at sites of narrowed fetal capillaries.

4.4.4 – Egfl7 loss-of-function results in differential expression of genes involved in inflammatory response, extracellular matrix signaling, and reproductive structure development

Egfl7 loss-of-function results in placental vascular patterning defects and reduced placental perfusion. To determine the molecular pathways regulated through *Egfl7*, RNA Sequencing (RNA-seq) analysis was performed on RNA isolated from E12.5 placentas of C57BL/6 control and Egfl7 KO mice (**Figure 4.4A-C**). TopHat and Cufflinks software was used to align the RNA-seq reads

to a reference genome and to assemble the reads into transcripts. Differentially expressed transcripts were analyzed using in-house software at the Genomics Core Facility at WCMC.

RNA-seq analysis revealed that expression of 219 genes were significantly upregulated with a fold change greater than two in Egfl7 KO placentas, while only 6 genes were downregulated (**Figure 4.4A-B**). The top ten genes upregulated in Egfl7 KO placentas include Prss29, Wfdc15b, Gm5294, Eif2s3y, Ddx3y, Uty, Slc13a1, Akr1b, Sult1d1, and Klk1, while the six downregulated genes include Btg3, Amd1, Rps27, Lcn4, Tex13, and RhD.

To identify the biological processes affected by *Egfl7* loss-of-function in the placenta, gene ontology (GO) analyses using DAVID functional annotation software (*30*) was performed. GO results indicated that processes associated with extracellular matrix signaling, inflammatory response, and reproductive structure development were upregulated in Egfl7 KO placentas (**Figure 4.4C**). Fewer genes, and therefore fewer biological processes, were downregulated in Egfl7 KO mice.

Eleven upregulated genes and one downregulated gene were validated by Real Time RT-PCR, including Csf1, Emr1, Ccl20, Cxcl16, Prap1, Serpina1e, Apoa4, Tgfb2, MMP7, TMEM213, Tmprss4, and RhD (**Figure 4.4D**). Representative genes of GO categories were chosen for validation. For example, (i) Csf1 (Colony stimulating factor 1), an important signaling molecule for macrophage function, was chosen for inflammatory signaling; (ii) Prap1 (Proline rich acidic protein 1), a factor suggested to be important in the uterus

A

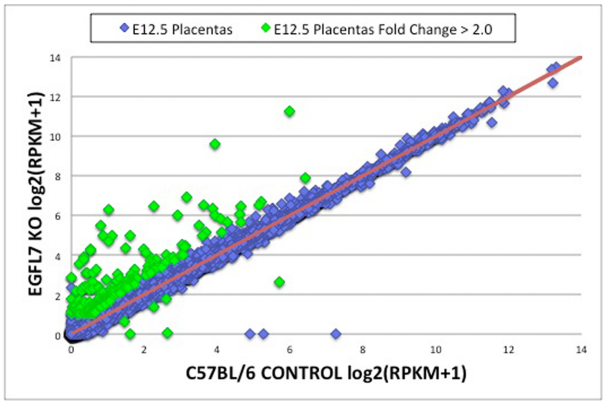

B

Upregulated	Downregulated
219	6

C

GO Terms: Upregulated
Extracellular matrix/signal peptide
Inflammatory response/platelet activation/wound healing
Regulation of hormone levels/metabolic processes
Cell adhesion
Blood vessel development/vasculature remodeling
Ion transport
Regulation of kinase activity

D

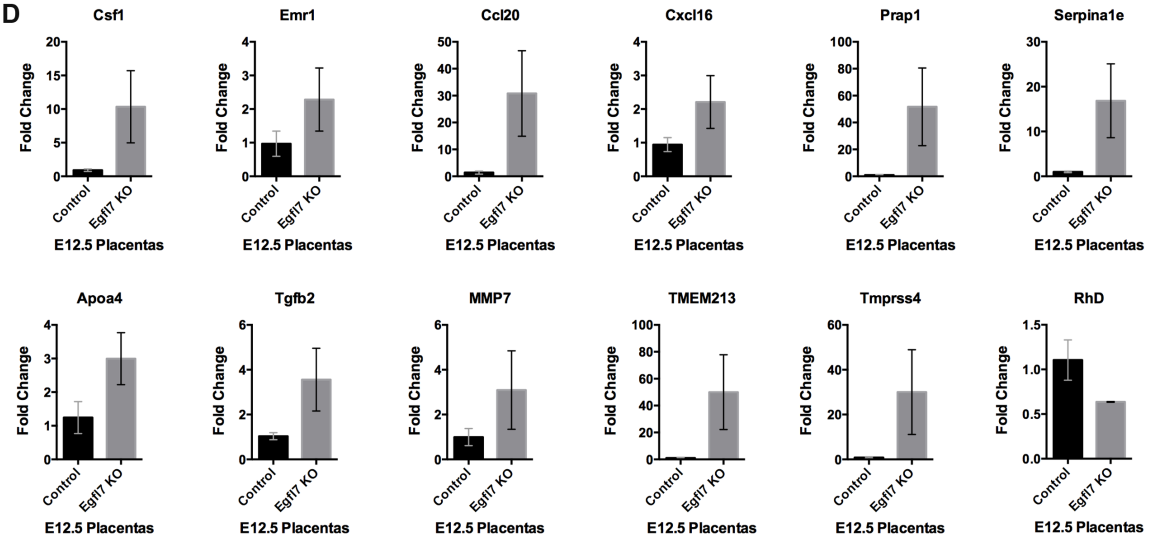

<u>FIGURE 4.4</u> Transcriptional profiling of Egfl7 KO mouse placentas results in differential expression of genes related to immune function and extracellular matrix signaling. (A) Scatterplot of transformed relative RPKM expression values in E12.5 placentas from C57BL/6 and Egfl7 KO mice. Differentially expressed genes with a fold change greater than 2 are marked in green. (B) The number of genes differentially expressed in E12.5 placentas from Egfl7 KO mice compared to C57BL/6 control. (C) Gene ontology enrichment analysis listing Gene Ontology terms upregulated in E12.5 Egfl7 KO placentas. (D) Real Time RT-PCR of eleven upregulated (Csf1, Emr1, Ccl20, Cxcl16, Prap1, Serpina1e, Apoa4, Tgfb2, MMP7, TMEM213, Tmprss4) and 1 downregulated (RhD) genes validating RNA-seq transcriptome analysis.

during pregnancy (*31*), was chosen for reproductive structure development; and (iii) Tmprss4 (Transmembrane protease serine 4) a transmembrane serine protease demonstrated to be involved with extracellular matrix modification, cell adhesion, and embryonic development was chosen for the gene ontology category of extracellular matrix signaling (**Figure 4.4D**).

Furthermore, to dissect the molecular pathways regulated through *Egfl7* specifically in the endothelial cell lineage, we isolated E12.5 placental endothelial cells from C57BL/6 control and Egfl7 KO mice by fluorescence activated cell sorting (FACS) with an antibody against the pan-endothelial marker, CD31. RNA-seq analysis was performed on RNA isolated from the sorted placental endothelial cells and performed as above. RNA-seq analysis revealed that expression of 12 genes were significantly upregulated with a fold change greater than two in Egfl7 KO placentas, while 32 genes were downregulated (**Supplemental Figure 4.4**). The top ten genes upregulated in Egfl7 KO placentas include Hist1h4j, Kdm5d, Uty, Ddx3y, Eif2s3y, S100g, Ucn, Cd52, Ly6h, and Cd74, while the top ten downregulated genes include Amd1, Ear1, Guca2b, Fam162b, Prap1, Gkn2, Afp, Pet117, C3, and Psg16. Results revealed that *Egfl7* loss-of-function in the placenta affects differential signaling pathways in placental endothelial cells as compared to whole placentas.

4.5 – Discussion

Disruptions in vascular development of the placenta can result in intrauterine growth restriction, fetal demise, or placental pathologies such as PE. Although several signaling pathways have been implicated in labyrinth development,

especially chorionic branching morphogenesis, the number of mouse mutants with a primary defect in placental vascularization is limited (*7*). Defects in fetal labyrinth development and vascularization can be classified as resulting either from defects in chorionic branching morphogenesis with secondary vascular defects, or primarily resulting from vascular-specific defects (*7*). In this study, we have revealed that Egfl7 KO mice exhibit patterning defects in the fetal labyrinth vasculature that results in reduced fetal blood space area and reduced perfusion. Many mouse mutants that exhibit vascular defects are primarily expressed in the trophoblast compartment. Egfl7, however, is primarily expressed and secreted by endothelial cells of the fetal labyrinth and not in labyrinthine trophoblasts. Egfl7 is, nevertheless, expressed in spongiotrophoblast cells of the junctional zone (*16*), a cell type that has been implicated to be important for vascular development in the fetal labyrinth. For example, HtrA-1 deficient mice exhibit irregularly patterned fetal labyrinth vessels at E14.5, although its expression is restricted to spongiotrophoblast cells (*32*). Furthermore, RNA-seq results revealed that *Egfl7* loss-of-function affects different signaling pathways in placental endothelial cells as compared to whole placentas, suggesting that it may have distinct, non-overlapping roles in placental trophoblast and endothelial cells. Additionally, reciprocal communication between trophoblast and endothelial cells is important for branching morphogenesis in the fetal labyrinth (*8*). Consequently, a role for spongiotrophoblast expressed EGFL7 cannot be ruled out as our *Egfl7* loss-of-function mice exhibit global knockout of the *Egfl7* gene.

It will be important to determine the cell-type specific role of *Egfl7* in placental trophoblast and endothelial cells through conditional knockout experiments.

EGFL7 has recently been shown to function *in vitro* in human trophoblast cells through activation of MAPK, PI3K, and NOTCH signaling (*26*). In these studies, overexpression of EGFL7 in human choriocarcinoma cells resulted in significantly increased cell migration and invasiveness, suggesting that trophoblast-derived EGFL7 may play an indirect role in the vascularization of the placenta. The ERK/MAPK pathways have been implicated in placental development and formation of the blood-placental barrier (*33, 34*), with functions in both endothelial cells and pericytes.

Egfl7 expression is also upregulated in response to hypoxia and exerts a protective effect against ischemia (*35-38*). Furthermore, *Egfl7* plays a critical role in vascular patterning and tubulogenesis *in vitro* and in mouse, zebrafish, and Xenopus embryos (*21, 23, 24, 39, 40*). It is possible that the hypoxic environment present during placental development may contribute to its upregulation, thereby regulating the patterning of the fetal labyrinth vasculature to ensure a large surface area for nutrient and gas exchange.

Placental vascular defects in Egfl7 KO mice appear to be partially resolved at late gestation, as seen in the slight decrease in Mendelian ratios of embryos and lack of a significant difference in placental weights at E18.5. Since extensive vascular remodeling occurs after E12.5, it is conceivable that the overall size and extent of vascularization of the placenta can change to compensate for primary defects (*7*). Of interest, a switch in placental gene expression patterns from genes that are primarily involved in growth and development to genes predominantly involved in maturation and increased metabolic processes occurs at E13.5 (*29*). Egfl7 expression is downregulated

in the placenta as gestation approaches completion (*16*). Vascular remodeling and additional compensatory factors could therefore correct, during late gestation, the defects observed in Egfl7 KO mice at E12.5.

Several of the biological processes predicted to be dysregulated in the Egfl7 KO placentas could contribute to the observed placental phenotype. Several genes identified in the transcriptome analysis are involved in inflammatory signaling, such as Csf1, Emr1 (F4/80), Ccl20, and Cxcl16. Additionally, genes involved in reproductive structure development were upregulated in Egfl7 KO placentas, including Prap1, several members of the Psg family (Psg17/18/27), Prl7a2, and Ctsq. TMPRSS4 plays a role in both cancer and embryonic development (*41*). Zebrafish knockdown of TMPRSS4 results in defects in vascular development, global organogenesis, and cell-cell adhesion (*42*). Thus, the upregulation of these genes and their involvement in vascular patterning of other vascular beds support the notion that these processes may also contribute to vascular patterning of the fetal labyrinth, and that they are regulated by *Egfl7* signaling.

Determining the specific role of *Egfl7* during vasculogenesis and angiogenesis has been complicated by the presence of an intronic mircoRNA miR-126 (*28*). A previous study by Kuhnert *et al.* using an Egfl7 KO model that did not affect miR-126 expression reported no vascular defects and no lethality in developing embryos (*28*). It is important to note, however, that these studies were performed in a mixed genetic background, presenting the possibility that modifying factors could have compensated during vascular development. In this study, miR-126 levels are unchanged and the global Egfl7 KO mice were

bred into a C57BL/6 congenic background. Our results demonstrate that mice with *Egfl7* loss-of-function exhibit defects in placental development, including altered vascular patterning, reduced fetal blood space, and poor placental perfusion resulting in embryos with reduced placental weights and reduced crown-to-rump lengths at midgestation. Egfl7 expression has been shown to be reduced in human PE placentas and placentas from a mouse model of PE (*16*). It will therefore be important to determine if the constriction of fetal vessels and reduction in placental perfusion in Egfl7 KO mice results in preeclampsia-like phenotypes.

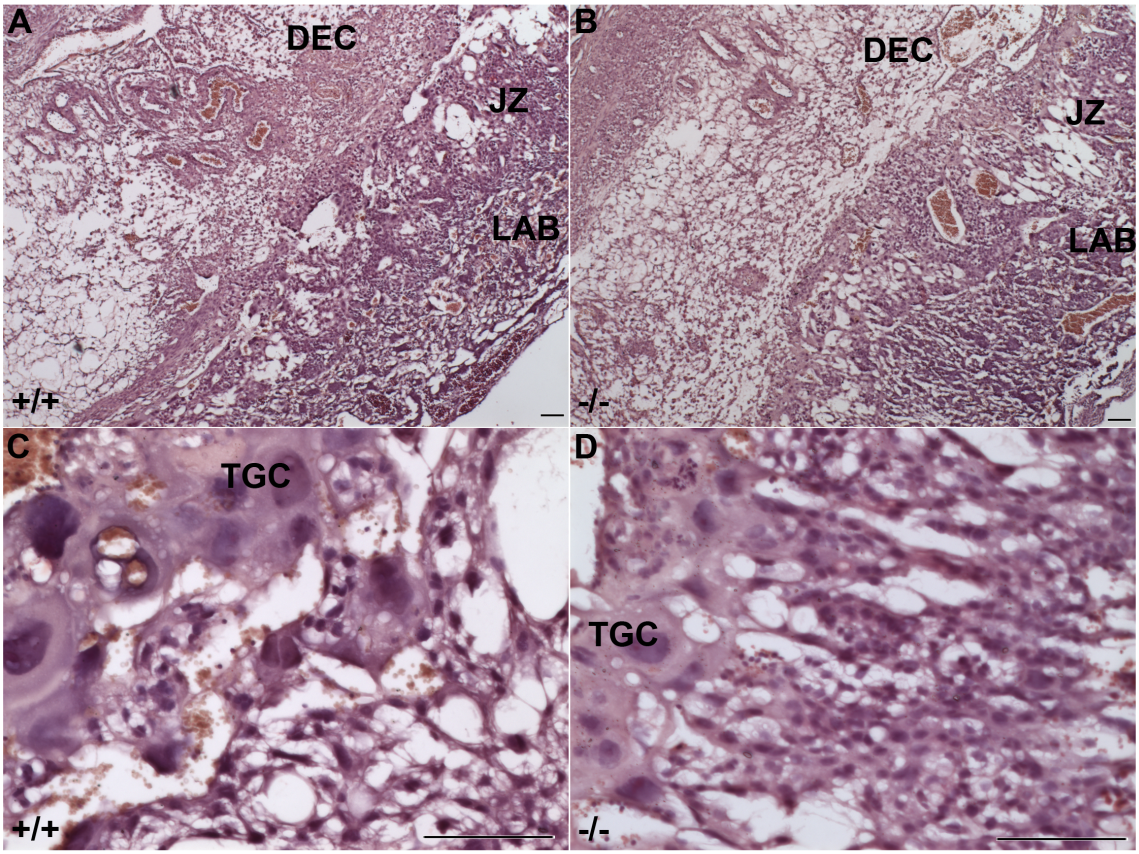

SUPPLEMENTAL FIGURE 4.1 Egfl7 KO placentas do not exhibit defects in maternal decidua or junctional zone placental layer formation. (A-B) Hematoxylin and eosin stained cross sections of E12.5 C57BL/6 control (+/+) (A) and Egfl7 KO (-/-) (B) placentas, demonstrating no overt defects in placental zone formation. (C-D) High magnification images of the junctional zone demonstrating no over defects in Egfl7 KO (-/-; D) placentas as compared for C57BL/6 controls (+/+; C). Scale bars = 100μm. *DEC-decidua, JZ-junctional zone, LAB-fetal labyrinth, TGC-trophoblast giant cell*

SUPPLEMENTAL FIGURE 4.2 Egfl7 loss-of-function does not affect proliferation of placental cells. (A-B) Triple immunfluorescent staining of E12.5 placentas from C57BL/6 (+/+; A) and Egfl7 KO (-/-; B) mice for the pan-trophoblast marker, CYTOKERATIN (CK; red), pan-endothelial marker, CD31 (green), and proliferation marker, EdU (white). (C-D) Double immunfluorescent staining of E12.5 placentas from C57BL/6 (+/+; C) and Egfl7 KO (-/-; D) mice for CD31 (green) and nuclear endothelial marker, ERG (red). (E-F) Double immunfluorescent staining of E12.5 placentas from C57BL/6 (+/+; E) and Egfl7 KO (-/-; F) mice for ERG (green) and EdU (red). (G-H) Quantification of the percentage of proliferating endothelial and non-endothelial cells in C57BL/6 (+/+) and Egfl7 KO (-/-) placentas. Scale bars = 100μm.

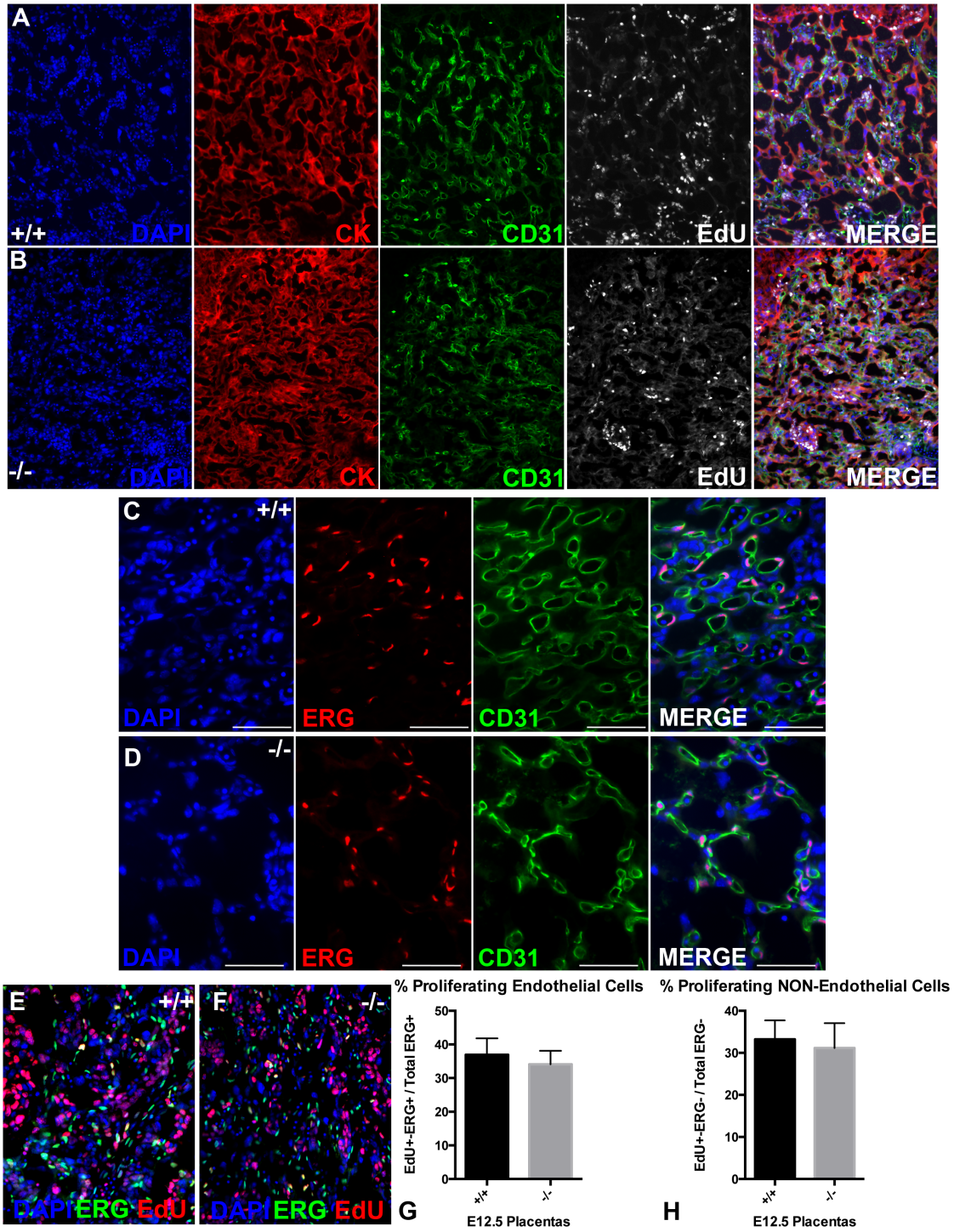
A
+/+
DAPI
CK
CD31
EdU
MERGE
B
-/-
DAPI
CK
CD31
EdU
MERGE
C
+/+
DAPI
ERG
CD31
MERGE
D
-/-
DAPI
ERG
CD31
MERGE
E
+/+
DAPI ERG EdU
F
-/-
DAPI ERG EdU
% Proliferating Endothelial Cells
EdU+-ERG+ / Total ERG+
50
40
30
20
10
0
+/+
-/-
E12.5 Placentas
G
% Proliferating NON-Endothelial Cells
EdU+-ERG- / Total ERG-
40
30
20
10
0
+/+
-/-
E12.5 Placentas
H

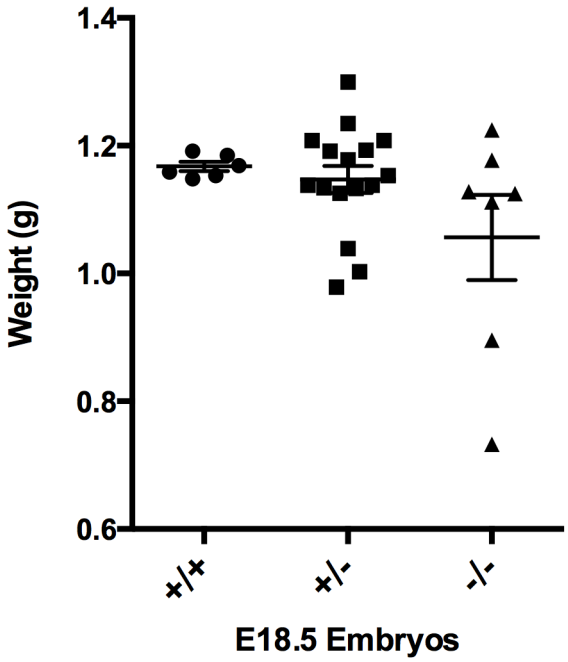

SUPPLEMENTAL FIGURE 4.3 Variable weights observed in late-stage Egfl7 KO embryos. E12.5 embryonic weights from Egfl7+/- intercrosses demonstrating a variable, but trend to decreased weights in Egfl7-/- embryos.

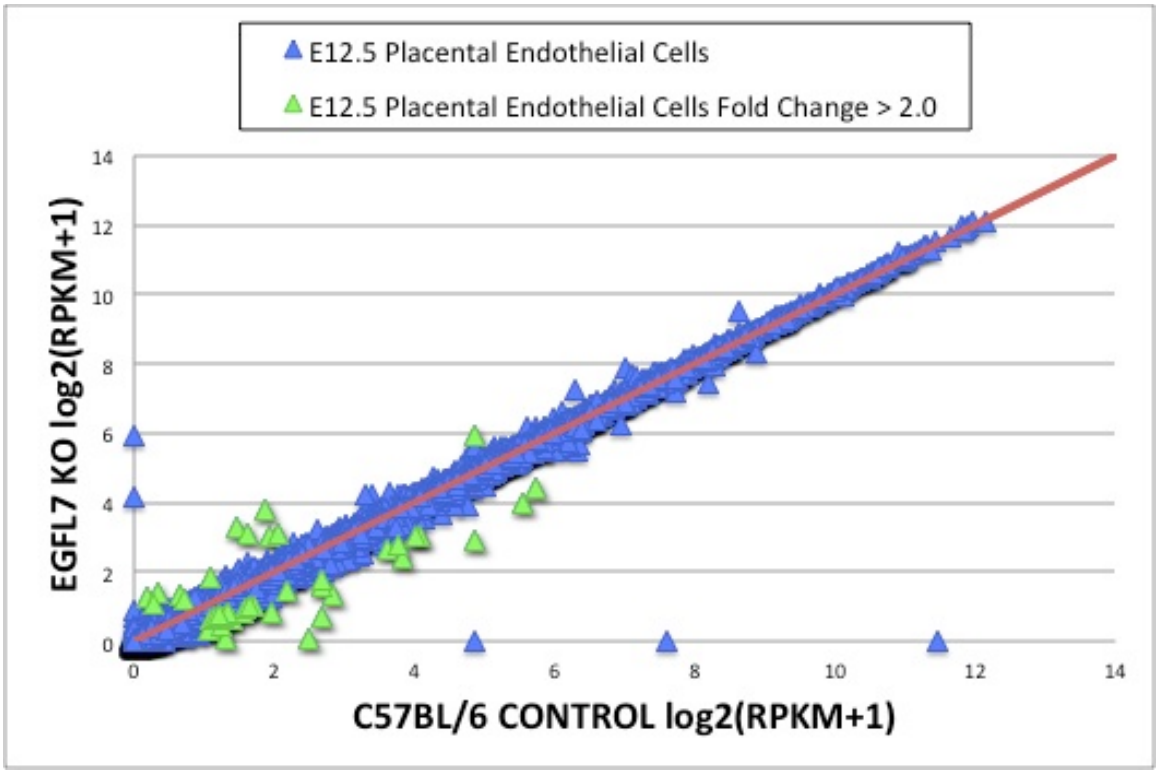

SUPPLEMENTAL FIGURE 4.4 Transcriptional profiling of FACS sorted placental endothelial cells. Scatterplot of transformed relative RPKM expression values in isolated E12.5 placental endothelial cells from C57BL/6 and Egfl7 KO mice. Differentially expressed genes with a fold change greater than 2 are marked in green.

4.6 – Materials and Methods

Mice

All animal protocols were approved and are in accordance with the Institutional Animal Care and Use Committee (IACUC) at Weill Cornell Medical College of Cornell University. C57Bl/6 mice were obtained from Jackson Laboratories and Egfl7-KO mice were derived at the Mouse Genetics Core at Memorial Sloan Kettering Cancer Center from embryonic stem cells of Velocigene clone #1501 (Regeneron Pharmaceuticals, Inc), a generous gift from Dr. Nick Gale of Regeneron. Velocigene clone #1501 contains a 12-bp deletion of the N-terminal MQTM sequence (including the two 5' ATG start codons) and insertion of a hygromycin cassette flanked by loxP sites. Founder mice were backcrossed into the C57Bl/6 background for 10 generations to obtain congenic mice. To remove the hygromycin cassette, Egfl7 knockout mice were bred to CAG-Cre transgenic mice (MSKCC Transgenic Core), a strain that retains Cre Recombinase activity in mature oocytes, irrespective of *cre* transgene transmission (*43*). Mice that were identified by PCR as positive for removal of the hygromycin cassette and negative for Cre were used for all further studies.

Timed pregnancies were performed and date of visualization of the vaginal plug was designated embryonic day 0.5 (E0.5). Placentas and embryos were dissected, imaged on Zeiss Discovery.V20 stereoscope, and weighed after removal of excess fluid. Crown-to-rump lengths were measured using ImageJ software.

Immunohistochemistry

Placentas were isolated, fixed in 4% paraformaldehyde, and embedded in an OCT:30% sucrose mixture in PBS (2:1). Cryosections were permeablized in 0.5% Triton-X/0.1% Saponin/PBS (TSP) and blocked with 1% donkey serum in 0.1% TSP/PBS (PBS–TSP). Primary antibodies (CD31, BD Biosciences, 553370, 5*μ*g/ml; CYTOKERATIN (DAKO Z0622, 12*μ*g/ml; ERG, Abcam, ab110639, 0.17*μ*g/ml) were incubated overnight at 4°C in block, followed by incubation with secondary antibodies in block (Alexa488-donkey-α-rat and Cy3-donkey-α-rabbit, Jackson Immunoresearch, 1.5 *μ*g/ml), and mounted with Prolong Gold + DAPI (Invitrogen). Images were acquired using an Axioplan 2 imaging microscope (Carl Zeiss).

Hematoxylin and Eosin Staining

Placentas were isolated, fixed in 4% paraformaldehyde, dehydrated through a series of alcohols, and embedded in paraffin. Sections were stained with hematoxylin and eosin, and mounted with Permount (Fisher Scientific). Images were acquired using an Axioplan 2 imaging microscope (Zeiss).

EdU Labeling

Proliferating cells were labeled using the Click-iT EdU Imaging Kit (Life Technologies, C10339). Female C57Bl/6 and Egfl7-KO mice were subjected to intraperitoneal injection of EdU at 50 μg per gram of body weight at day-12.5 of gestation. After 45 minutes, mice were euthanized and placentas were isolated and fixed in 4% paraformaldehyde overnight. Tissue was cryopreserved, embedded in a 2:1 OCT:30% sucrose mixture, and sectioned for further

processing. Sections were permeablized and EdU detection was carried out according to the manufacturer's protocol. Antibody staining was then performed as described above. Approximately every 10th section was used for quantification of labeling, for a total of five sections per placenta (n=3 per genotype), and analyzed using ImageJ, Metamorph and Prism software.

Quantifications

Fetal blood space was analyzed on 9 images from the fetal labyrinth zone of n=3 placentas from at least two litters of C57Bl/6 and Egfl7-KO mice. Fetal blood space was identified by CD31-positive staining surrounding DAPI-positive nucleated erythrocytes and traced using ImageJ software. The percentage of fetal blood space of the total area analyzed was quantified.

Microangiography

Females were sacrificed at day 12.5 of gestation by cervical dislocation, conceptuses were isolated in L15 medium (Invitrogen) and umbilical arteries exposed. A 40μl solution of tomato-lectin (Vector Labs, #DL-1177) in PBS containing heparin was injected into the umbilical artery. Each conceptus was incubated for 10minutes at 37°C in L15 medium (Corning), allowing the embryonic heart to circulate the injection throughout the feto-placental circulation. Placentas and embryos were then further dissected and fixed overnight at 4°C in 4% paraformaldehyde. Only conceptuses in which the fluorescent lectin had reached the embryo were kept for analysis. Placentas were incubated in 5% low melt agarose (Lonza) for 2hours at 42°C, and embedded in 5% low melt agarose through solidification at room temperature. Blocks were cut on a vibratome at 100μm thickness. Agarose was removed

and sections were either mounted in Prolong Gold (Life Technologies) using slide wells (Electron Microscopy Sciences) or processed for immunostaining.

Placenta vibratome sections were blocked for 3hours in 10% donkey serum in TSP, incubated in CD31 primary antibody (BD #550274; 1μg/ml) in 5% donkey serum in TSP, overnight at 4°C. Sections were washed in TSP, incubated in 488-donkey-α-rat secondary antibody (JacksonImmuno #712-546-150; 1:500), washed in TSP, and mounted in Prolong Gold (Life Technologies) using slide wells.

FACS analysis

Placentas from C57BL/6 and Egfl7 KO timed pregnant females were isolated at E12.5. Pooled placentas were digested with Collagenase/Dispase (Roche) and DNAse I (Roche) at 37°C for 20minutes. Digested placentas were passed through a 40μm cell strainer to form a single cell suspension. Samples were then depleted using lineage cell depletion kit per manufacturer's protocol (Miltenyi Biotec). Cells were resuspended in PBS+2%FBS and incubated in primary-conjugated antibody for CD31 (APC-CD31, BD Pharmingen) for 30minutes at room temperature. Stained cells were washed in PBS-2%FBS, sorted using the BD FACSAriaII SORP high-speed cell sorter and analyzed using BD FACSDiva software (BD Biosciences) with the aid of Dr. Jason McCormick at the Weill Cornell Medical College Department of Pathology and Laboratory Medicine Flow Cytometry Core for FACS.

RNA-seq

Total RNA was isolated from E12.5 placentas or isolated placental endothelial cells using Trizol Reagent. RNA was digested with DNase I (Zymo Research) and purified using the DNA-free RNA kit (Zymo Research). RNA quality was verified using an Agilent Technologies Bioanalyzer 2100 and samples were processed for next-generation sequencing by the Genomics Core Facility at Weill Cornell Medical College.

RNA was converted into cDNA using the Illumina TruSeq sample preparation kit, and cDNA hybridization and cluster amplification was performed using a cBOT fluidic device, following protocols offered by Illumina, Inc. (San Diego, CA). Templates were then sequenced on the HiSeq2500 (Illumina) by performing single read clustering (51 cycle sequencing). Analysis of the reads was performed with the help of the Genomics Core Facility (Dr. Tuo Zhang) using TopHat and Cufflinks software, and alignment to the University of California, Santa Cruz mm9 reference genome. Differentially expressed transcripts were analyzed using in-house software.

Real Time RT-PCR

Placentas from C57BL/6 and Egfl7 knockout mice were dissected and flash frozen in liquid nitrogen. RNA was isolated using Trizol (Invitrogen) and reverse transcribed using qScript cDNA Synthesis Kit (Quanta Biosciences). Gene expression was measured quantitatively using PerfeCTa SYBR Green SuperMix for iQ (Quanta Biosciences) and specific primer sets for ß-actin, Egfl7 (as described in (*24*)). Additional primer sequences are listed in

Supplemental Table 4.1. Differences among target expression were quantified using the ΔΔCT method and normalized to ß-actin.

For analysis of miR-126 expression, ten nanograms of E12.5 placenta RNA was reverse transcribed using TaqMan MicroRNA Reverse Transcription Kit (Life Technologies #4366596) with RT primers specific for miR126 (*002228*), miR126* (*000451*), and control snoRNA234(0001234). Real Time PCR was performed using TaqMan Universal PCR Master Mix (Life Technologies #4324018) and TaqMan probes for miR126 (*002228*), miR126* (*000451*), and control snoRNA234 (0001234).

Statistics

Data are represented as mean ± SEM. The data were analyzed using a student's t-test with statistical significance defined as $*P < 0.05$, $**P<0.001$ unless otherwise noted.

SUPPLEMENTAL TABLE 4.1 Real Time RT-PCR primers.

Primer	Forward Sequence (5' ➔ 3')	Reverse Sequence (5' ➔ 3')
Egfl7Δ12bp	ATGCAGACCATGTGGGGCTC	GGTCTCCGAGATGGAACCTCCG
Csf1	TCTCCTTGAAAAGGACTGGAACA	GCAGTTGCAATCAGGCTTGG
Emr1	CCAGGCTTTGTCTTGAATGGC	AGCTTCCGAGAGTGTTGTGG
Ccl20	AACTGGGTGAAAAGGGCTGT	CCTTGGGCTGTGTCCAATTC
Cxcl16	GTTGCAGTCCAAAAGCGTGT	CCCATGACCAGTTCCACACT
Prap1	TTTCTCCTGGCCACCTGTTTG	ACACATGTTTGCCTTTGGTCTT
Serpina1e	AGGAAAGATAGTTGAGGCTGTGA	AGGATCGAATGGCTTCTTCCA
Mmp7	GCGGAGATGCTCACTTTGAC	GTGGCCAAATTCATGGGTGG
Tgfb2	AAAATCGACATGCCGTCCCA	TGAGACATCAAAGCGGACGA
Apoa4	GATGCCCCATGCCAACAAAG	TCTGATCTTGCAGGTCCACG
TMEM213	CCTTCCACTTATCCTGCGGT	TCGACATTGGCACACTGCT
Tmprss4	TGAGCCTGATAGCCCTCGT	CCCCTCTGAATGAAGGTCAGG
Btg3	AAGCAAGGAAGTGGACGTGA	AAGGGTGCCACATTGGAAGA
Amd1	GCTGGAGGTCTGGTTTTCCA	TGAGCACTGCACATCCTTCAA
Rps27	AACATGCCTCTCGCAAAGGA	TAGGAATTGGGGCTCTGCAC
Rhd	GGTGCAGGGAACAATCTTGC	CAGCACAGGTAAGGTGCTCA

REFERENCES

1. L. L. Waite, A. K. Atwood, R. N. Taylor, Preeclampsia, an implantation disorder. *Rev Endocr Metab Disord* **3**, 151-158 (2002).
2. P. Merviel, L. Carbillon, J. C. Challier, M. Rabreau, M. Beaufils, S. Uzan, Pathophysiology of preeclampsia: links with implantation disorders. *Eur J Obstet Gynecol Reprod Biol* **115**, 134-147 (2004).
3. B. C. Young, R. J. Levine, S. A. Karumanchi, Pathogenesis of preeclampsia. *Annu Rev Pathol* **5**, 173-192 (2010).
4. C. E. Powe, R. J. Levine, S. A. Karumanchi, Preeclampsia, a disease of the maternal endothelium: the role of antiangiogenic factors and implications for later cardiovascular disease. *Circulation* **123**, 2856-2869 (2011).
5. M. V. Naljayan, S. A. Karumanchi, New developments in the pathogenesis of preeclampsia. *Adv Chronic Kidney Dis* **20**, 265-270 (2013).
6. J. Rossant, J. C. Cross, Placental development: lessons from mouse mutants. *Nat Rev Genet* **2**, 538-548 (2001).
7. E. D. Watson, J. C. Cross, Development of structures and transport functions in the mouse placenta. *Physiology (Bethesda)* **20**, 180-193 (2005).
8. J. C. Cross, H. Nakano, D. R. Natale, D. G. Simmons, E. D. Watson, Branching morphogenesis during development of placental villi. *Differentiation* **74**, 393-401 (2006).
9. G. C. Gurtner, V. Davis, H. Li, M. J. McCoy, A. Sharpe, M. I. Cybulsky, Targeted disruption of the murine VCAM1 gene: essential role of VCAM-1 in chorioallantoic fusion and placentation. *Genes Dev* **9**, 1-14 (1995).
10. L. Kwee, H. S. Baldwin, H. M. Shen, C. L. Stewart, C. Buck, C. A. Buck, M. A. Labow, Defective development of the embryonic and extraembryonic circulatory systems in vascular cell adhesion molecule (VCAM-1) deficient mice. *Development* **121**, 489-503 (1995).
11. L. Anson-Cartwright, K. Dawson, D. Holmyard, S. J. Fisher, R. A. Lazzarini, J. C. Cross, The glial cells missing-1 protein is essential for branching morphogenesis in the chorioallantoic placenta. *Nat Genet* **25**, 311-314 (2000).
12. S. L. Adamson, Y. Lu, K. J. Whiteley, D. Holmyard, M. Hemberger, C. Pfarrer, J. C. Cross, Interactions between trophoblast cells and the maternal and fetal circulation in the mouse placenta. *Dev Biol* **250**, 358-373 (2002).
13. D. G. Simmons, D. R. Natale, V. Begay, M. Hughes, A. Leutz, J. C. Cross, Early patterning of the chorion leads to the trilaminar trophoblast

cell structure in the placental labyrinth. *Development* **135**, 2083-2091 (2008).
14. M. Kar, Role of biomarkers in early detection of preeclampsia. *J Clin Diagn Res* **8**, BE01-04 (2014).
15. S. Rana, S. A. Karumanchi, M. D. Lindheimer, Angiogenic factors in diagnosis, management, and research in preeclampsia. *Hypertension* **63**, 198-202 (2014).
16. L. A. Lacko, M. Massimiani, J. L. Sones, R. Hurtado, S. Salvi, S. Ferrazzani, R. L. Davisson, L. Campagnolo, H. Stuhlmann, Novel expression of EGFL7 in placental trophoblast and endothelial cells and its implication in preeclampsia. *Mech Dev* **133**, 163-176 (2014).
17. K. Junus, M. Centlow, A. K. Wikström, I. Larsson, S. R. Hansson, M. Olovsson, Gene expression profiling of placentae from women with early- and late-onset pre-eclampsia: down-regulation of the angiogenesis-related genes ACVRL1 and EGFL7 in early-onset disease. *Mol Hum Reprod* **18**, 146-155 (2012).
18. M. Zanello, P. DeSanctis, G. Pula, C. Zucchini, M. C. Pittalis, N. Rizzo, A. Farina, Circulating mRNA for epidermal growth factor-like domain 7 (EGFL7) in maternal blood and early intrauterine growth restriction. A preliminary analysis. *Prenat Diagn* **33**, 168-172 (2013).
19. L. Campagnolo, I. Moscatelli, M. Pellegrini, G. Siracusa, H. Stuhlmann, Expression of EGFL7 in primordial germ cells and in adult ovaries and testes. *Gene Expr Patterns* **8**, 389-396 (2008).
20. M. J. Fitch, L. Campagnolo, F. Kuhnert, H. Stuhlmann, Egfl7, a novel epidermal growth factor-domain gene expressed in endothelial cells. *Dev Dyn* **230**, 316-324 (2004).
21. L. H. Parker, M. Schmidt, S. W. Jin, A. M. Gray, D. Beis, T. Pham, G. Frantz, S. Palmieri, K. Hillan, D. Y. Stainier, F. J. De Sauvage, W. Ye, The endothelial-cell-derived secreted factor Egfl7 regulates vascular tube formation. *Nature* **428**, 754-758 (2004).
22. F. Soncin, V. Mattot, F. Lionneton, N. Spruyt, F. Lepretre, A. Begue, D. Stehelin, VE-statin, an endothelial repressor of smooth muscle cell migration. *EMBO J* **22**, 5700-5711 (2003).
23. M. S. Charpentier, K. S. Christine, N. M. Amin, K. M. Dorr, E. J. Kushner, V. L. Bautch, J. M. Taylor, F. L. Conlon, CASZ1 promotes vascular assembly and morphogenesis through the direct regulation of an EGFL7/RhoA-mediated pathway. *Dev Cell* **25**, 132-143 (2013).
24. D. Nichol, C. Shawber, M. J. Fitch, K. Bambino, A. Sharma, J. Kitajewski, H. Stuhlmann, Impaired angiogenesis and altered Notch signaling in mice overexpressing endothelial Egfl7. *Blood* **116**, 6133-6143 (2010).
25. L. Campagnolo, A. Leahy, S. Chitnis, S. Koschnick, M. J. Fitch, J. T. Fallon, D. Loskutoff, M. B. Taubman, H. Stuhlmann, EGFL7 is a

chemoattractant for endothelial cells and is up-regulated in angiogenesis and arterial injury. *Am J Pathol* **167**, 275-284 (2005).
26. M. Massimiani, L. Vecchione, D. Piccirilli, P. Spitalieri, F. Amati, S. Salvi, S. Ferrazzani, H. Stuhlmann, L. Campagnolo, Epidermal growth factor-like domain 7 promotes migration and invasion of human trophoblast cells through activation of MAPK, PI3K and NOTCH signaling pathways. *Mol Hum Reprod*, (2015).
27. P. Georgiades, A. C. Ferguson-Smith, G. J. Burton, Comparative developmental anatomy of the murine and human definitive placentae. *Placenta* **23**, 3-19 (2002).
28. F. Kuhnert, M. R. Mancuso, J. Hampton, K. Stankunas, T. Asano, C. Z. Chen, C. J. Kuo, Attribution of vascular phenotypes of the murine Egfl7 locus to the microRNA miR-126. *Development* **135**, 3989-3993 (2008).
29. K. Knox, J. C. Baker, Genomic evolution of the placenta using co-option and duplication and divergence. *Genome Res* **18**, 695-705 (2008).
30. d. W. Huang, B. T. Sherman, R. A. Lempicki, Systematic and integrative analysis of large gene lists using DAVID bioinformatics resources. *Nat Protoc* **4**, 44-57 (2009).
31. J. Kasik, E. Rice, A novel complementary deoxyribonucleic acid is abundantly and specifically expressed in the uterus during pregnancy. *Am J Obstet Gynecol* **176**, 452-456 (1997).
32. M. Z. Hasan, M. Ikawati, J. Tocharus, M. Kawaichi, C. Oka, Abnormal development of placenta in HtrA1-deficient mice. *Dev Biol* **397**, 89-102 (2015).
33. S. Giroux, M. Tremblay, D. Bernard, J. F. Cardin-Girard, S. Aubry, L. Larouche, S. Rousseau, J. Huot, J. Landry, L. Jeannotte, J. Charron, Embryonic death of Mek1-deficient mice reveals a role for this kinase in angiogenesis in the labyrinthine region of the placenta. *Curr Biol* **9**, 369-372 (1999).
34. V. Nadeau, J. Charron, Essential role of the ERK/MAPK pathway in blood-placental barrier formation. *Development* **141**, 2825-2837 (2014).
35. M. V. Badiwala, L. C. Tumiati, J. M. Joseph, R. Sheshgiri, H. J. Ross, D. H. Delgado, V. Rao, Epidermal growth factor-like domain 7 suppresses intercellular adhesion molecule 1 expression in response to hypoxia/reoxygenation injury in human coronary artery endothelial cells. *Circulation* **122**, S156-161 (2010).
36. M. Gustavsson, C. Mallard, S. J. Vannucci, M. A. Wilson, M. V. Johnston, H. Hagberg, Vascular response to hypoxic preconditioning in the immature brain. *J Cereb Blood Flow Metab* **27**, 928-938 (2007).
37. D. Xu, R. E. Perez, I. I. Ekekezie, A. Navarro, W. E. Truog, Epidermal growth factor-like domain 7 protects endothelial cells from hyperoxia-induced cell death. *Am J Physiol Lung Cell Mol Physiol* **294**, L17-23 (2008).

38. Y. S. Liu, Z. W. Huang, A. Q. Qin, Y. Huang, F. Giordano, Q. H. Lu, W. D. Jiang, The expression of epidermal growth factor-like domain 7 regulated by oxygen tension via hypoxia inducible factor (HIF)-1α activity. *Postgrad Med* **127**, 144-149 (2015).
39. A. Durrans, H. Stuhlmann, A role for Egfl7 during endothelial organization in the embryoid body model system. *J Angiogenes Res* **2**, 4 (2010).
40. M. Schmidt, K. Paes, A. De Mazière, T. Smyczek, S. Yang, A. Gray, D. French, I. Kasman, J. Klumperman, D. S. Rice, W. Ye, EGFL7 regulates the collective migration of endothelial cells by restricting their spatial distribution. *Development* **134**, 2913-2923 (2007).
41. A. L. de Aberasturi, A. Calvo, TMPRSS4: an emerging potential therapeutic target in cancer. *Br J Cancer* **112**, 4-8 (2015).
42. A. Ohler, C. Becker-Pauly, Morpholino knockdown of the ubiquitously expressed transmembrane serine protease TMPRSS4a in zebrafish embryos exhibits severe defects in organogenesis and cell adhesion. *Biol Chem* **392**, 653-664 (2011).
43. K. Sakai, J. Miyazaki, A transgenic mouse line that retains Cre recombinase activity in mature oocytes irrespective of the cre transgene transmission. *Biochem Biophys Res Commun* **237**, 318-324 (1997).

Chapter 5 – Conclusion and Future Perspectives

5.1 – Summary

The work described in this thesis demonstrates that Egfl7 plays a functional role during organogenesis. Using Egfl7 overexpressing and knockout mice, as well as a mouse model for preeclampsia, I have demonstrated that dysregulation of Egfl7 expression results in aberrant pancreatic and placental development and function. In the pancreas, endothelial EGFL7 regulates pancreatic progenitor cell proliferation and stem cell maintenance, and thus pancreatic size. In the placenta, EGFL7 affects vascular patterning and perfusion of the fetal labyrinth. Results of these studies have provided insight into the function of Egfl7 during organogenesis and its implications in pathological pancreatic and placental development.

5.2 – Implications of Egfl7 signaling during pancreatic development

Endothelial cells play a critical role in pancreatic growth and development (*1-3*). In chapter 2, I revealed that Egfl7 signaling from the endothelium influences the size of the developing pancreas *in vivo* by facilitating proliferation of pancreatic progenitor cells. The laboratory of Dr. Shuibing Chen demonstrated the stage-dependent role of EGFL7 in pancreatic progenitor cell self-renewal *in vitro* using hESCs. Furthermore, collaborative studies with the Chen laboratory uncovered the functional consequences of Egfl7 overexpression and aberrant pancreatic development by revealing that adult Egfl7 overexpressing mice have impaired beta cell function. Taken together, these results provide insight into

understanding normal pancreatic development and have clinical implications for diseases of the pancreas, such as diabetes mellitus.

Diabetes mellitus is a chronic health condition characterized by prolonged hyperglycemia resulting from defects in insulin production or insulin action (*4*), and is expected to reach a prevalence of 4.4% of the worldwide population by 2030 (*5*). A promising strategy to treat diabetes involves the transplantation of mature, insulin-producing, glucose-responding beta cells derived from stepwise differentiation of human embryonic stem cells (hESC) *in vitro* for cell replacement therapy (*6*). The studies presented in chapter 2 suggest that EGFL7 can be used as a therapeutic tool for developing methods to increase the functional beta cell population in diabetic patients.

5.3 –Implications of Egfl7 signaling during placental development

Despite its critical role during pregnancy, the placenta remains under-studied. Many of the dynamic changes that occur in the placenta throughout gestation remain elusive. The lack of progress in understanding placental physiology and development is largely due to the difficulty in obtaining human placental tissue early in gestation, and a lack of animal and *in vitro* models that faithfully recapitulate human placental development. The mouse placenta, however, shares many structural, morphological, and genetic similarities to the human placenta, making it an excellent model for studying the development of this organ (*7, 8*). Indeed, several genetic mutant mice have elucidated much of what we know today about placental development (*8*). In this thesis, I have

utilized a mouse model of PE and developed a genetic knockout mouse of Egfl7 to study normal and pathological placental development.

The studies described in chapter 3 provide much needed insight into the role of *Egfl7* in placental development. Detailed characterization of the spatiotemporal expression profile in the placenta revealed a novel expression domain for Egfl7 in trophoblast cells. Spongiotrophoblast cells of the junctional zone of the mouse placenta are known to play a structural role and to produce hormones, however, the molecular mechanisms underlying spongiotrophoblast function remain poorly characterized. Dissecting the trophoblast-specific role of *Egfl7* during placental development may shed insight into the function and physiology of this subset of spongiotrophoblast cells, as *Egfl7* may mark a specialized, distinct group of trophoblast cells in the junctional zone of the placenta.

Furthermore, communication between trophoblast and endothelial cells has been suggested as an important mechanism in fetal labyrinth formation and patterning (*9*). Consistent with these functions, *Egfl7* has been shown to have both a paracrine and autocrine effect. It is plausible that *Egfl7* may play distinct, non-overlapping roles in these two cell types. Ongoing and future studies dissecting the differential roles that *Egfl7* plays in placental endothelial and trophoblast cell function and determining if *Egfl7* is involved in interactive trophoblast and endothelial cell communication will elucidate the mechanisms by which *Egfl7* affects normal and pathological placental development. Spongiotrophoblast-specific ablation of *Egfl7* using a Tpbpa-Cre mouse, and endothelial-specific ablation of *Egfl7* using a VE-cadherin-Cre mouse, will shed insight into the cell-specific functions of Egfl7 during placental development.

Furthermore, these studies can be complimented by *in vitro* studies using cells derived from C57BL/6 control and *Egfl7* knockout mice, including trophoblast stem cells and isolated placental endothelial cells.

The studies described in chapter 3 also have clinical implications for PE. Abnormal placental function underlies the maternal presentation of the disease, as PE resolves after delivery of the placenta and fetus (*10-12*). Although the clinical presentation of PE occurs in late gestation, studies suggest that the pathogenesis of the disease begins as early as implantation (*13, 14*). In chapter 3, I have shown that Egfl7 is downregulated in placentas of a PE mouse model preceding elevated blood pressure and proteinuria, suggesting a possible causative role in its pathophysiology. It is well established that a dysregulation of pro- and anti-angiogenic signaling factors is involved in PE, and it is likely that several signaling pathways are dysregulated, including signaling through EGFL7. With that, development of novel diagnostic and therapeutic tools will be needed for treatment of the disease. Indeed, studies are underway to diagnose PE using a panel of markers (*15-17*). Because Egfl7 is downregulated in the BPH/5 mouse model of PE early in gestation, and downregulation of *Egfl7* has been associated with human PE placentas, as well as in the serum of PE patients, utilizing *Egfl7* in a diagnostic test for PE may prove beneficial. Future studies involve developing an ELISA test to detect EGFL7 in maternal serum of patients throughout pregnancy to determine if it is suitable for diagnostic use.

Identifying the EGFL7 signaling pathway in the placenta will be important for understanding the functional role of *Egfl7* during normal placental development

and potentially the pathogenesis of PE. In chapter 4 I have demonstrated that knockout of *Egfl7* in mice results in altered placental vascular patterning and reduced placental perfusion. Together with results from transcriptome analysis, these studies provided insights into possible molecular mechanisms by which *Egfl7* could be working in the placenta. It is evident that Egfl7 affects immune regulation and signaling, which play a critical role in immune tolerance during normal pregnancy and has been implicated in PE (*18, 19*). Interestingly, Notch signaling was largely unchanged in Egfl7 KO placentas at E12.5, despite its known modulation by *Egfl7* in other vascular beds, as well as in human PE placentas and human trophoblast cells *in vitro (20-22)*. Thus, it is likely that *Egfl7* works through several signaling pathways to exert its effects on placental development, or that *Egfl7* may function, in part, through modulating Notch signaling in the placenta in a stage-dependent manner.

Understanding the cellular and molecular processes that underlie normal placentation will shed insight into the pathophysiology of PE and other placental pathologies, such as intrauterine growth restriction. To this end, future studies are underway to determine if *Egfl7* knockout results in the presentation of PE-like symptoms of elevated blood pressure, proteinuria, and global endothelial dysfunction.

5.4 –Conclusion

Collectively, the studies presented in this thesis have elucidated novel roles for *Egfl7* during organogenesis of the pancreas and the placenta. Studies presented here reveal that Egfl7 stimulates pancreatic progenitor proliferation

and pancreatic development in addition to regulating vascular patterning and perfusion in the placenta. These studies have carefully determined *Egfl7*-specific function during development of endocrine organs by utilizing mouse models that maintain miR-126 expression, a microRNA embedded in the non-coding region of the Egfl7 gene. Notably, these results reveal that dysregulation of *Egfl7* has implications in common diseases such as diabetes and preeclampsia. Endothelial-derived EGFL7 increases the number of pancreatic progenitor cells produced during step-wise differentiation of hESC into functional beta cells. These findings enhance the strategy to produce sufficient numbers of functional beta cells for transplantation into diabetic patients. Furthermore, downregulation of *Egfl7* early in gestation, its detection in maternal serum, and its function in fetoplacental vascular patterning and perfusion make it a candidate for diagnosing and/or treating PE. Future studies on *Egfl7* function during pancreatic and placental development will reveal the potential of using *Egfl7* for diagnostic and therapeutic purposes.

REFERENCES

1. J. Magenheim, O. Ilovich, A. Lazarus, A. Klochendler, O. Ziv, R. Werman, A. Hija, O. Cleaver, E. Mishani, E. Keshet, Y. Dor, Blood vessels restrain pancreas branching, differentiation and growth. *Development* **138**, 4743-4752 (2011).
2. E. Lammert, O. Cleaver, D. Melton, Induction of pancreatic differentiation by signals from blood vessels. *Science* **294**, 564-567 (2001).
3. D. Eberhard, M. Kragl, E. Lammert, 'Giving and taking': endothelial and beta-cells in the islets of Langerhans. *Trends Endocrinol Metab* **21**, 457-463 (2010).
4. A. D. Association, Diagnosis and classification of diabetes mellitus. *Diabetes Care* **32 Suppl 1**, S62-67 (2009).
5. S. Wild, G. Roglic, A. Green, R. Sicree, H. King, Global prevalence of diabetes: estimates for the year 2000 and projections for 2030. *Diabetes Care* **27**, 1047-1053 (2004).
6. D. I. Kao, S. Chen, Pluripotent stem cell-derived pancreatic β-cells: potential for regenerative medicine in diabetes. *Regen Med* **7**, 583-593 (2012).
7. P. Georgiades, A. C. Ferguson-Smith, G. J. Burton, Comparative developmental anatomy of the murine and human definitive placentae. *Placenta* **23**, 3-19 (2002).
8. J. Rossant, J. C. Cross, Placental development: lessons from mouse mutants. *Nat Rev Genet* **2**, 538-548 (2001).
9. J. C. Cross, H. Nakano, D. R. Natale, D. G. Simmons, E. D. Watson, Branching morphogenesis during development of placental villi. *Differentiation* **74**, 393-401 (2006).
10. B. C. Young, R. J. Levine, S. A. Karumanchi, Pathogenesis of preeclampsia. *Annu Rev Pathol* **5**, 173-192 (2010).
11. C. E. Powe, R. J. Levine, S. A. Karumanchi, Preeclampsia, a disease of the maternal endothelium: the role of antiangiogenic factors and implications for later cardiovascular disease. *Circulation* **123**, 2856-2869 (2011).
12. M. V. Naljayan, S. A. Karumanchi, New developments in the pathogenesis of preeclampsia. *Adv Chronic Kidney Dis* **20**, 265-270 (2013).
13. L. L. Waite, A. K. Atwood, R. N. Taylor, Preeclampsia, an implantation disorder. *Rev Endocr Metab Disord* **3**, 151-158 (2002).
14. P. Merviel, L. Carbillon, J. C. Challier, M. Rabreau, M. Beaufils, S. Uzan, Pathophysiology of preeclampsia: links with implantation disorders. *Eur J Obstet Gynecol Reprod Biol* **115**, 134-147 (2004).

15. H. S. Cuckle, Screening for pre-eclampsia--lessons from aneuploidy screening. *Placenta* **32 Suppl**, S42-48 (2011).
16. M. Hund, D. Allegranza, M. Schoedl, P. Dilba, W. Verhagen-Kamerbeek, H. Stepan, Multicenter prospective clinical study to evaluate the prediction of short-term outcome in pregnant women with suspected preeclampsia (PROGNOSIS): study protocol. *BMC Pregnancy Childbirth* **14**, 324 (2014).
17. B. Huppertz, H. Meiri, S. Gizurarson, G. Osol, M. Sammar, Placental protein 13 (PP13): a new biological target shifting individualized risk assessment to personalized drug design combating pre-eclampsia. *Hum Reprod Update* **19**, 391-405 (2013).
18. S. Saito, A. Shiozaki, A. Nakashima, M. Sakai, Y. Sasaki, The role of the immune system in preeclampsia. *Mol Aspects Med* **28**, 192-209 (2007).
19. E. Laresgoiti-Servitje, A leading role for the immune system in the pathophysiology of preeclampsia. *J Leukoc Biol* **94**, 247-257 (2013).
20. M. Massimiani, L. Vecchione, D. Piccirilli, P. Spitalieri, F. Amati, S. Salvi, S. Ferrazzani, H. Stuhlmann, L. Campagnolo, Epidermal growth factor-like domain 7 promotes migration and invasion of human trophoblast cells through activation of MAPK, PI3K and NOTCH signaling pathways. *Mol Hum Reprod*, (2015).
21. D. Nichol, C. Shawber, M. J. Fitch, K. Bambino, A. Sharma, J. Kitajewski, H. Stuhlmann, Impaired angiogenesis and altered Notch signaling in mice overexpressing endothelial Egfl7. *Blood* **116**, 6133-6143 (2010).
22. M. H. Schmidt, F. Bicker, I. Nikolic, J. Meister, T. Babuke, S. Picuric, W. Müller-Esterl, K. H. Plate, I. Dikic, Epidermal growth factor-like domain 7 (EGFL7) modulates Notch signalling and affects neural stem cell renewal. *Nat Cell Biol* **11**, 873-880 (2009).